UNIVERSITA' DEGLI STUDI DI MILANO

Dottorato di Ricerca in Scienze Biochimiche
XXXIII ciclo

Dipartimento di Biotecnologie Mediche

e Medicina Traslazionale

Evaluation of the GM1 oligosaccharide role in neuronal differentiation

Pamela Fato
Matricola n. R11944

Tutor:
Dott.ssa Laura Mauri

Coordinatore del Dottorato:
Prof. Alessandro Prinetti

Anno Accademico 2019-2020

Contents

Abstract

GM1 is a mono-sialo ganglioside with amphiphilic character due to the presence of a hydrophobic group, ceramide, and a hydrophilic head (oligosaccharide chain). GM1 represents one of the most important modulator in the nervous system where it is involve in maturations of neurons, differentiation, increase responses to neurotrophic factors, protection against neuronal death and reduction brain damage. The effects of GM1 are known *in vitro* and *in vivo*, but the molecular mechanism of action underlying the GM1 properties is unknown. The present work aims to analyze the mechanism of action of GM1, and in particular to demonstrate that the effects of this ganglioside are attributable to the action of its oligosaccharide portion (OligoGM1) and not to the entire molecule. To reach our purpose we used mouse neuroblastoma cell line Neuro2a (N2a). Like GM1, OligoGM1 promotes neurodifferentiation by increasing both neurite elongation and the expression of neurofilament proteins in N2a cell. A similar effect was obtained with the use of fucosyl-OligoGM1 but not with the administration of asialo-OligoGM1, OligoGM2, OligoGM3, sialic acid or galactose (single components of Oligo GM1). OligoGM1, in N2a cells, activates ERK1/2 pathway binding to the NGF specific receptor TrkA present on the cell surface. To study this mechanism of action we used tritium labeled derivative of OligoGM1. The activator for GM1 mediated functions (differentiation and protection) is the interaction between OligoGM1 and TrkA. This was established with the use of a TrkA inhibition.

With a bioinformatics study it was established that OligoGM1 inserts in a pocket of the TrkA-NGF complex. An increase in energy associated to the complex TrkA-NGF-OligoGM1 indicates greater stability of intermolecular interactions.

All the results lead to the conclusion that the bioactive portion of GM1, in neuronal differentiation and protection, is represented by its hydrophilic chain (OligoGM1). These conclusions open up new perspectives on the therapeutic use of gangliosides.

Introduction

1. Chemical properties of gangliosides

Gangliosides **(Figure I-1)** are glycosphingolipids (GSLs) containing one or more sialic acid residues **(Figure I-2)** in the sugar moiety. These GSLs are amphiphilic components of cells membrane. Gangliosides are inserted into membranes by their lipid moiety while the glycan moiety is extending outside. They are present in different tissues but in mammalian they are abundant in plasma membranes of nervous cells.

Gangliosides were first extracted from brain tissue in 1935 by Ernest Klenk (*Klenk 1935*). In 1930s Ernst Klenk was investigating ganglia cells of patients affected by some peculiar neurolipidoses like Niemann-Pick disease, characterized by accumulation of sphingomyelin and other lipids in reticuloendothelial cells, and Tay-Sachs disease, an autosomal-recessive lysosomal storage metabolic disorders caused by β-hexosaminidase A (HexA) enzyme deficiency, resulting in GM2 ganglioside accumulation predominantly in lysosomes of nerve cells (*Solovyeva et al. 2018*). In this ganglia cells Klenk discovered a new glycosphingolipid differed from the cerebrosides by its solubility in water, its acidic nature and by a characteristic purple colour reaction with Bial's sugar reagent. The word "ganglioside" was proposed because this kind of glycolipids resulted largely in ganglia cells of the grey matter (*Klenk 1970*).

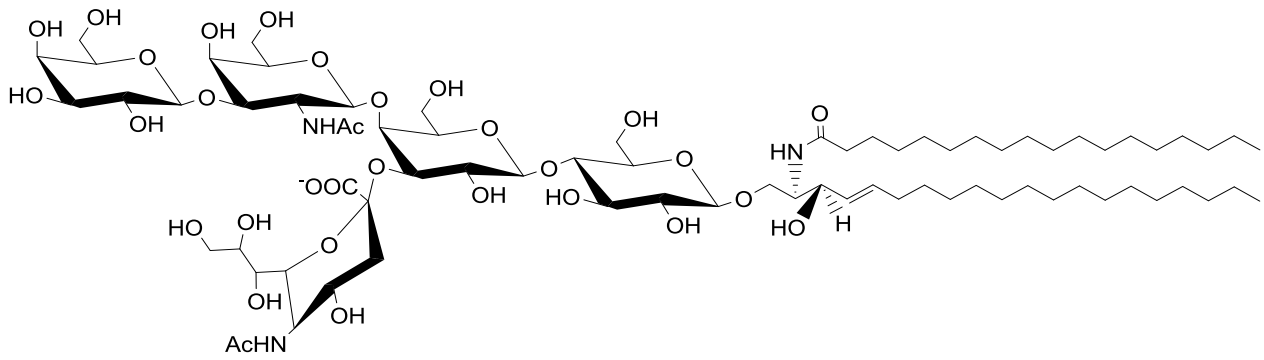

(A)

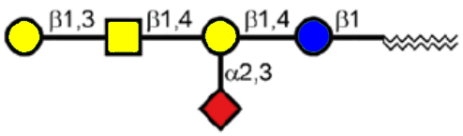

(B)

Figure I-1. Monosialoganglioside GM1a. (A) Schematic sturcture β-Gal-(1–3)-β-GalNAc-(1–4)-[α-Neu5Ac-(2–3)-]β-Gal-(1–4)-Glc-(1–1)-Cer. GM1a: according to Svennerholm (*Svennerholm 1980*). $II^3Neu5AcGg_4Cer$: abbreviations according to IUPAC-IUB (*IUPAC-IUB 1997*). (B) Glycan symbol of GM1a. Yellow circle: galactose (Gal). Yellow square: *N*-Acetylglucosamine (GalNAc). Blu circle: glucose (Glc). Red rhombus: 5-*N*-Acetylneuraminic acid (Neu5Ac).

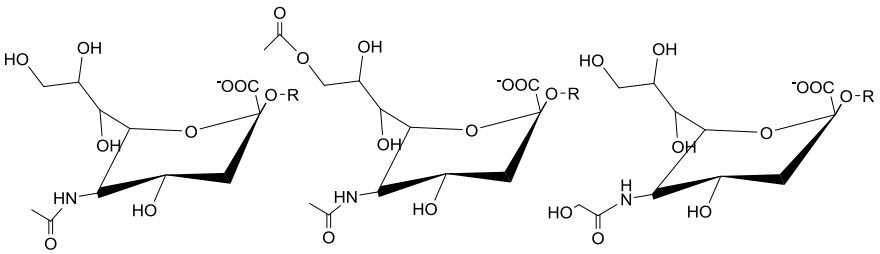

(A) **(B)** **(C)**

Figure I-2. Structure of 5-*N*-acetyl- (Neu5Ac) (**A**), 5-*N*-acetyl-9-*O*-acetyl- (Neu5,9Ac$_2$) (**B**), and 5-*N*-glycolyl-neuraminic acid (Neu5Gc) (**C**).

But the structure of gangliosides was described in 1963 by Kuhn and Wiegandt (*Kuhn et al. 1963*).
Gangliosides are complex lipids with a strong amphiphilic character due to the presence of a hydrophobic group (lipid moiety, named ceramide) **(Figure I-3A)** linked with a β-glycosidic linked to a hydrophilic head group (oligosaccharide chain). Ceramide, inserted in the plasma membrane outer layer, can be involved in a lot of cellular signaling like regulating differentiation, proliferation, and programmed cell death. Ceramide is the simplest kind of two-chained sphingolipids, one of its chain is an amino alcohol (Roisen et al. 1981) with a trans double bond in the 4,5 position (2S, 3R, 4E) 2-amino-1,3-dihydroxy-octadec-4-ene (sphingosine) **(Figure I-3B)**, linked to a fatty acyl chain with an amide bond. According to the number of carbon atoms we can have different kind of sphingosine like C18 or C20. In mammalian sphingolipids, the molecular species C18 is the most abundant. Other sphingosine with more or less C in alkyl chain have been identified in specific cells and tissues. C20-sphingosine is present quite totally into the brain. Sometimes is also present a minor amount of the saturated species, named sphinganine **(Figure I-3C).**

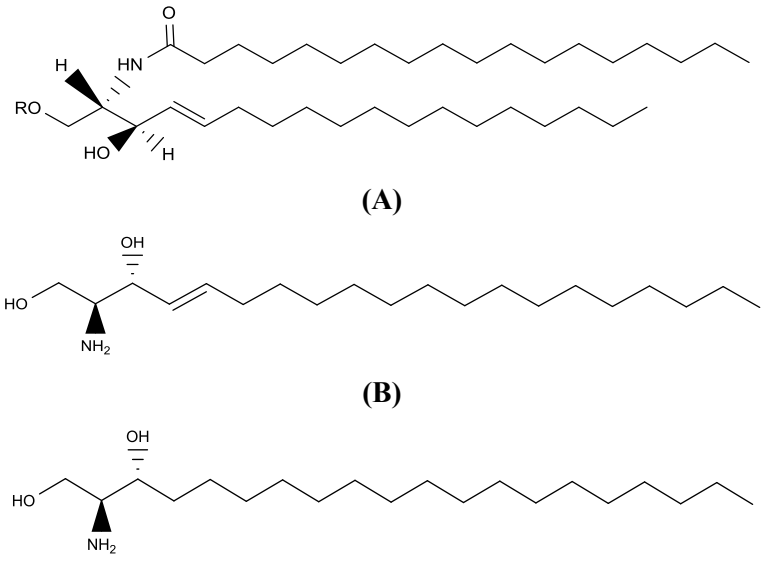

(A)

(B)

(C)

Figure I-3. Structure of ceramide **(A)**, sphingosine **(B)** and sphinganine **(C)**.

The fatty acid of ceramide is highly variable as regards the length and presence of unsaturated bonds. The length of the ceramide fatty acid chain is regulated by the tissue specific enzyme, ceramide synthase. Mainly, stearic acid (C18, 18:0) prevails in the nervous system (over 90%) (*Schengerund et al. 1969*). In the other tissues, fatty acids are more heterogeneous and often they have a very long chain.

The oligosaccharide chain of gangliosides is extremely changeable, from one galactose residue in galactosyl-ceramide, one of the main lipids present in myelin, to a very complex structure like in polysialylated gangliosides, characteristic of the nervous system. Oligo chain is linked to ceramide with a β-glycosidic bond between the sugar C1 and the sphingosine C1.

Sialic acid is the sugar, containing a carboxyl group, that differentiates gangliosides from neutral glycosphingolipids and sulfatides. Sialic acid, a nine-carbon backbone sugar, represents all derivatives of 5-amino-3,5-didooxy-D-glycero-D-galact-non-2-ulopyranosonic acid or neuraminic acid. The sialic acid is linked to the neutral oligosaccharide portion by an α-glycosidic bond, while other hexoses are present as β-anomers. The most common sialic acid linked to gangliosides in humans is N-acetylneuraminic acid (Neu5Ac. In humans, sialic acid is also present as 5-N-acetyl-9-O-acetylneuraminic but it is absent in the form 5- N-glycolyneuramine (Neu5Gc) present in other mammals (*Irie et al. 1998*). Neu5Ac and Neu5Gc differ by one oxygen atom which is added by the enzyme cytidine monophosphate N-acetylneuraminic acid hydroxylase (CMAH) in the cytosol. Humans do not biosynthesize Neu5Gc because CMAH gene, on chromosome 6p21.32, encoding for the hydroxylase / monooxygenase enzyme responsible for the conversion of CMP-5-*N*-acetyl-neuraminic acid to CMP-5-*N*-glycolylneuraminic acid, is inactive (*Varki 2007*). Neu5Gc has been found on the cell surface of human tumors and in lower amount in normal human tissues. Neu5Gc in human comes likely from the consumption of animal-derived diets, such as red meat and animal milk (*Kooner et al. 2019*). The number of sialic acid residues in ganglioside is variable from 1 to 7.

Gangliosides are usually classified according to the number and location of hexoses and sialic acid residues. The nomenclature that is usually used was proposed by Svennerholm (*Svennerholm 1964*). Gangliosides are named by applying a three-character code (two letters and a number). The first letter is G, indicating that the molecule is a ganglioside. The second letter indicate the number of sialic acid: monosialo (M), disialo (D), trisialo (T), tetrasialo (Q) and pentasialo (P) gangliosides. An Arabic number is then assigned to indicate the length of the gangliotetraose core as either all four neutral sugars (1), three sugars (2) or two sugars (3). This number initially was referring to its migration order in a certain chromatographic system (*IUPAC-IUB 1997*):

1= Gal (β1---3)GalNac(β1---4)Gal(β1---4)Glcβ1

2= GalNac(β1---4)Gal(β1---4)Glcβ1

3= Gal(β1---4)Glcβ1

Finally, to indicate the number of sialic acid residues linked to internal galactose, a lower case letter is used (a = 1, b = 2, c = 3) (*Svennerholm 1963*).

For monosialogangliosides like GM1, one of the most studied gangliosides, the lower case "a" is optional and most often omitted. However, GM1b have a "b" in its name, although is 0-series gangliosides (no sialic acids on the internal galactose) (*Kolter 2012*). The corresponding IUPAC-IUBMB name of GM1 is $II^3Neu5AcGg_4Cer$. This first structure of GM1 was established in 1963 by Kuhn and Wiegandt (*Kuhn and Wiegandt 1963*). Then in 1975 a different GM1, called GM1b, has been identified into the brain (*Stoffyn et al, 1975*) **(Figure I-4)**. The two structures differ in the position of the sialic acid.

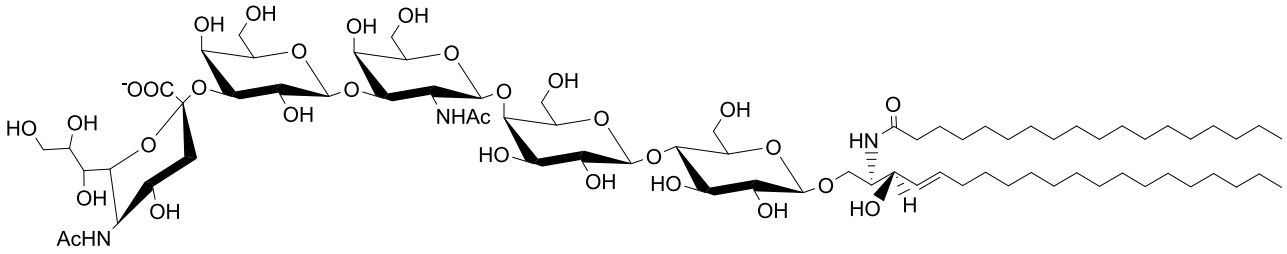

(A)

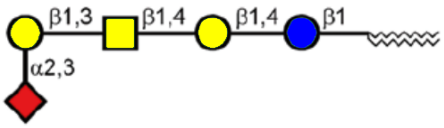

(B)

Figure I-4. Monosialoganglioside GM1b. (A) Schematic sturcture [α-Neu5Ac-(2–3)-]β-Gal-(1–3)-β-GalNAc-(1–4)-β-Gal-(1–4)-Glc-(1–1)-Cer. GM1b: abbreviation according to Svennerholm (*Svennerholm 1980*). $IV^3Neu5AcGg_4Cer$: abbreviations according to IUPAC-IUB (*IUPAC-IUB 1997*). (B) Glycan symbol of GM1b. Yellow circle: galactose (Gal). Yellow square: *N*-Acetylglucosamine (GalNAc). Blu circle: glucose (Glc). Red rhombus: 5-*N*-Acetylneuraminic acid (Neu5Ac).

2. Biosynthesis of gangliosides

The biosynthesis of glycosphingolipids and in particular of gangliosides is described as a combinatorial process, in wich biomolecules are product by the combination of different building blocks (*Kolter et al. 2002*) starting from a few reactions catalysed by glycosyltransferases, enzymes able to use precursors and intermediates to produce different molecules. Gangliosides, like other glycosphingolipids, are biosynthesized at intracellular membranes and then they are transported to the plasma membrane. In particular, the Golgi apparatus is the subcellular organelle in which occurs glycan modifications of glycoconjugates in transit to the cell surface or extracellular destinations (*Varki 2011*).
Ganglioside biosynthesis starts with the formation of ceramide in the endoplasmic reticulum (ER).
De novo synthesis of gangliosides can be distinguished from salvage processes, in which sialic acids, sugars, fatty acids, and sphingoid bases are recycled (*Kolter 2012*). Gangliosides are degraded after endocytosis by degrading enzymes, activator proteins, and negatively charged lipids (*Breiden and Sandhoff 2018*).

2.1. Ceramide

The biosynthesis of gangliosides starts from ceramide formation at the cytoplasmic side of the endoplasmic reticulum (ER). In mammals, ceramide is the precursor of many important compounds such as phosphosphingolipids (sphingomyelin (SM) and Cer1-phosphate (Cer-1P)) and glycosphingolipids (galactosilceramide (GalCer) and glucosilceramide (GlcCer)), and complex glycosphingolipids (*Merrill 2002*). The production of ceramide occurs mainly following three metabolic pathways: de novo biosynthesis, degradation of complex sphingolipids and recycling of sphingosine **(Figure I-5)**.

2.1.1 De novo biosynthesis

In 1967 Braune in 1968 Stoffel (*Braun and Snell 1967; Stoffel et al. 1968*) have demonstrated that the first reaction of sphingolipids metabolism occurs in the cytosolic side of the ER where the amino acid L-serine condenses with an activated fatty acid (mainly palmitoyl-CoA) giving 3-ketosphinganine. This reaction is catalyzed by serine palmitoyltransferase (SPT), which requires pyridoxal 5'-phosphate (PLP) as cofactor for the decarboxylative, and represents the biosynthesis limiting reaction. In the brain, the external supply of L-serine by astrocytes is crucial for neuronal lipid biosynthesis and brain development (*Hirabayashi and S. Furuya 2008*).
The condensation reaction is followed by the rapid reduction of 3-ketosphinganine (catalyzed by 3-ketosphinganine reductase) to produce sphinganin in presence of NADPH.
The ceramidesyntase then catalyzes the condensation reaction between the oh-group in position 2 of sphinganin and a fatty acid, with the formation of dihydroceramide. The enzymes that lead to the formation of dihydroceramide are located on the cytosolic surface of the ER. The final step in the formation of ceramide is the introduction of a double bond in position 4-5 catalyzed by dihydroceramide desaturase (DES) located in the ER.

The ceramide formed in this way is transported to the Golgi by the ceramide transport protein (CERT) (*Hanada et al. 2003*) or by vesicular transport. In this apparatus ceramide - 1 - phosphate (C1P), sphingomyelin (SM) and glucosylceramide (GluCer) are synthesized.

2.1.2 Degradation of complex sphingolipids

De novo biosynthesis is only a minor pathway for sphingolipid formation in different cell types (*Kolter and Sandhoff 2006*). Ceramide is also generated during the catabolism of all complex sphingolipids. The catabolism of glycosphingolipids takes place in lysosomes and endosomes by glycohydrolases which cleaved the individual monosaccharide units from the non-reducing end of the oligosaccharide chain. The cleavage of the hydrophilic head groups, happens in a sequential manner, from glycosphingolipids finally generates sphingosine, fatty acids, monosaccharides, sialic acids, and sulphate. The final degradation products are able to leave the lysosome (*Kolter and Sandhoff 2005*). The sphingolipids of the plasma membrane reach the lysosomes via the endocytotic pathway. There is also a different pathway of degradation of gangliosides which consists in breaking the β-glucosidic bond between glucose and ceramide with the release of the ceramide and oligosaccharide (*Ito and Yamagata 1986; Ito and Yamagata 1989*). The enzymes involved in this reaction are endoglycoceramidases, each specific for a substrate and probably activated by specific proteins. The proteins required for GM1 degradation is GM1-*β*-galactosidase (*Kolter 2012*), a 64 kDa protein. This protein is part of a lysosomal multienzyme complex, together with the protective protein (carboxypeptidase A), sialidase, and *N*-acetylaminogalactose-6-sulfate sulfatase. GM1-*β*-galactosidase catalyzes the hydrolytic cleavage of several *β*-galactosides. The hydrolysis of ganglioside GM1 to GM2 requires the presence of either the GM2-activator protein, or saposin-B, or, *in vitro*, of an appropriate detergent. Also the plasma membrane-associated sialidase Neu3 can degrade gangliosides.

2.1.3 Recycling of sphingosine

Ceramide synthase is able to use sphinganin and sphingosine with similar efficiency so ceramide can be produced by N-acylation of sphingosine deriving from the catabolism of complex sphingolipids. The amount of sphingosine recycled during the catabolism of GM1 ganglioside contributes significantly to the cellular free sphingosine. The ceramide thus obtained can enter numerous biosynthetic pathways leading to the synthesis of sphingolipids.

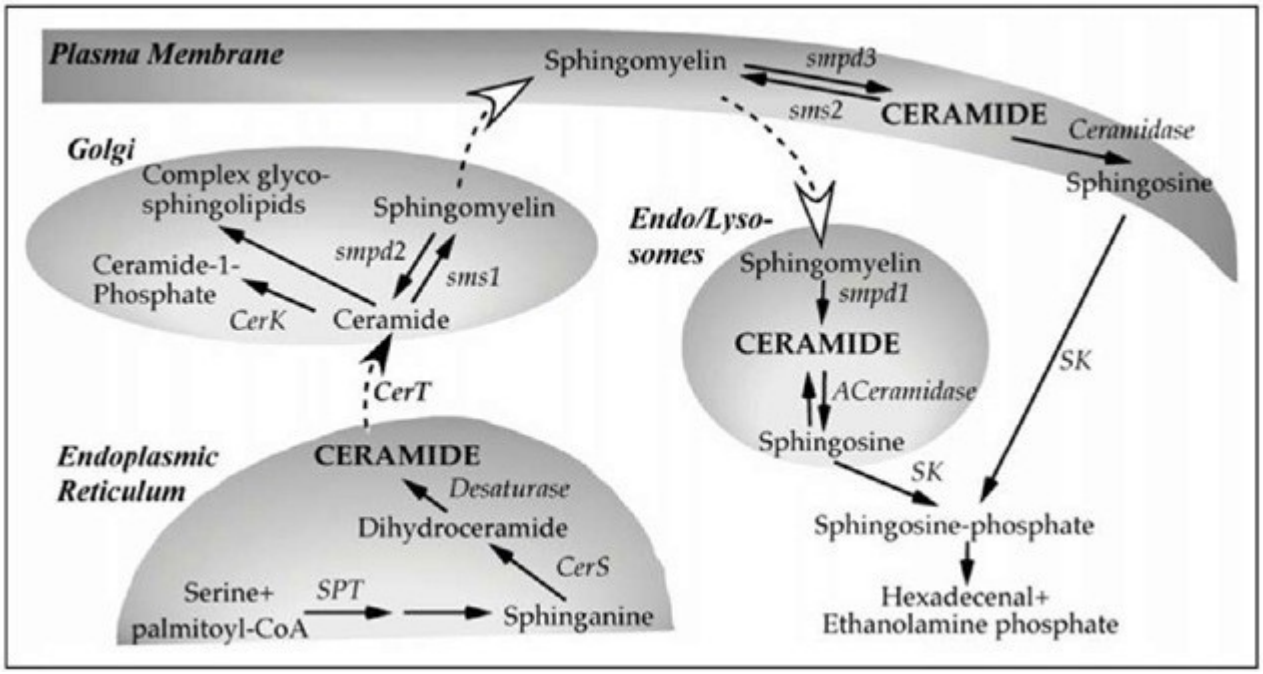

Figure I-5. Metabolic pathways responsible for ceramide synthesis and degradation. SPT: Serine Palmitoyltransferase; Cers: Ceramide synthases; CerT: ceramidetransfer protein. SMS1 & 2: sphingomyelin synthase 1 & 2; smpd1: Acid Sphingomyelinase, smpd2: Neutral sphingomyelinase1, smpd3: Neutral sphingomyelinase 2. CerK1, CeramideKinase1; SK: sphingosine Kinase. ACeramidase: Acid Ceramidase (*Nikolova-Karakashian and Reid 2011*).

2.2. Metabolism of Sialic Acid

The sialylation, the addition of sialic acid units to oligosaccharides and glycoproteins **(Figure I-6)**, is an important modification involved in embryonic development, neurodevelopment, reprogramming, oncogenesis and immune responses (*Li and Ding 2019*). Sialic acids, negatively charged nine carbon monosaccharides located terminally on glycoproteins and glycolipids, are linked to both O- and N-linked glycans either at their galactose (Gal) or N-acetylgalactosamine (GalNAc) units via α-2,3- or α-2,6-bonds, or to other sialic acid moieties via α-2,8- or α-2,9-bonds by specific enzymes (*Angata and Varki 2002*). The most common sialic acid linked to gangliosides in humans is N-acetylneuraminic acid (Neu5Ac). It is synthesized from UDP-N-acetyl-glucosamine (UDP-GlcNAc), which in turn is produced by the hexosamine pathway in the cytosol (Hanover 2001).

UDP-N-acetylglucosamine-2-epimerase/N-acetylmannosamine kinase (UDP-GlcNAc 2-epimerase), whose encoding human gene is *GNE*, convert UDP-GlcNAc in ManNAc and the same enzyme convert ManNAc to N-acyl-D-mannosamine6-phosphate (ManNAc-6P).

ManNAc-6P is converted to N-acylneuraminate 9-phosphate (Neu5Ac-9P) by N-acetyl-neuraminate-9-phosphate synthase (NeuAC-9-P-synthase, encoding gene NANS).

The last reaction is the dephosphorylation of the Neu5Ac-9P in Neu5Ac by N-acylneuraminate-9-phosphatase (NeuAC-9-P-phosphatase, encoding gene NANP) that takes place in the cytosol.

Neu5Ac enters the nucleus and is converted to cytidine 5′-monophosphate N-acetylneuraminicacid (CMP-Neu5Ac) by CMP-NeuNAc synthase (CMAS).

In most non-human species, however, a part of CMP-Neu5Ac is converted to cytidine 5′-monophosphate N-glycolylneu-raminic acid (CMP-Neu5Gc) by CMP-Neu5Ac hydroxylase (*Li and Ding 2019*).

CMP-Neu5Ac is transported into the Golgi apparatus where sialyltransferases (ST) that are cell-and tissue-dependent, generate α-2,3- (ST3GAL1-6), α-2,6- (ST6GAL1-2/ST6GALNAC1-6), or α-2,8-linked (ST8SIA1-6) sialoglycoconjugates (sialoglycoproteins or gangliosides).

The 20 mammalian sialyltransferases are classified into four families (ST3Gal, ST6Gal, ST6GalNAc, or ST8Sia) based on the linkage they generate (α2–3, α2–6, or α2–8) and their primary saccharide acceptor (Gal, GalNAc, or Sia) (*Schnaar et al. 2014*).

Sialoglycoconjugates are hydrolyzed by neuraminidases (NEU1-4), which regenerate sialic acids that can be recovered to synthesize more sialo-glycoconjugate (*Du et al. 2009*).

Four types of mammalian sialidases have been described: NEU1, NEU2, NEU3 and NEU4. They are encoded by different genes and characterized by different subcellular localization. NEU1, the most abundant neuroaminidase in mammals, is primarily intra-lysosomal and is active on glycoproteins but not on gangliosides. NEU2, with cytoplasmic localization, has the ability to remove Sia from different classes of glycans. NEU3 is located on the plasma membrane and is selective for gangliosides. NEU4, mainly expressed on the intracellular membrane remove terminal sialic acid residues from various sialo derivatives, such as glycoproteins, glycolipids, oligosaccharides, and gangliosides (*Glanz 2019*).

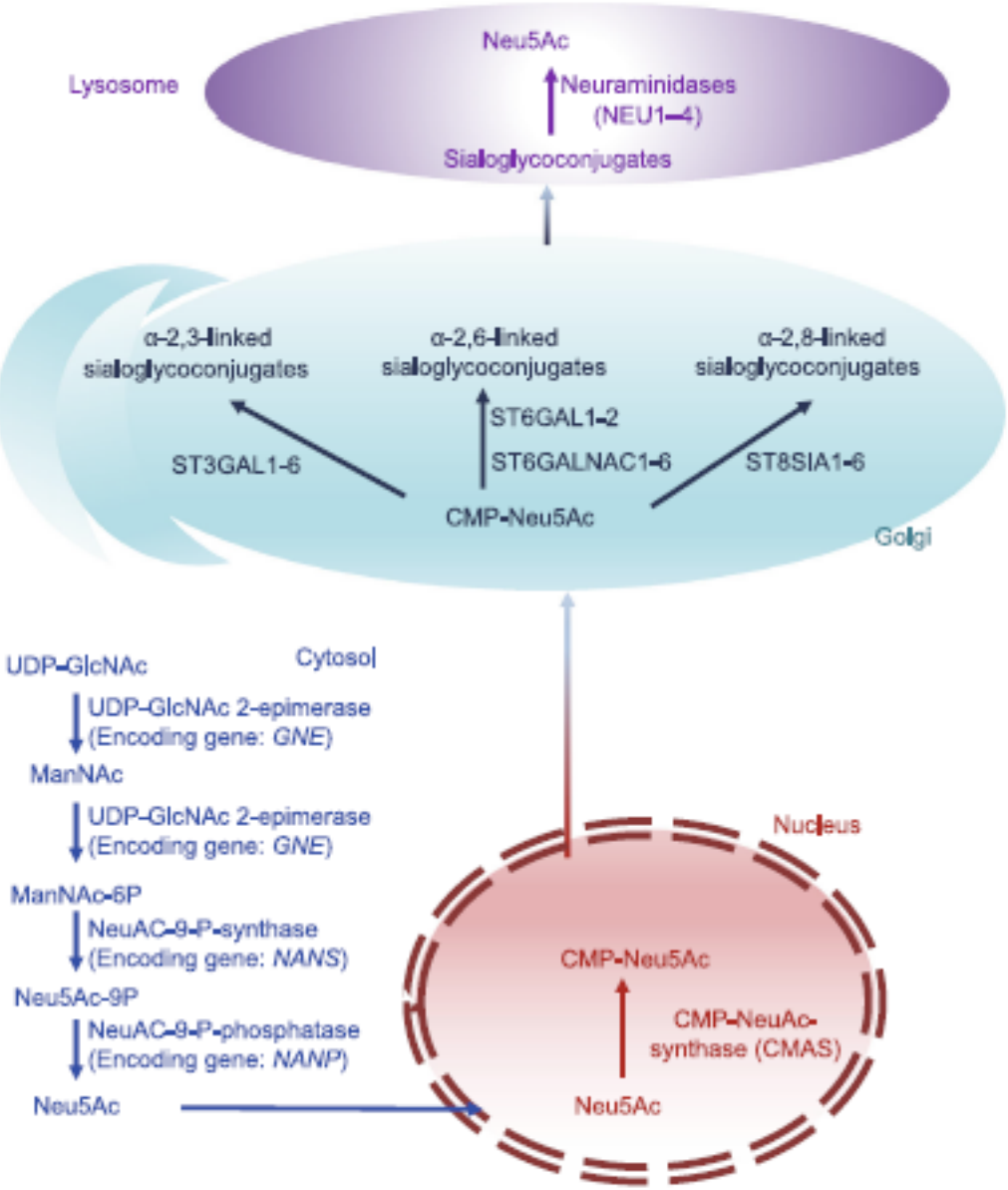

Figure I-6. The biosynthesis pathway of sialylation (*Li and Ding 2019*).

2.3. Biosynthetic pathways of gangliosides

The initial biosynthesis phases of glycosphingolipids including gangliosides occur in the endoplasmic reticulum and continues in the Golgi apparatus by sequential addition of a carbohydrate moieties to an acceptor lipid molecule. Ceramide is the common precursor of glycosphingolipids and sphingomyelin **(Figure I-7).**

A molecule of Glc or Gal is transferred from UDP-glucose (glucose in active form) or UDP-galactose to ceramide to give glucosilceramide (Glc-Cer) or galactosylceramide (Gal-Cer). GlcCer is transported to the trans-Golgi by FAPP2 (phosphateadaptorprotein 2) to start the synthesis of complex GSLs (*D'Angelo et al. 2012*). The reactions are catalyzed respectively by the enzymes glucosyltransferase (Glc T) and galactosyltransferase (Gal T3).

Galactosyltransferase I (Gal T1) catalyzed the addiction of one galactose residue from UDP-galactose to glucosylceramideto Glc-Cer to produce lactosylceramide (LacCer).

With the exception of GM4 (a minor component of human brain gangliosides, where it is localized in myelin), which is derived from GalCer in presence of sialyltransferases ST6 VI (GM4-synthase), gangliosides are synthesized from LacCer (*Yu et al. 2011*).

The biosynthesis of higher gangliosides occurs on the luminal side of the Golgi apparatus, so that their glycan chains are extracytoplasmic.

The addition of the first sialic acid to LacCer leads to its transformation into GM3 by the enzyme sialyltransferase 1 (ST1) also called GM3-synthase (*Yu et al 2004*).

The addition of a sialic acid residues to GM3 generates GD3 (catalyzed by ST2 or GD3-synthase) and the sialic acid addition to GD3 produced GT3 (catalyzed by ST3 or GT3-synthase).

GM3, GD3 and GT3 are the precursors for complex gangliosides of the 0-, a-, b-, and c-series. These different series are characterized by the presence of no (0-series), one (a-series), two (b-series), or three sialic acid residues (c-series) linked to the 3-position of the inner galactose moiety.

In 1988 (*Pohlentz et al 1988*) it was shown that equivalent passages in the parallel synthesis pathways are catalyzed by the same enzymes. The stepwise glycosylation of the precursors of the 0-, a-, b-, and c-series is performed by only a few glycosyltransferases of limited specificity: GalNac T *(N*-acetylgalactosaminyltransferase I or GM2/GD2/GT2-synthase), Gal T2(galactosyltransferase II or GM1-synthase), ST4 (sialyltransferase IV or GD1a-synthase), ST5 (sialyltransferase V or GT1a-synthase).

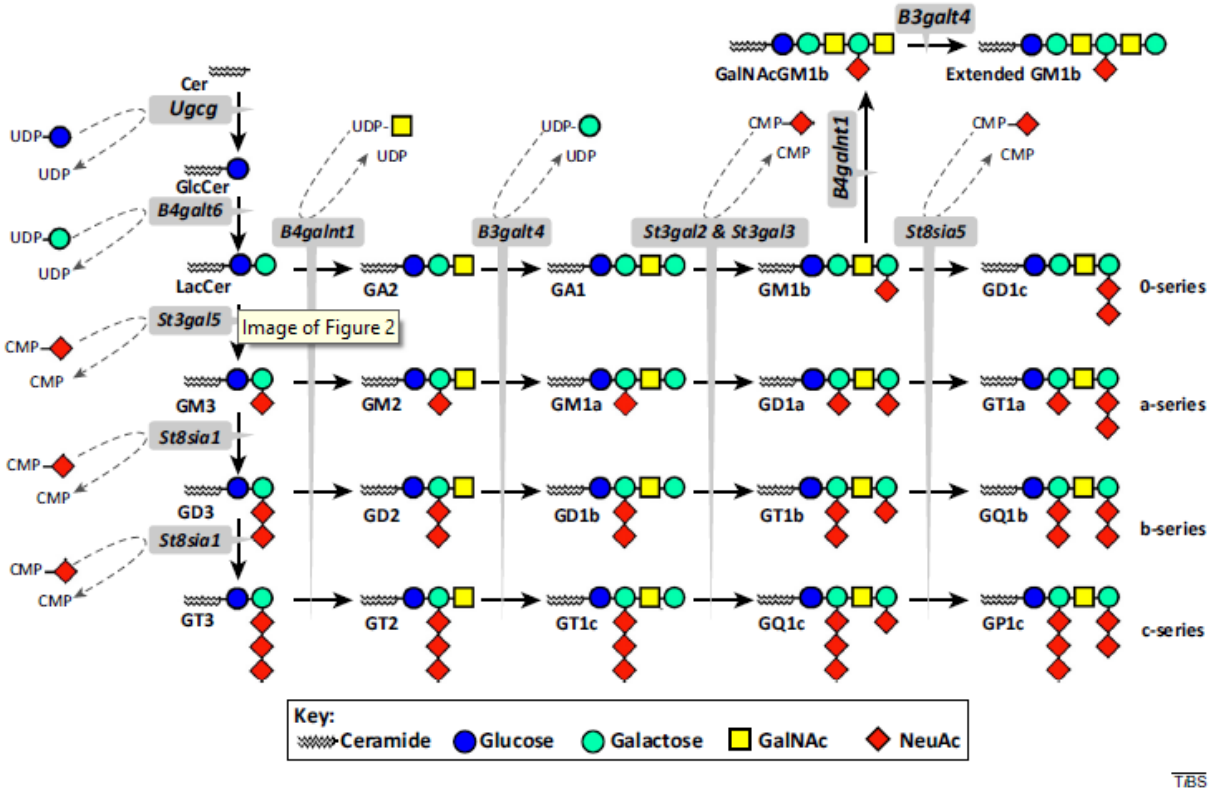

Figure I-7. Biosynthetic pathways of ganglio-series gangliosides. Glycosylation sequences for biosynthesis of the a-, b-, c-, and o-series are shown (*Ledeen and Wu 2015*).

3. Gangliosides in membrane organization and their structural proprieties

Biological membranes are the start point in the eukaryotic cell organization with their primary function of physical barriers. But cell membranes are also a specific compartment in cell functions including communication with the environment, transport of molecules and metabolic functions. The basic molecular organization of biological membranes is represented by a bilayer of amphipathic phospholipids, characterize by a polar moiety (hydrophilic) and an apolar moiety (hydrophobic) where the hydrophobic tails face each other and hydrophilic heads interact with the surrounding environment. The properties of membrane lipids determine structural and functional properties of biological membranes.

In 1972 Singer and Nicolson (*Singer and Nicolson 1972*) called "fluid mosaic" a model to describe structure and functions of cellular membrane. For this model, membranes are made up of lipids, proteins and carbohydrates that gives the membrane a fluid character. The maintenance of structural and physical properties (fluidity, rigidity and fusion temperature) of the plasma membrane is the co-localization of cholesterol and ganglioside in specific areas. The presence of gangliosides in this areas results in an increased rigidity of the plasma membrane. In 1982, was proposed the theory about organization of the lipid components of membranes into "domains" as a consequence of the presence of different phases in the membrane lipid environment. This organization requires the presence of lateral interactions between the different components of the plasma membrane because these components will be able to stabilize different substructures with their own local order. This domain differs in lipid and/or protein composition from the surrounding membrane environment (*Lindner and Naim 2009*). Heterogeneity of membrane lipids, with their different physical and chemical propeties, is the first step for the lateral organization of biological membranes. The difference of transition temperature (melting temperature of the aliphatic chains) imputable to the structure of the acyl chain composition is one of the main forces leading to phase separation in lipids membrane organization (*Sonnino and Prinetti 2013*). For example the transition temperature of the GM1 containing stearic acid (C18) and a sphingosine C18 is 11.7 °C, however sphingosine C20 determines a variation of the transition temperature to 23.2 °C (*Mauri et al. 2018*).

Biological membranes are not homogeneous and its components are not randomly distributed. Cell membrane components are organized in small domains (10-200 nm), named lipid raft **(Figure I-8).** Lipid rafts are signalling subdomains of the plasma membrane involved in the neurons development, neuronal survival, axon growth and interactions between neurons and glial cells (*Sonnino et al. 2015*). Nervous system diseases, like several neurodegenerative diseases, can be associate with unusual lipid raft functions. Most neurodegenerative disease is represented by a structural and functional alteration in a cellular protein. Examples of altered protein involved in neurodegenerative disease are amyloid β peptide (Aβ) in Alzheimer's Disease (AD), α-Synuclein in Parkinson's Disease (PD) and scrapie isoform of the prion protein(PrP^{Sc}) in transmissible encephalopaties.

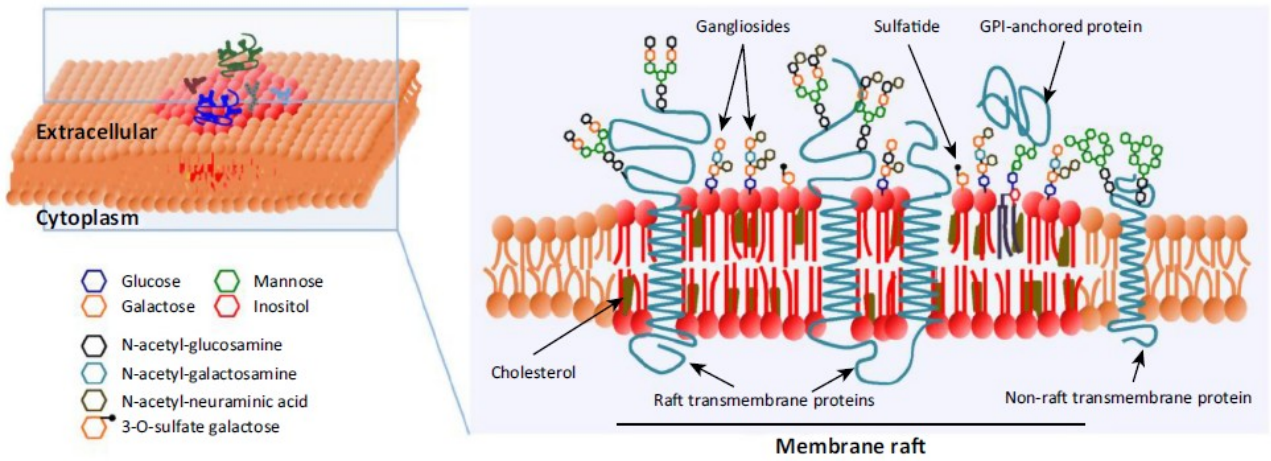

Figure I-8. Structure and composition of a membrane raft. 3D scheme of a portion of plasma membrane containing a lipid raft, indicated in red (left panel). The plane indicated in left panel is shown as a 2D scheme (right panel) indicating the different components of the raft (*Abad-Rodrıguez and Dìez-Revuelta 2015*).

There are two types of lipid rafts: caveolae **(Figure I-9)** and planar rafts. The caveolae are characterized biochemically by the presence of the structural protein caveolin with the functions of the transport of cholesterol, vesicular transport and signal transduction. Caveolae are very enriched in cholesterol. Different sphingolipids have been shown to partition differentially between caveolae and non-caveolar membrane areas (*Sonnino and Prinetti 2009*). Planar rafts are, on the other hand, are small and morphologically indistinguishable platforms of the cell membrane. Lipid raft are enriched in gangliosides, sphingomyelin, sterols (cholesterol in neurons) with ceramide and various proteins involved in signal transduction mechanisms (*Kolesnick et al. 2000*). The presence of GM1 in lipid rafts was demonstrated using its ability to bind subunit B of cholera toxin (*Holmgren et al. 1973*). For their composition those lipid rafts are called SEMD (Sphingolipid - Enriched Membrane Domains). SEMDs have a high transition temperature due to the presence of hydrogen bonds and present high resistance to solubilisation with non-ionic detergents and with other substances that break up the membrane structure. For this reason, SEMDs are described as "Detergent Resistant Membranes" (DRM).

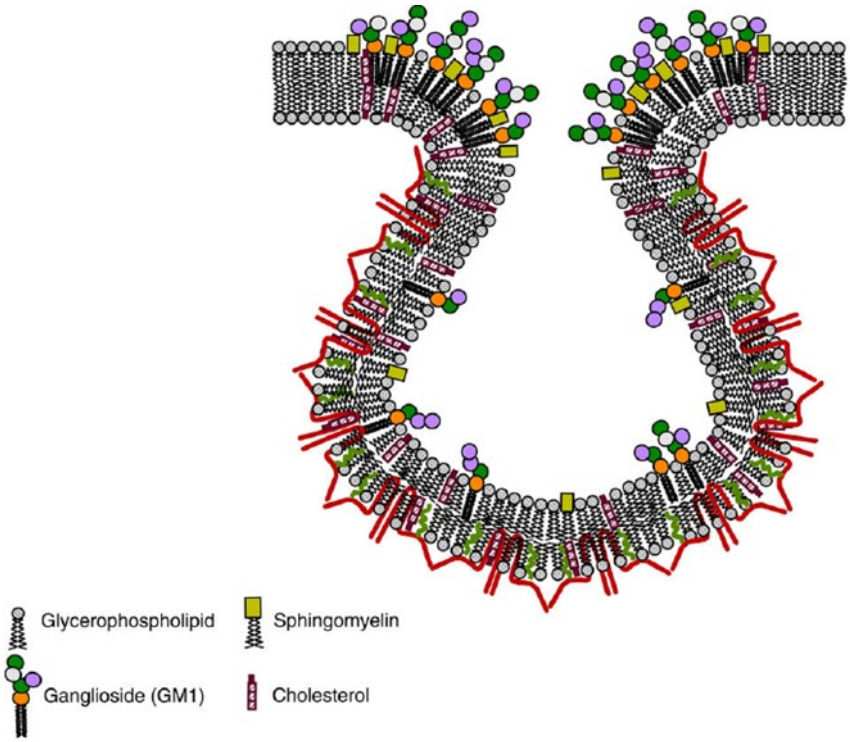

Figure I-9. Structure of caveola (*Sonnino and Prinetti 2009*).

Gangliosides are implicated in a lot of cell surface phenomena. For example they play important function in animal cells as antigens, and receptors for microbial toxins as well as mediators of cell adhesion and modulators of signal transduction. (*Todeschini and Hakomori 2008*). The role of gangliosides in these processes derives from the peculiar features dependent to the chemical and physicochemical properties which control their interactions with the other lipid and protein components of the membrane (*Corti et al. 1980*). Gangliosides molecular complexity is very pronounced. The double tailed hydrophobic moiety of gangliosides, ceramide, is heterogeneous in terms of chain length and presence of instaurations. Ceramide influence the interaction with other complex lipids and proteins. It represents a structural and functional modulator of plasma membrane. Also oligosaccharide portions give to gangliosides structural properties finely connect to biological functions. Oligosaccharide chain represent the interactive point of gangliosides with other molecules in extracellular environment. It is extremely variable in sugar structure, number, and is characterized by the presence of one or more negative charges in the sialic acid residues. The volume of the oligosaccharide head groups is more variable and determines level of phase separation and geometry in a specific membrane microenvironment. With the increase of the volume of the head group **(Figure I-10)** is required a progressively large interfacial area for the ganglioside interaction in the bilayer (*Mauri et al. 2018*). Big interfacial area leads to a more marked segregation of ganglioside in the phospholipid bilayer, and the consequence is a more positive curvature of the resulting ganglioside-rich membrane microenvironment.

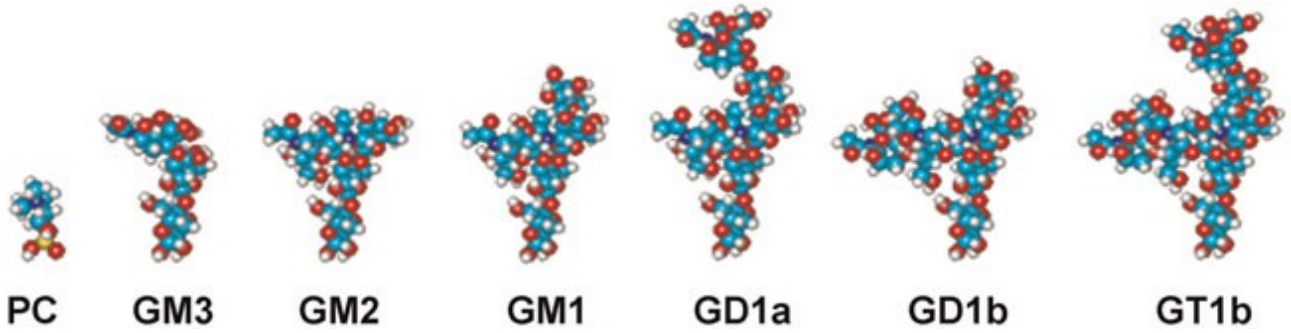

Figure I-10. Schematic representation of the progressive increase in the volume of the oligosaccharide chain of gangliosides (*Sonnino et al. 2007*).

The three most important characteristic of the oligosaccharide head groups are: geometry and dynamics of the different glycosidic linkages; the presence of the negative charge(s) of the sialic acid residue(s); and the amount of hydration water associated with the oligosaccharide chains (*Sonnino et al. 2018*).
Oligosaccharide chains of gangliosides (glycolipids), glycoproteins and proteoglycans are the components of the glycocalyx, a surface coat of glycans which constitutes the cell's interface with outside environment. Cell surface glycans mediate cell-cell recognition, cell differentiation and regulate cell to cell interactions. Many glycoproteins and glycolipids of vertebrates in glycocalyx are terminated with sialic acids. The functions of sialic acids depend on sialoglycan structures at several levels, from the modifications on each sialic acid carbon to their context within oligosaccharides, larger glycans, and multiglycan complexes (*Schnaar et al. 2014*). Sialic acids are also receptors for pathogens and toxins. Mutations in sialic acid metabolism lead to different human diseases.

Geometrical structure and aggregation properties of ganglioside is determinate by the number of sialic acid and by sugars composition. Gangliosides in aqueous solution form small ellipsoidal micelles. Micelles **(Figure I-11)** are formed by a hydrophobic ceramide core and the hydrophilic domain in contact with surrounding environment. Micelles are in equilibrium with monomers and present a critical micellar concentration (c.m.c.) in the range of 10^{-5} M–10^{-9} M (*Sonnino et al. 1994; Chiricozzi et al. 2020*). Brain GM1 has a c.m.c. between 10^{-8} M–10^{-9} M. This value is influenced by the length of the acyl chain. From 18 to 2 carbons c.m.c. had an increase of three orders and this is a demonstration of the importance of ceramide in chemical and physicochemical properties of gangliosides.

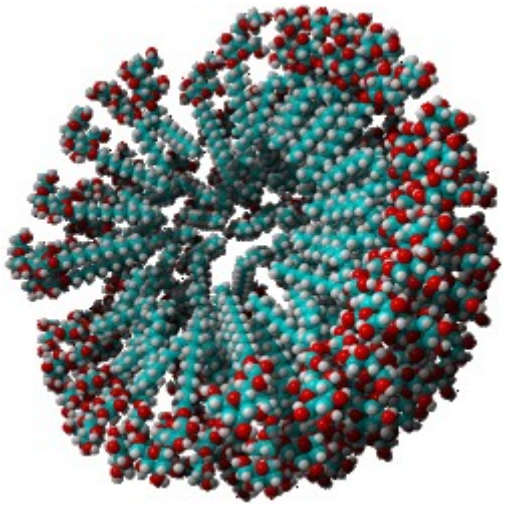

Figure I-11. Section of a ganglioside micelle.

Aggregative properties of gangliosides are important when they are administered to cells. In water gangliosides are present in different physical forms: monomers and micelle. In particular, under c.m.c. gangliosides are in monomers form and over this concentration they are present like monomer and micelle together in equilibrium. Only the monomeric GM1 becomes part of the plasma membrane when administered to cells, while the micelles reach lysosomes after the binding with proteins (*Saqr et al. 1993*). It is possible to follow how gangliosides associate to the plasma membranes and what happen when they are uptaken by the cells. For follow this is possible to add to the cell medium of cultured cells gangliosides with probe like a radionuclide, a paramagnetic, a fluorescent or a photoactivable group (*Schwarzmann 2018*). Three possible forms of GM1 association are known: “serum-removable”, “trypsin-removable” and “trypsin-stable” (*Chiricozzi et al. 2020*). The association form depends by the experimental conditions like the presence of proteins in the cell culture medium, time of incubation and ganglioside concentration. This because the presence of proteins reduce the number of free micelles. Long-time of incubation permit to have a lot of monomers for the trypsin-stable form and a lower concentration of ganglioside leads to a higher percentage of monomers in solution.

4. GM1, neurotrophins and neuroprotection

Gangliosides organization in the PM is specific for the cell type and their presence is regulated during the cell development. GM1 ganglioside is one of the principal modulator in the nervous system where is involve in maturations of neurons, differentiation, increases responses to neurotrophic factors, protects against neuronal death and reduces brain damage acting on neurotrophic factors. Aging and/or epigenetic influences can reduce the level of GM1 with a damage in the neuronal functions. A lot of studies have attributed neuroprotective and neurorestorative properties to GM1 in animal models and in clinical trials (*Ledeen et al. 2015*).

Neurotrophins (NT) are regulators for neural survival, development, function and differentiation both in central than in peripheral neurons. GM1 modulating the interaction between neurotrophins and their receptors, including the GDNF (glia cell-derived neurotrophic factor) receptor complex and neurotrophin tyrosine kinase family receptors (Trk). The neurotrophin family includes nerve growth factor (NGF), brain-derived neurotrophic factor (BDNF), transforming growth factor (TGF)-β. Neurotrophins binding to Trk induces receptor dimerization and autophosphorylation and from this interaction take place a complex cascade of signal events **(Figure I-12)**.

NGF causes Trk receptor homodimerization, and leads to transphosphorylation on at least five tyrosine residues. Activation of TrkA induces the phosphorylation and activation of SHC, PI3K, and PLCγ1. Ras/MAPK and AKT are activated downstream of these pathways. Tyrosine phosphorylated SHC associates with the adapter protein GRB2, which in turn binds the SOS-Ras guanine nucleotide exchange factors. SOS enhances the rate of GDP-GTP exchange on Ras, leading to Ras activation. Ras sequentially activates a series of kinases, including RAF1, MEK (MAPK kinase), ERK (MAPK), and RSK. MAPK and RSK translocate to the nucleus to participate in the activation of transcription factors that regulate NGF-inducible genes, resulting in survival and neuronal differentiation (*Brodeur et al. 2009*). Trk expression is impostant for the normal development of the peripheral nervous system. The expression of TrkA is important for the development of normal sympathetic neurons and NGF is necessary for the survival and differentiation of these neurons *in vitro* and *in vivo*.

Exogenous GM1 is able to stimulate Trk receptor kinase activity. GM1 was shown to be necessary for the membrane insertion and function of tropomyosin-related kinase A (TrkA), the protein tyrosine kinase receptor for NGF that is situated in lipid rafts. Overexpressed GM1 also caused disruption of microdomain integrity, resulting in suppression of NGF signaling and suggesting the need for tight regulation of GM1 content in lipid rafts. Sialidases Neu3 is an enzyme that plays a crucial role in modifying the cell surface ganglioside composition, producing GM1 from polysialo gangliosides. Neu3 increase the surface concentration of GM1 in neurons, thus affecting the biological activity of the TrkA neurotrophin receptor (*Sonnino et al. 2018*). GM1 also associates with TrkB, the tyrosine kinase receptor for brain-derived neurotrophic factor (BDNF), the activity of this receptor is modulated by the amount of GM1 in the membrane environment (*Pitto et al. 1998*). Something similar happen in the receptor of glial cell line-derived neurotrophic factor (GDNF) (*Hadaczek et al. 2015*), a member of the transforming growth factor (TGF)-β

superfamily, which functions to preserve the viability of catecholaminergic neurons. GM1 was shown to associate with the GDNF receptor complex comprising Ret, the tyrosine kinase component, and GFRα, a GPI-anchored co-receptor; Ret asso-ciation with GFRa was severely damaged in neurons of the *B4galnt1* $^{-/-}$ mouse (mouse deficient in ganglio-series gangliosides) and partially damaged in the *B4galnt1*$^{+/-}$ heterozygote (model of sporadic Parkinson's disease).

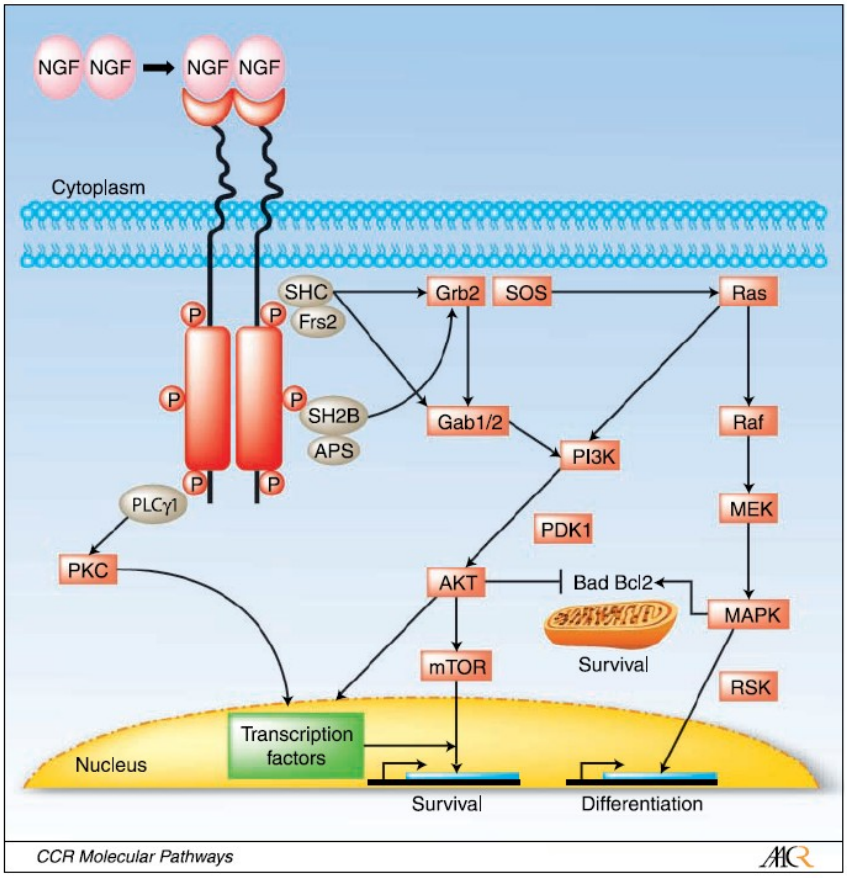

Figure I-12. Trk signaling pathways. In brown: adaptor proteins that interact directly with TrkA. In red: downstream signaling proteins (*Brodeur et al. 2009*).

5. Gangliosides in the nervous system: differentiation and aging

Neurons are the main site of gangliosides (*Svennerholm et al. 1994*). Gangliosides in nervous system are involved in different process like ion transport mechanisms, receptor modulation (neurotrophic factor receptors), stem cell biology and neurodegenerative disorders. The gangliosides content change during neuron differentiation, aging and neurodegenerative diseases.

Neural stem cells (NSCs) are the starting point from which the central nervous system is generated. These are undifferentiated neural cells characterized by the capacity for self-renewal and multipotency (*Itokazu et al. 2018*). Gangliosides are implicated in brain development and NSC maintenance. At the beginning of rodent brains formation, in undifferentiated neurons during neuronal tube formation and NSC proliferation, the ganglioside content is characterized by the presence of a large quantity of simple gangliosides with small hydrophilic head, like GD3 and GM3 **(Figure I-13)**. In subsequent development, during the axons and synapses formation, complex gangliosides prevail, like GM1, GD1a, GD1b, and GT1b.

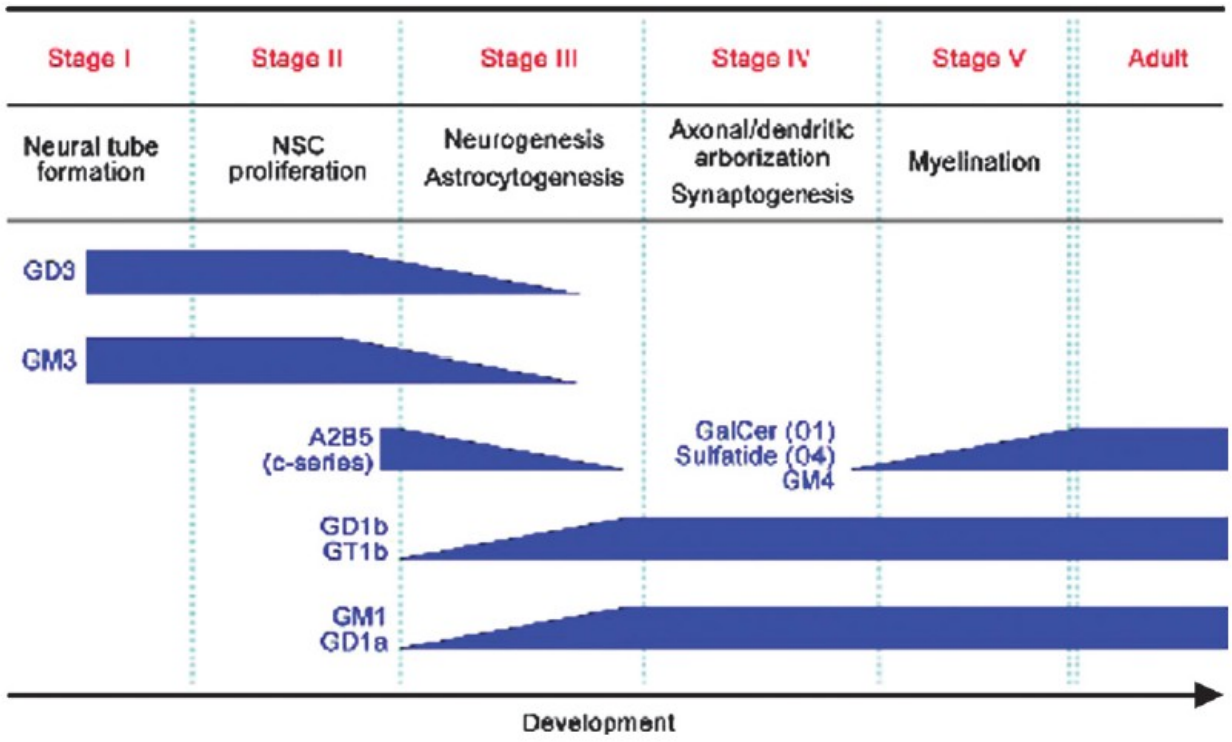

Figure I-13. Neurodevelopmental and changes in GSL expression (*Yu et al. 2009*).

Variations in the expression of gangliosides indicate the biological needs of GalNAc-containing gangliosides, at particular moment, in brain development (Itokazu et al. 2018). The modification of brain ganglioside content reflects the differences in expression or in activities of specific glycosyltransferases (*Sonnino et al. 2010*).

Exogenous GM1 induce neurite outgrowth in N2a cell (*Ledeen 1984; Faccci et al. 1984*) and in primary neuronal cultures (*Skaper et al. 1985*). Increase of GM1 using sialidase (*Wu and Ledeen 1991*), induce neurite outgrowth associated with increased Ca^{2+} influx (*Wu and Ledeen 1994*). Sialidase increases GM1and stimulate axonogenesis through removal of GD1a and GT1b, which inhibit axon outgrowth via trans-interaction with myelin-associated glycoprotein (MAG) (*Yang et al. 2006; Mountney et al 2010*). Increase of endogenous membrane GM1 by Neu3 is essential for axonal specification during early neuronal differentiation (*Da Silva et al. 2005*) as well as for peripheral nerve regeneration (*Kappagantula et al. 2014*). Neu3-induced GM1 elevation triggered the signaling pathway controlling axon growth, which included extracellular-signal-regulated kinase (ERK) activation (*Chierzi et al 2005; Waetzig and Herdegen 2005*).

Ganglioside changes in central nervous system with aging. There are changes in ganglioside profiles during development till senescence in mice and rats (*McGonigal et al. 2016*). In human brain gangliosides, there have been reports on the alteration of ganglioside profiles with aging. Generally, ganglioside contents gradually decreased (*Segler-Stahl et al. 1983*), and a-series gangliosides tended to decrease mainly in frontal cortex. In turn, b-series gangliosides reduced with aging in cerebellum (*Svennerholm et al. 1991*).

The content of membrane lipids diminished continuously up to 90 years of age, when a marked diminution in level of gangliosides and cerebrosides occurred (*Kracun et al. 1992*). In a study of 118 subjects, age 20–100 years, gangliosides showed an almost constant concentration between 20 and 70 years of age (*Svennerholm et al. 1994*). The brain sialic acid ganglioside amount progressively decreases, being reduced of about 30% in centenary in comparison with 20-year-old people. The ganglioside pattern undergoes changes during aging with an increased proportion of b-series gangliosides, particularly GD1b, and a reduced content of a-series gangliosides, including GM1 and GD1a; this latter can be considered as a reservoir for the production of GM1 at the plasma membrane. Thus, GM1 and GD1a are the two gangliosides mainly responsible for the decrease of sialic acid ganglioside content along the aging of humans. Alterations of ganglioside pattern can be found in different neurodegenerative diseases, including Parkinson, Alzheimer and Huntington diseases.

6. Ganglioside GM1 in neurodegenerative diseases

Gangliosides have extensively been tested in different clinical applications. Until the early 1990s, a ganglioside extract, or the pure GM1, produced from calf brains was marketed in Europe as treatment for acute or chronic PNS diseases. The drugs were withdrawn from the European market after reports of Guillain-Barré-Syndrome (GBS), a rare misdirected immune response to gangliosides causing peripheral nerve damage, often following infections. Changes in the ganglioside profile were reported in degenerative CNS conditions, including Alzheimer's (AD) (*Blennow et al. 1992*), Parkinson's disease (PD) (*Wu et al.*

2012), Huntington's disease (HD) (*Maglione et al 2010*), multiple sclerosis (MS) (*Zaprianova et al. 2001*), and amyotrophic lateral sclerosis (ALS) (*Dodge et al. 2015*). GM1 deficiencies in particular have been detected in PD and HD, whereas GM1 expression and distribution were shown to be affected in CNS injury caused by trauma or disease (*Rubovitch et al. 2017*). GM1 is one of the predominant brain gangliosides, with demonstrated antineurotoxic, neuroprotective, and neurotrophic actions *in vitro* and *in vivo*. The medical need for new treatments of neurodegenerative conditions continues to increase and remains largely unmet. In parallel, preclinical evidence of potentially beneficial GM1 effects in such indications has evolved.

*7. **The oligosaccharidic chain of GM1***

GM1 ganglioside performs many functions, both in the plasma membrane and intracellular loci (*Ledeen and Wu 2015*). The effects of GM1 are known *in vitro* and *in vivo*, but the molecular mechanism of action underlying the GM1 properties like neurodifferentiation, neuroprotection and its involvement in neurodegeneration, remain difficult to elucidate. GM1 is one of the most studied gangliosides not only in its complete structure but also for the features of the oligosaccharide chain.

Shengrund and Prouty, in 1988 (*Schengrund and Prouty 1988*), described for the first time the ability of OligoGM1 to increase neuritogenesis in S20Y murine neuroblastoma cells. They observed that the increase of neuritogenesis in presence of OligoGM1 was the same looked in presence of the intact GM1. Shengrund and Prouty concluded that was the oligosaccharide portion of GM1 that was responsible for the ability of GM1 to increase of neuritogenesis in S20Y neuroblastoma cells.

Important studies were performed using GM1 derivatives characterized by the same oligosaccharide chain structure, with the substitution of the fatty acid of ceramide by a different group, such as acetylene in LIGA4 **(Figure I-14)** (Manev et al. 1990) or dichloroacetylene in LIGA20 **(Figure I-15)**.

Manev and coworkers, demostred that the delayed neuronal death induced by glutamate on primary cultures of cerebellar granule cells can be prevented by pretreating the cultures with GM1, LIGA4 and LIGA20 (protection of LIGA20 was greater than or equal to LIGA4 greater than GM1).

In 2002, Rabin and coworkers (*Rabin et al. 2002*) used NIH-3T3 fibroblasts expressing the different Trk receptors to analyse if GM1 ganglioside and LIGA20 activate neurotrophin receptors. In this study they observed that both GM1 and LIGA20, activated TrkB tyrosine phosphorylation.

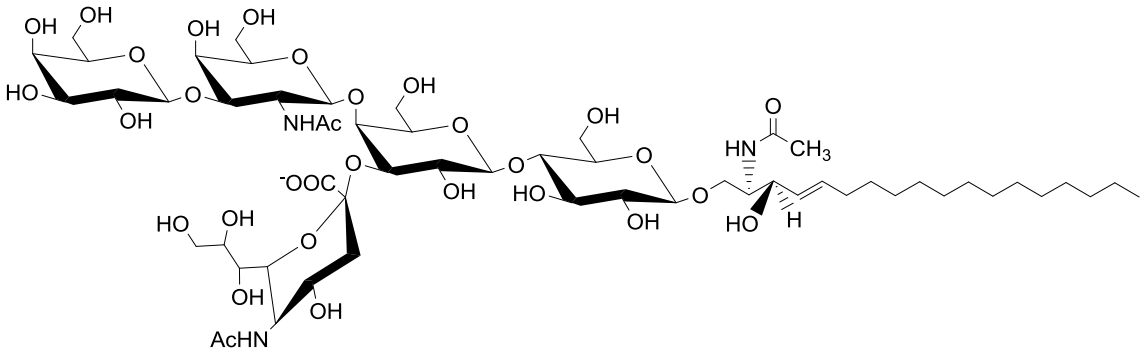

Figure I-14. Structure of LIGA4: GM1 derivatives containing N-acetyl-sphingosine.

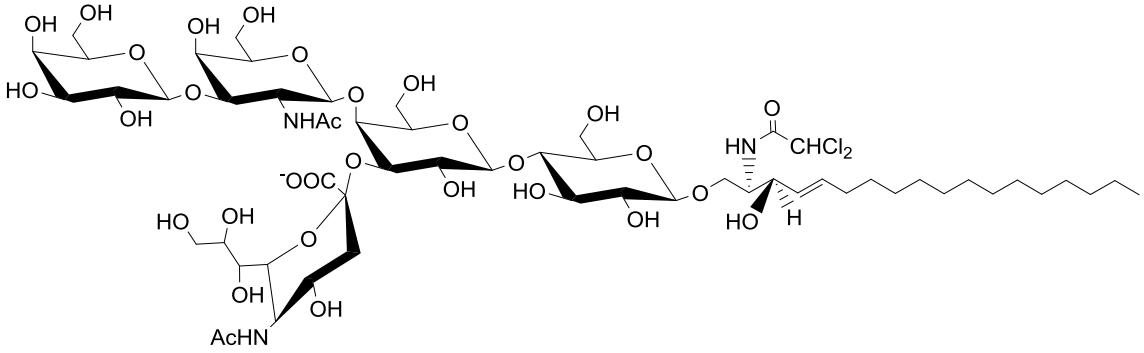

Figure I-15. Structure of LIGA20: GM1 derivatives containing N-dichloroacetyl-sphingosine.

GM1 derivatives (LIGA4 and LIGA20) differ from GM1 in the capacity to penetrate the blood–brain barrier (BBB) and neuronal plasma membrane. LIGA20 incremented membrane permeability (*Ledeen and Wu 2015*) but it was more toxic, in the long-term, if compared with GM1. Genetically engineered mice *B4galnt1*$^{(-/-)}$, animal models of Parkinson's disease, treated with LIGA20, present beneficial effects, including the reduction of substantia nigra alpha-synuclein aggregates (*Wu et al. 2012*).

All this study suggested that the ceramide structure is not involved in GM1 modulatory effcts.

Aim

GM1 is one of the major gangliosides into the nervous system, with demonstrated antineurotoxic, neuroprotective, and neurotrophic properties *in vitro* and *in vivo*. The gangliosides content change during neuron differentiation, aging and neurodegenerative diseases. In later neuronal developmental, during the axons and synapses formation, prevail complex gangliosides like GM1, GD1a, GD1b, and GT1b. It is known that the increase in the content of GM1 favours neuronal differentiation. If the functions of GM1 are known, its mechanism of action is not clear. GM1 is one of the most studied gangliosides not only in its complete structure but also for the features of the oligosaccharide chain.

The ability of OligoGM1 to increase neuritogenesis in S20Y murine neuroblastoma cells was described for the first time by Shengrund and Prouty in 1988 (*Schengrund and Prouty 1988*). Important studies were performed also using GM1 derivatives characterized by the same oligosaccharide chain structure, with the substitution of the fatty acid of ceramide by a different group, such as the acetyl in LIGA4 or the dichloroacety in LIGA20. These GM1 derivatives differ from GM1 in the capacity to penetrate the blood–brain barrier (BBB) and neuronal plasma membrane. LIGA20 incremented membrane permeability (*Ledeen and Wu 2015*) but it is more toxic, in the long-term, if compared with GM1. Genetically engineered mice *B4galnt1*$^{(-/-)}$, animal models of Parkinson's disease, treated with LIGA20, present beneficial effects, including the reduction of substantia nigra alpha-synuclein aggregates (*Wu et al. 2012*).

All this study suggested that the ceramide structure is not involved in GM1 modulatory effects. Past studies demonstrated the activation of the TrkA-Erk1/2 pathways by ganglioside GM1.

The aim of this study is to explain the molecular mechanism of GM1 in particular to explain the role of its oligosaccharide chain using different experimental approaches *in vitro* (murine neuroblastoma call, N2a). The use of this cells *in vitro* allow to study neuronal development and maturation. To study the TrkA–GM1 interaction, we synthesized two radioactive and photoactivable GM1 derivatives and a radioactive and photoactivable OligoGM1. The first GM1 derivative was tritium labeled in position C-6 of external galactose and had a photoactivable nitrophenylazide group at the end of lipid moiety. The second one GM1 tritium labeled at position C-3 of the sphingosine and had a photoactivable nitrophenylazide group at position 6 of external galactose.

Materials and Methods

Materials

Commercial chemicals were of the highest purity available, common solvents were distilled before use and water was doubly distilled in a glass apparatus.

Mouse neuroblastoma Neuro2a (N2a) cells (RRID: CVCL_0470), phosphate-buffered saline (PBS), perchloric acid, potassium hydroxide, sodium acetate, sodium octyl sulphate, paraformaldehyde (PFA), Triton X-100, chloroform, acetone, methanol, ethanol, 12-aminododecanoic acid, sodium dodecyl sulfate (SDS), 1-propanol, 2-propanol, 2,3-dichloro-5,6-dicyanobenzoquinone (DDQ), sodium hydroxide, sodium cyanoborohydride, ammonium acetate, ethyl acetate, ammonium hydrogen carbonate, tetrahydrofuran, formic acid, 3-(4,5,-dimethylthiazole-2yl)-2,5-diphenyltetrazolium bromide (MTT), phosphate buffer solution, Trypan blue, galactose, galactose oxidase, sialic acid, anti-rabbit FITC conjugate, dimethylsulfoxide (DMSO), sodium borohydride, HPR-conjugated cholera toxin subunit B (CT-B), fetal calf serum, o-phenylenediamine tablets, hydrogen peroxide solution (H_2O_2), vibrio cholerae sialidase, bovine serum albumin (BSA), Dako fluorescent mounting medium, ammonia 33%, dimethylformamide (DMF), triethylamine, tributylamine, ethylenediaminetetraacetic acid (EDTA), 4-fluoro-3-nitrophenylazide, retinoic acid (RA), sodium orthovanadate (Na_3VO_4), buffered saline solution (BSS), sucrose, calcium chloride, calcium magnesium free (CMF)-PBS, glucose, RNAase-free water, aprotinin, , mouse α-tubulin antibodies, and trypsin were from Sigma-Aldrich (St. Louis, MO, USA).

Cell culture plates and Transfectagro™ reduced serum medium were from Corning (Corning, NY, USA).

Dulbecco's modified Eagle's high glucose medium (DMEM), fetal bovine serum (FBS), L-glutamine (L-Glut), penicillin (10.000 U/mL), streptomycin and 30% acrylamide were from EuroClone (Paignton, UK).

Gibco™ OptiMEM™ I reduced serum medium, Lipofectamine® 2000, mouse anti-calnexin (RRID: AB_397884), Hoechst-33342 fluorescent stain, Oligo(dT)20 Primer and goat anti-mouse IgG (H+L) antibody (RRID: AB_228307) were from Thermo Fischer Scientific (Waltham, MA, USA).

TrkA inhibitor (CAS 388626-12-8) was from Merk Millipore (Billerica, MA, USA).

The short interfering RNAs (siRNAs) were from Quiagen (Velno, Netherlands).

Rabbit anti-TrkA (RRID: AB_10695253), rabbit antiphospho- TrkA (tyrosine 490, Tyr490) (RRID: AB_10235585), rabbit anti-p44/42 MAPK (Erk1/2) (RRID: AB_390779), rabbit antiphospho-p44/42 MAPK (pErk1/2) (Thr202/Tyr204) (RRID:B_2315112), and anti-rabbit IgG (RRID: AB_2099233) antibodies were from Cell Signaling Technology (Danvers, MA, USA).

Rabbit anti-pan Neurofilament (NF) antibody (RRID: AB_10539699) was from Biomol International (Plymouth Meeting, PA, USA).

Chemiluminescent kit for western blot was from Cyanagen (Bologna, Italy).

Ultima gold was from Perkin Elmer (Waltham, MA, USA).

4–20% Mini-PROTEAN® TGX™ Precast Protein Gels, Criterion TGX™ Precast Gels, Turbo Polyvinylidene difluoride (PVDF) Mini-Midi membrane and DC™ protein assay kit was from BioRad (Hercules, CA, USA).

Polyvinylidene difluoride (PVDF) membrane was from GE Healthcare Life Sciences (Chicago, IL, USA).

Rabbit anti-flotillin (RRID: AB_941621) was from Abcam (Cambridge, UK).

High-performance thin-layer chromatography (HPTLC), silica gel 60, silica gel 100 and silica gel C-18 reversed phase (RP18) was from Merk Millipore (Frankfurten, Germany).

2. Methods

2.1 Preparation of gangliosides

2.1.1 GM1 ganglioside

GM1 ganglioside **(Figure M-1)** was purified from the total ganglioside mixture extracted from pig brains *(Tettamanti et al. 1973)*. Total brain lipids were extracted with solvent and gangliosides were separated by partitioning. The ganglioside mixture, 5 g as sialic acid, was dissolved in prewarmed (36 °C) 500 mL of 0.05 M sodium acetate, 1 mM $CaCl_2$ buffer, pH 5.5. Vibrio cholerae sialidase (1 unit) was added to the solution every 12 h *(Acquotti et al. 1994)*. Sialidase was used to increase the quantity of GM1 because it do non hydrolyze the α2-3 linkage between sialic acid and the internal galactose of the oligosaccharide chain. This is due to steric hindrance exerted by N-acetylgalactosamine *(Chiricozzi et al. 2020)*. After two-day incubation under magnetic stirring at 36 °C the solution was dialyzed at 23 °C for 4 days against 10 l of water changed 5 times a day. The sialidase treated ganglioside mixture was subjected to 150 cm × 2 cm silica gel 100 column chromatography eluted with chloroform/methanol/water 60:35:5 (v/v/v). The chromatography purification is necessary because sialidase treatment of the ganglioside mixture increase GM1 but a few quantities of GM2 and GalNAc-GD1a is always present. The fractions containing GM1, identified by HPTLC, were pooled and dried. The residue was dissolved in chloroform/methanol 2:1 (v/v) and precipitated with 4 volumes of cold acetone. After centrifugation (15.000 × g) the GM1 pellet was separated from the acetone, dried, dissolved in 50 mL of deionized water and lyophilized. The white powder was stored at -20 °C.

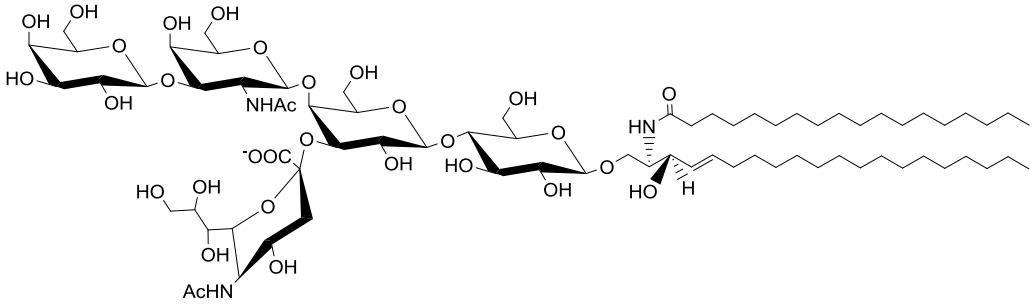

Figure M-1. Structure of GM1 (II3Neu5AcGg$_4$Cer).

2.1.2 Fucosyl-GM1 and GM2

Fucosyl-GM1 *(Ghidoni et al. 1976)* and GM2 **(Figure M-2)** gangliosides were purified, with the same procedure used for GM1, from the total ganglioside mixture extracted from pig brains *(Tettamanti et al. 1973),* submitted to sialidase hydrolysis *(Acquotti et al. 1994).*

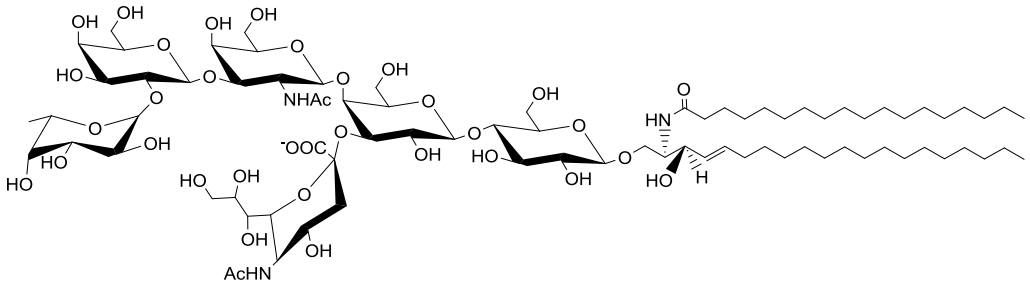

(A)

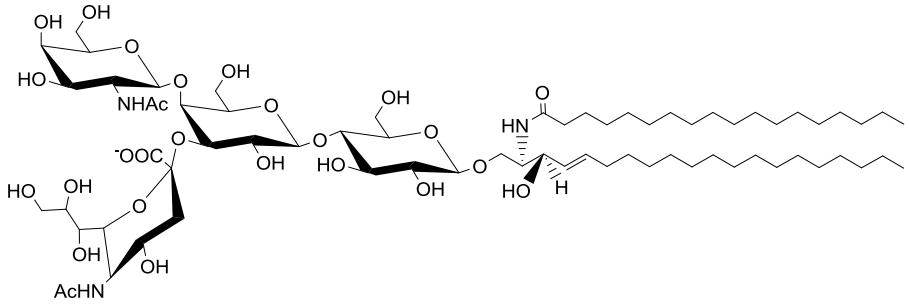

(B)

Figure M-2. Structure of: **(A)** Fucosyl-GM1 ($IV^2\alpha FucII^3Neu5AcGg_4Cer$) **(B)** GM2 ($II^3Neu5AcGg_3Cer$).

2.1.3 Desialylated GM1

Desialylated GM1 (asialo-GM1) **(Figure M-3)** was prepared by acid hydrolysis of GM1 and chromatographic purification *(Ghidoni et al. 1976).*

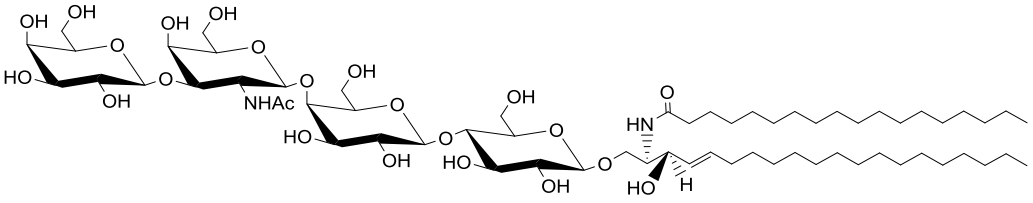

Figure M-3. Structure of desialylated GM1 (Gg_4Cer).

2.1.4 GM1 tritium labeled at position C-6 of the external galactose

GM1 containing tritium at position 6 of external galactose ([6-^{3}H(IV-Gal)]GM1) **(Figure M-4)** was prepared by enzymatic oxidation with galactose oxidase followed by reduction with sodium [^{3}H]$NaBH_4$ *(Sonnino et al. 1996)*. 13 mmol of the gangliosides GM1 was dissolved in 1 ml of chloroform/methanol, 2:1 (v/v), mixed with 180 mg of Triton X-100 and dissolved in 10 ml of the same solvent. The mixture was dried under vacuum and the residue was dissolved in 8 ml of 5 mM EDTA, 25 mM sodium phosphate buffer, pH 7.0, containing 450 U of galactose oxidase. The mixture was incubated at 37 °C under continuous stirring for 24 h; other 450 U of galactose oxidase were added after 6 h. The mixture was dried under vacuum and purified on a 110 cm x 2 cm silica gel 100 column with the solvent system chloroform/methanol/water 60:35:5 (v/v/v). Column elution was monitored by HPTLC. Plates were developed in chloroform/methanol/0,2% aqueous $CaCl_2$ 50:42:11 (v/v/v), and were colored with an anysaldehyde spray reagent. The fractions containing the oxidized GM1 were collected, pooled, and evaporated to dryness.

Oxidized GM1 was dissolved in propanol-0.1 M/NaOH, 7:3 (v/v), in a screw-capped tube, and treated at room temperature with solid [^{3}H]$NaBH_4$. After 5 h, 10 mg of cold $NaBH_4$ were added and the reaction was allowed to continue for 30 min. Under nitrogen pressure the solution was evaporated to a very small volume, the wet residue was then dissolved in 1 ml of water and again reduced to a small volume. The vapours were passed into a 5 M sulphuric acid trap to oxidize tritium to tritiated water. The final wet residue was dissolved in water and dialyzed.

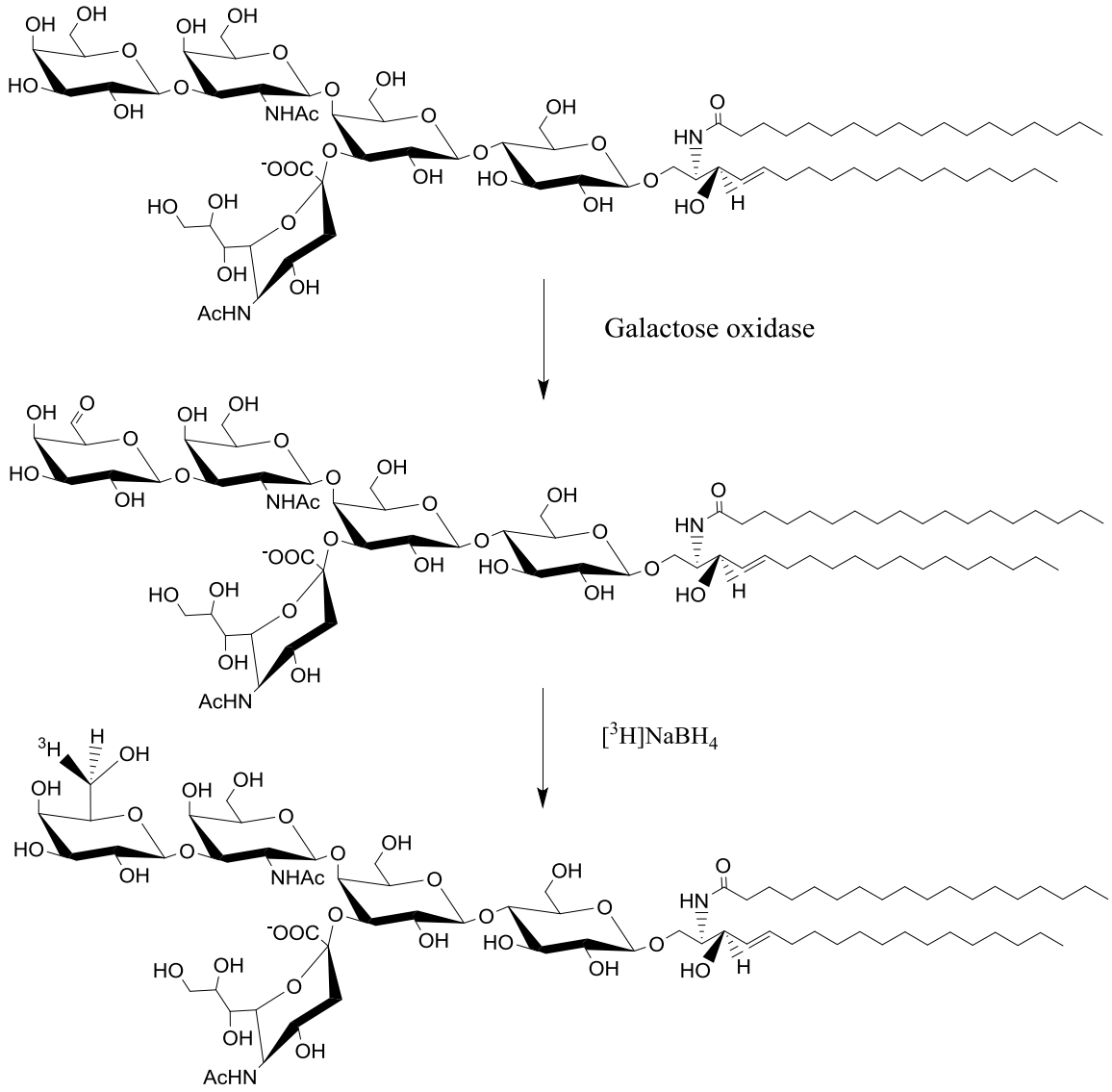

Figure M-4. Scheme for the preparation of GM1 tritium labeled at position C-6 of the external galactose ([6-^{3}H(IV-Gal)]GM1).

2.1.5 GM1 tritium labeled at position C-3 of the sphingosine

GM1 tritium labeled at the C-3 position of the sphingosine ([Sph-3-^{3}H]GM1) **(Figure M-5)** resulted from a oxidation of GM1 at position 3 of sphingosine with 2,3-dichloro-5,6-dicyanobenzoquinone (DDQ), a reagent that is specific for allylic hydroxyl groups. Then carbonyl group was reduced to alcohol with [^{3}H]$NaBH_4$ *(Sonnino et al. 1996).* 13 mmol of GM1 were dissolved in 10 ml of chloroform/methanol 2:l (v/v) and mixed with 10 ml of a solution of Triton X-100 in the same solvent (60 mg/ml). The solvent was evaporated and the residue was dissolved in 10 ml of DDQ solution (60 mg/ml, in sodium dehydrated toluene). The mixture reacted at 37 °C for 40 h under continuous stirring in a screw-capped tube. The solvent was then evaporated under vacuum at 37 °C. The dark brown residue was suspended in 10 ml of acetone, sonicated and centrifuged at 12000 rpm. The supernatant containing Triton X-100 and DDQ was discarded. The treatment was repeated four times to obtain a white precipitate. The oxidized GM1 was purified on a silica gel 100 column (110 cm × 2 cm) with the solvent system chloroform/methanol/water 60:35:5 by volume. The elution was monitored by HPTLC plates developed in chloroform/methanol/0,2% aqueous $CaCl_2$ 50:42:11 (v/v/v), and colored with an anysaldehyde spray reagent.

The fractions containing the oxidized GM1 were collected, evaporated to dryness, dissolved in few ml of propanol/water 7:3 (v/v) in a screw-capped tube, and treated at room temperature with solid [^{3}H]$NaBH_4$. Then 10 mg of cold $NaBH_4$ were added and the reaction continued for 30 min. The solution was evaporated, under nitrogen pressure, to a very small volume and the wet residue was dissolved in 1 ml of water and again reduced to a small volume. The vapours were passed into a 5 M sulphuric acid trap to oxidize tritium to tritiated water. The final wet residue was dissolved in water and dialyzed.

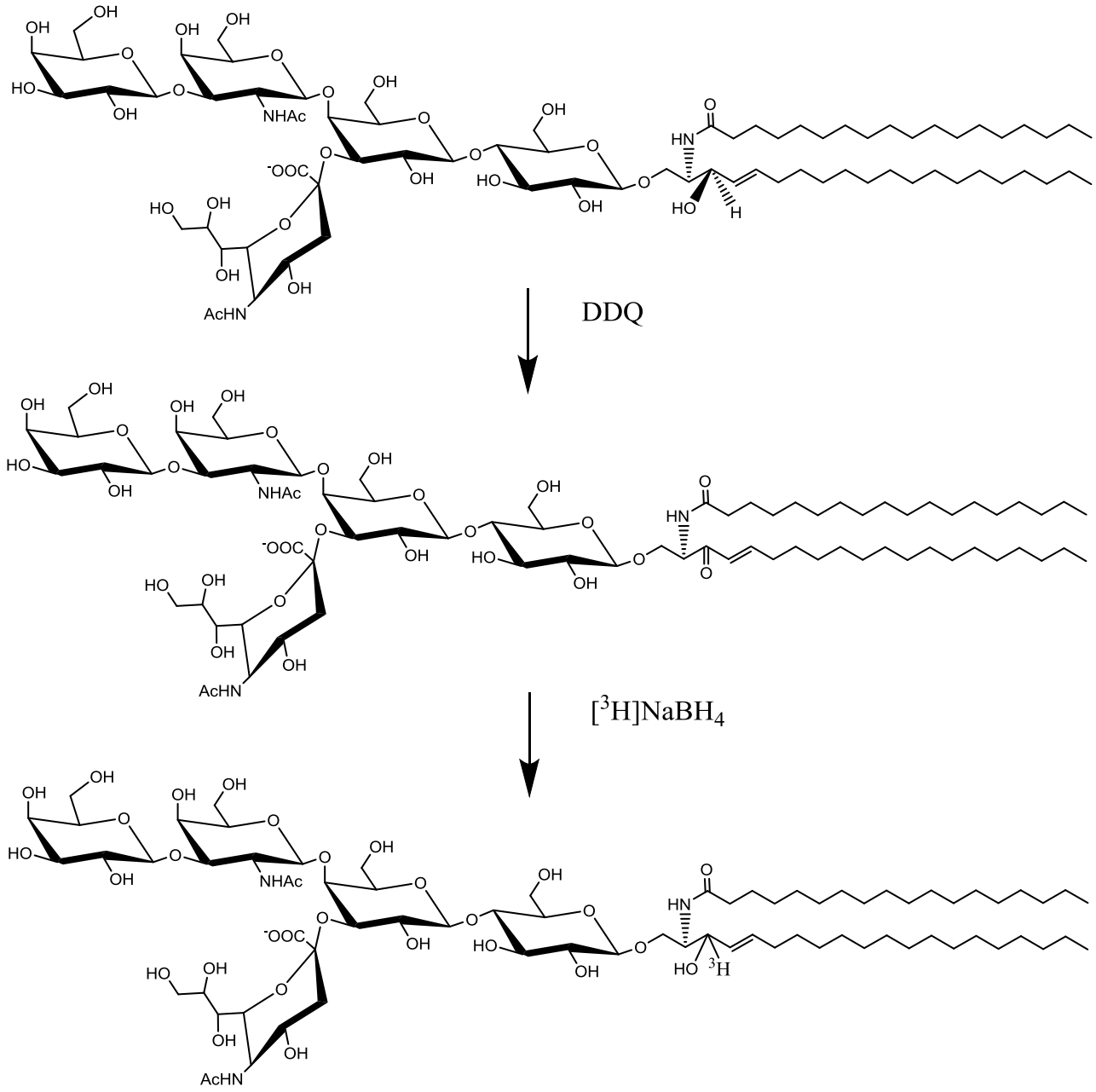

Figure M-5. Scheme for the preparation of GM1 tritium labeled at position C-3 of sphingosine ([Sph-3-^{3}H]GM1).

2.1.6 GM1 oligosaccharide and GM1 radiolabeled oligosaccharide preparation

OligoGM1 (II^{3}Neu5Ac-Gg$_4$) (**Figure M-6)** and [6-^{3}H(IV-Gal)]OligoGM1 (II^{3}Neu5Ac-[^{3}H]Gg$_4$) **(Figure M-7)** were prepared by ozonolysis followed by alkaline degradation *(Wiegandt and Bucking 1970)* of GM1 and [6-^{3}H(IV-Gal)]GM1, respectively. GM1 or [6-^{3}H(IV-Gal)]GM1 was dissolved in the minimum required methanol and maintained under ozone at 23 °C for 6 h under continuous stirring. The solvent was then evaporated under vacuum and the residue brought to pH 10.5–11.0 by the addition of triethylamine. After solvent evaporation, GM1 oligosaccharide or [6-^{3}H(IV-Gal)]GM1 oligosaccharide was purified by flash chromatography using chloroform/methanol/2-propanol/water 60:35:5:5 (v/v/v/v) as eluent. Oligosaccharides were dissolved in methanol and stored at 4 °C. NMR, mass Spectrometry **(Figure M-8)** and HPTLC analyses showed a purity over 99% for the prepared OligoGM1. HPTLC followed by radio-imaging showed a purity over 98% for the [6-^{3}H(IV-Gal)]OligoGM1.

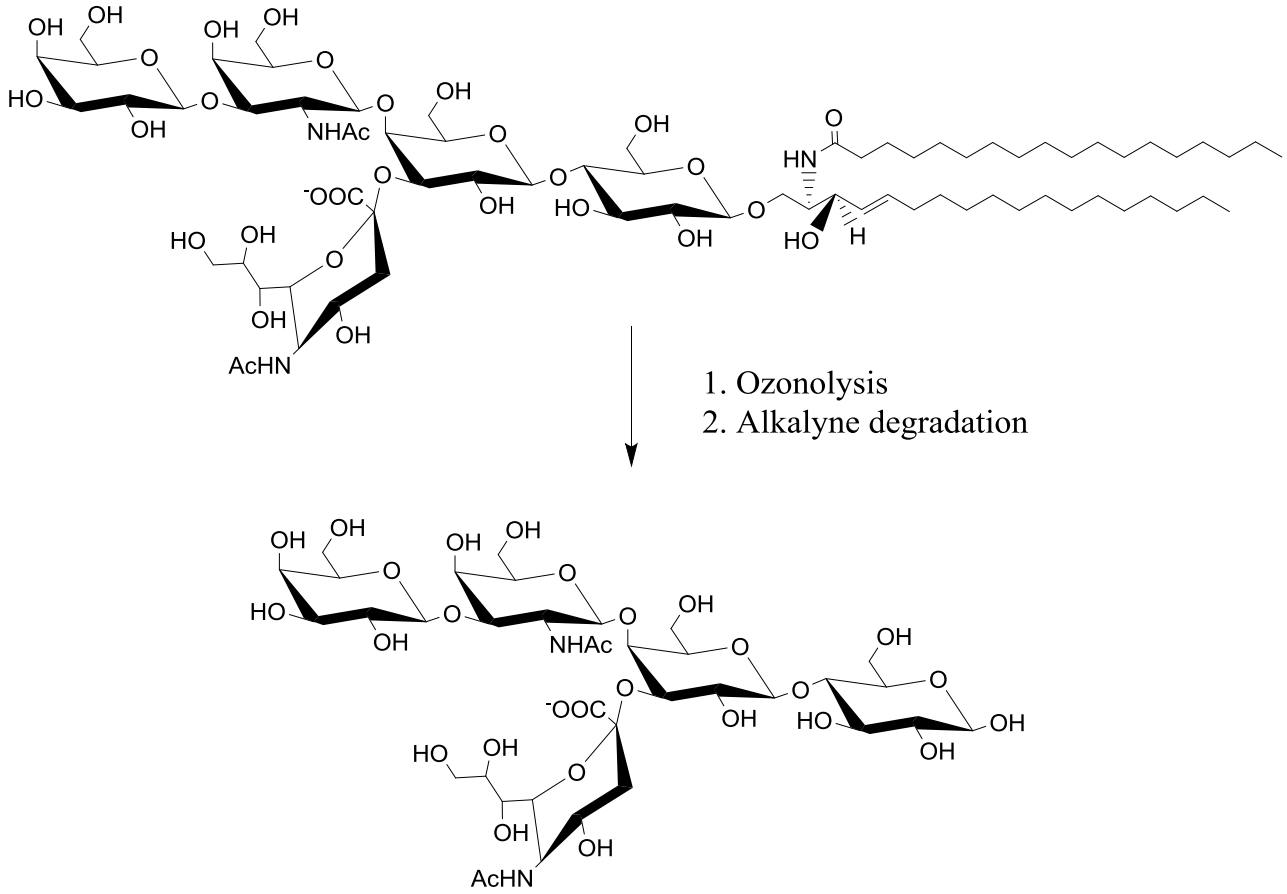

Figure M-6. Scheme for the preparation of OligoGM1 (II^{3}Neu5Ac-Gg$_4$).

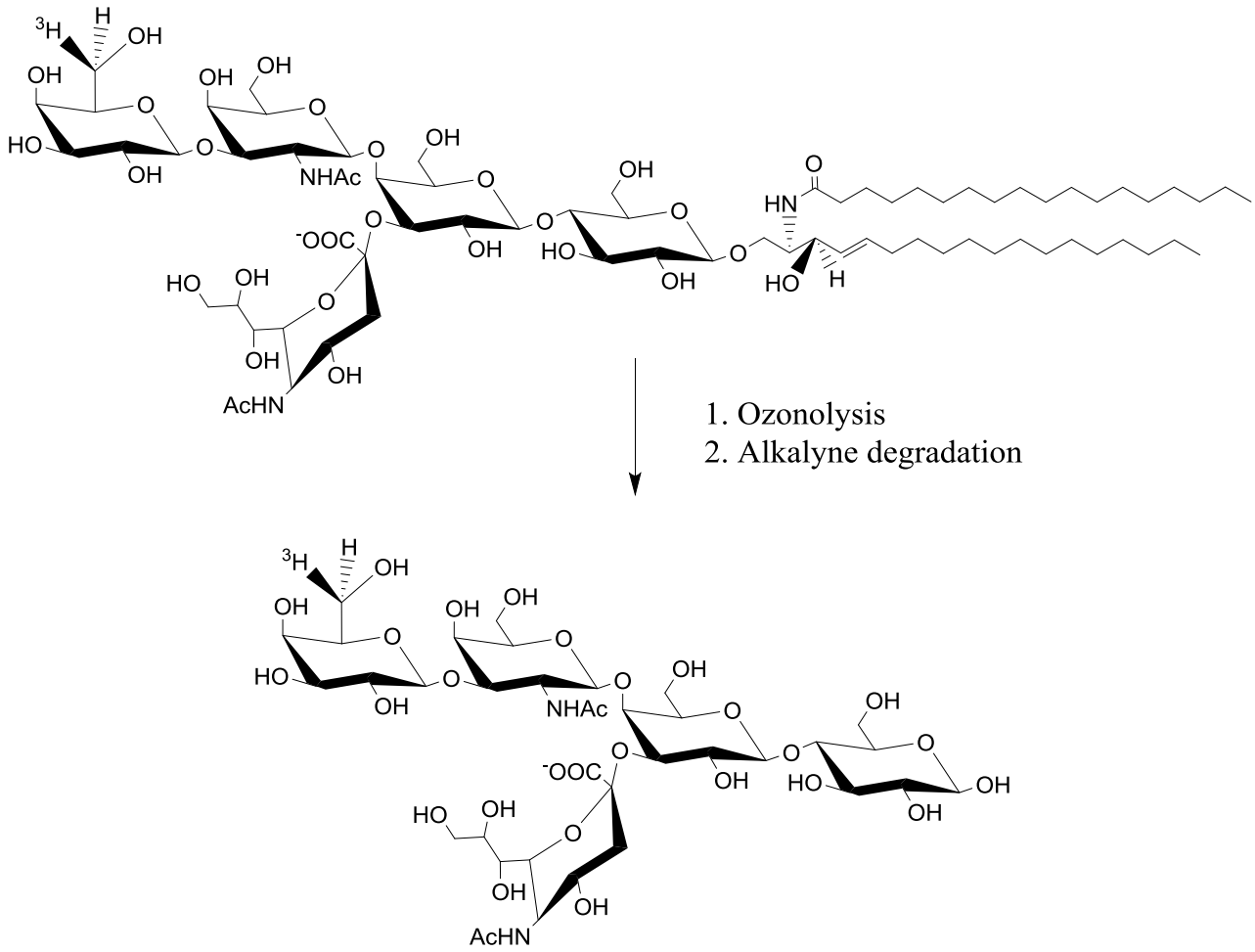

Figure M-7. Scheme for the preparation of [6-^{3}H(IV-Gal)]OligoGM1 (II^{3}Neu5Ac-[^{3}H]Gg$_{4}$).

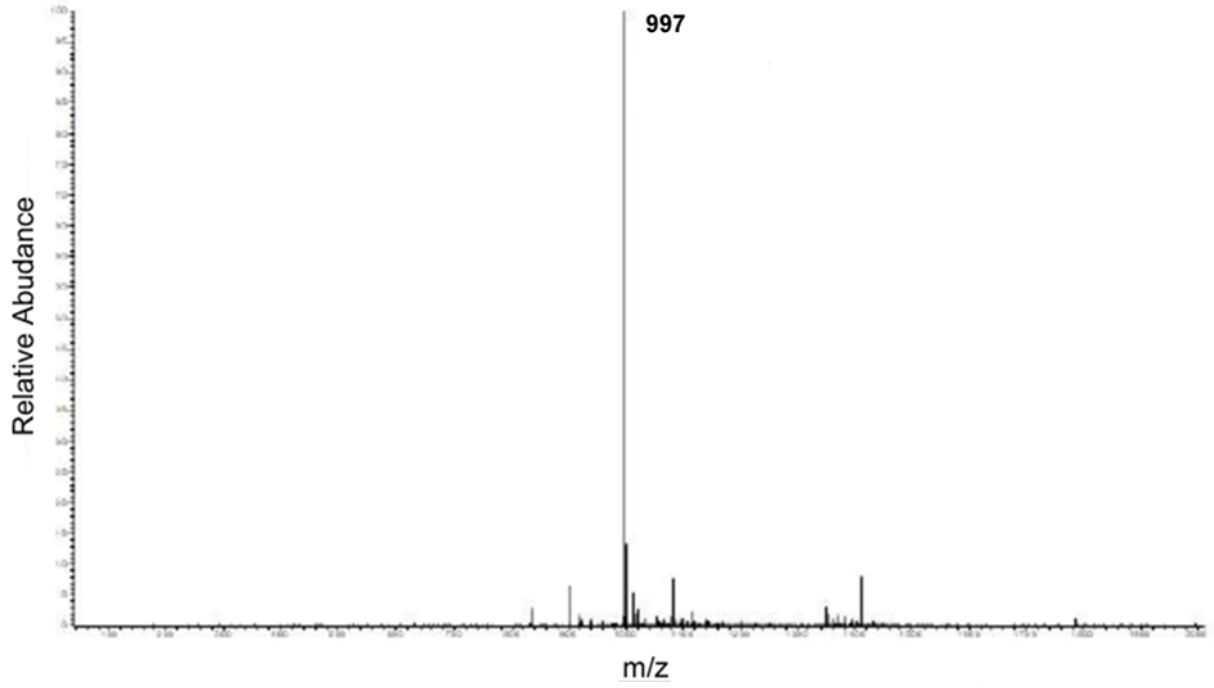

Figure M-8. OligoGM1 MS profile ESI-MS (negative-ion mode): m/z= 997 [M - H]$^{-}$.

2.1.7 NO_2-OligoGM1

NO_2-OligoGM1 **(Figure M-9)** was prepared from ozonolysis of deAcGM1. GM1, purified from a mixture of gangliosides using the DEAE ion-exchange chromatography, has been deacetylated on sialic acid residue by alkaline hydrolisis. Deacetyl-GM1 has been purified by flash chromatography and then submitted to ozonolysis and basic treatment with triethylamine (TEA) to cleave the apolar chain. Deacetyl-oligoGM1 has been purified from the reaction mixture using flash chromatographic chloroform/methanol/water 50:42:11 (v/ v/v) **(Figure M-10)**. From this reaction we obtained deacetyl-oligoGM1 (5% yield) and NO_2-OligoGM1(95% yield). In **Figure M-11** it's possible to see HPTLC of GM1, OligoGM1 and NO_2-OligoGM1.

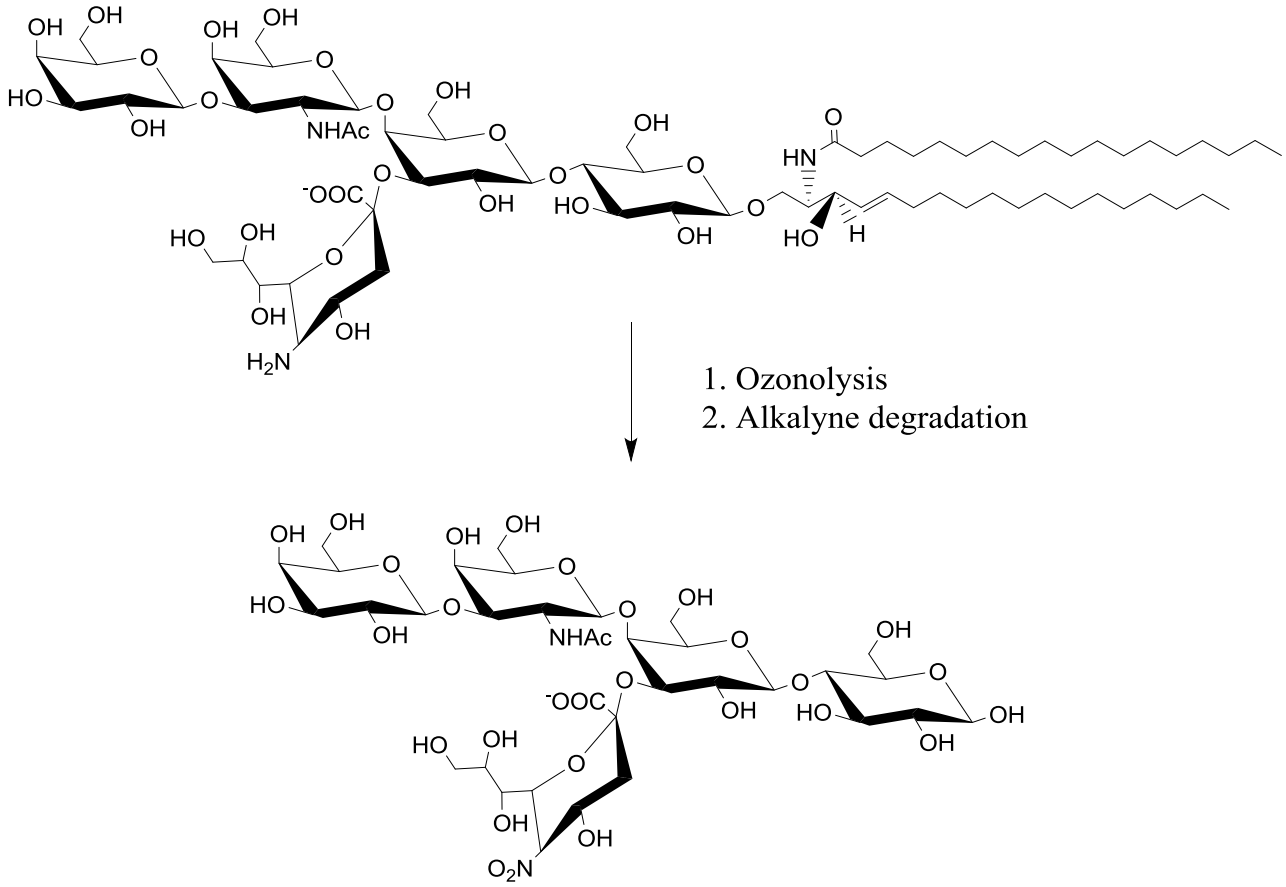

Figure M-9. Scheme for the preparation of NO_2-OligoGM1.

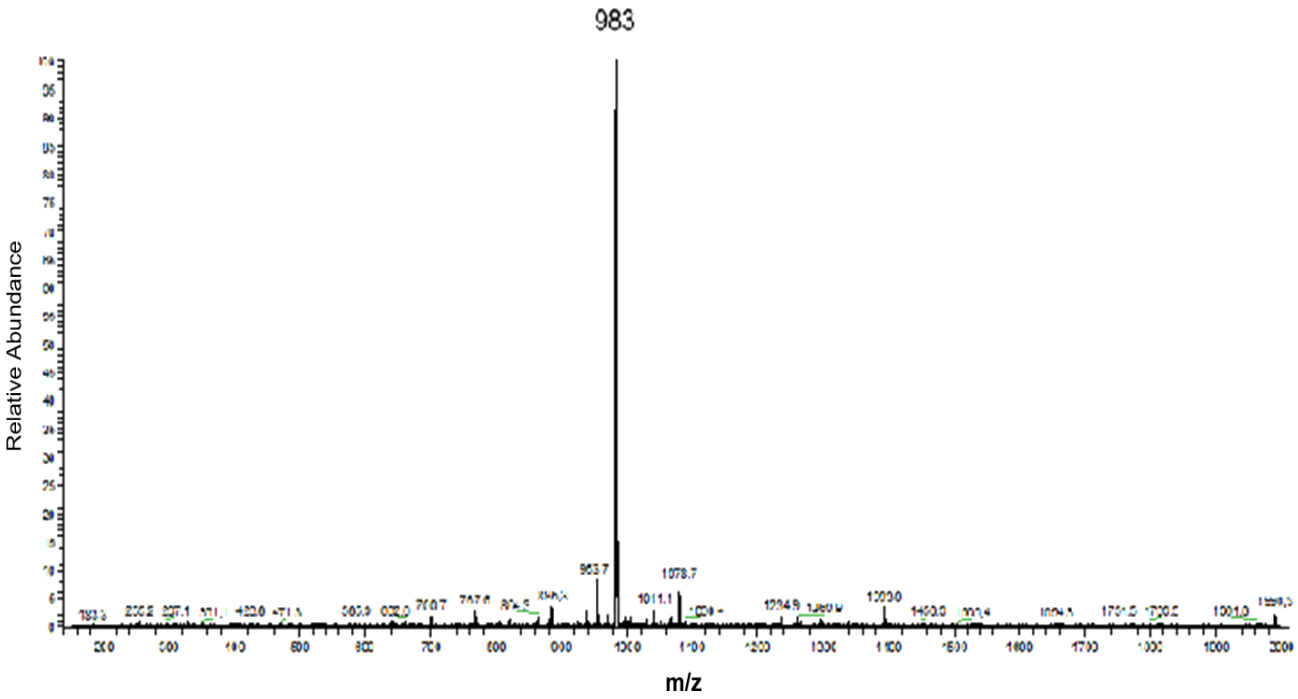

Figure M-10. NO_2-OligoGM1 MS profile ESI-MS (negative-ion mode): m/z= 983 $[M - H]^-$.

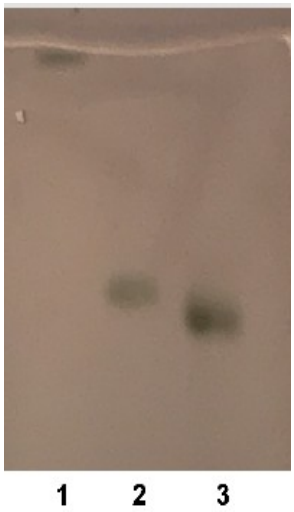

Figure M-11. HPTLC. **1**. GM1. **2**. OligoGM1. **3**. NO_2-OligoGM1. Mono-dimensional HPTLC using the solvent system $CHCl_3/CH_3OH/KCl$ 50 mM 30:50:13 (v:v:v). Gangliosides were recognized by specific detection spraying with anisaldehyde reagent.

2.1.8 Oligosaccharides

Gg_4, $II^3Neu5Ac$-Lac, $II^3Neu5AcGg_3$, $II^3Neu5Ac$-[^{3}H]Gg_3, $IV^2aFucII^3$-$Neu5AcGg_4$, were prepared by ozonolysis followed by alkaline degradation *(Wiegandt and Bucking 1970)* from tetrahexosylceramide, GM3, GM2, [^{3}H]GM2, Fucosyl-GM1, respectively **(Figure M-12).**

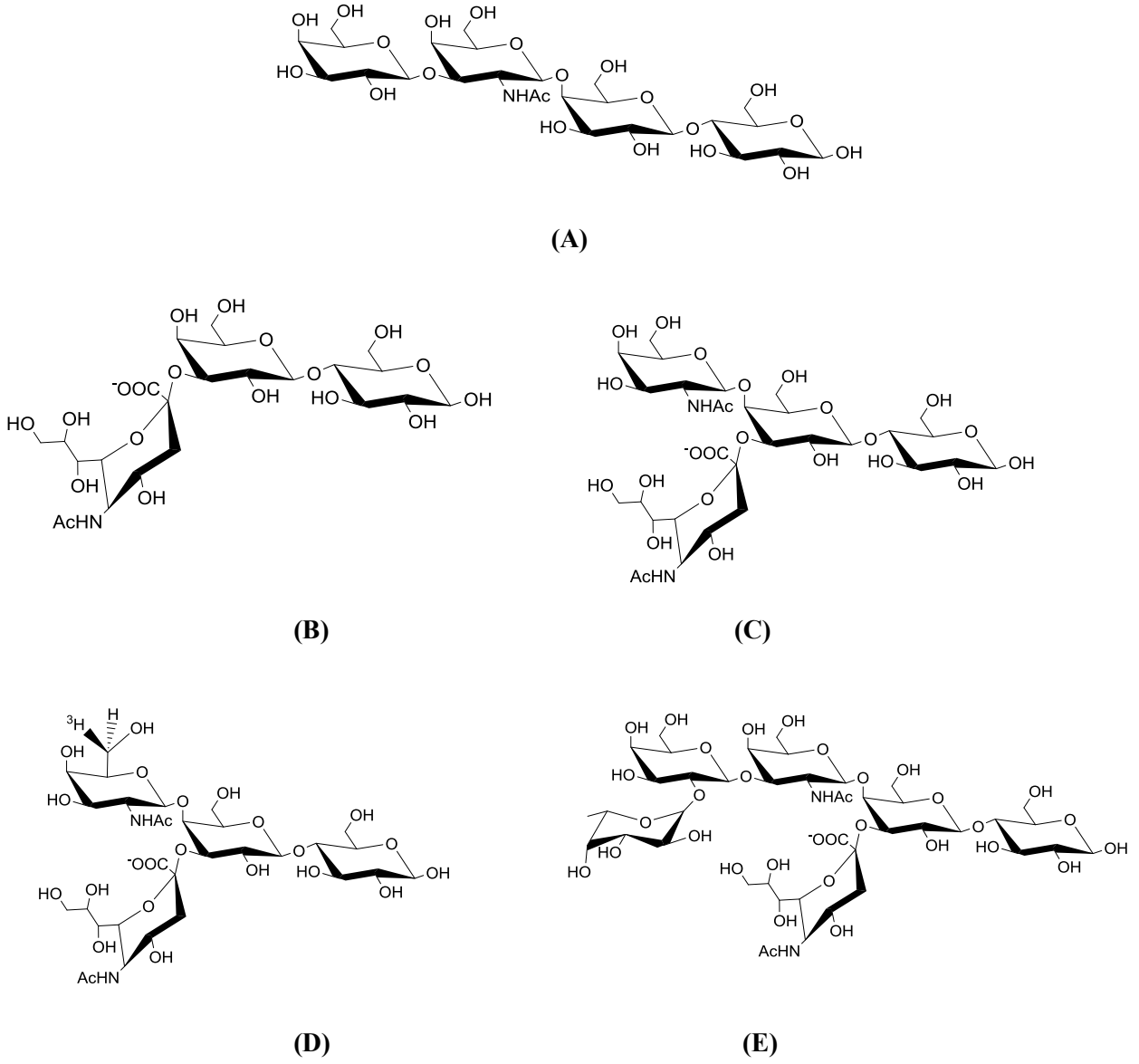

Figure M-12. Oligosaccharide structure: **(A)** Oligo asialo-GM1 (Gg_4). **(B)** Oligo GM3 (II3Neu5Ac-Lac). **(C)** Oligo GM2 (II3Neu5Ac-Gg_3). **(D)** Oligo [^{3}H]GM2 (II3Neu5Ac-[^{3}H]Gg_3). **(E)** Oligo Fucosyl-GM1 (IV2αFucII3-Neu5Ac-Gg_4).

2.1.9 tritium-labeled and photoactivable GM1

Two different tritium-labeled and photoactivable GM1 ([6-^{3}H(IV-Gal)]GM1(Cer-N_3) and [Sph-3-^{3}H]GM1(Gal-N_3) were prepared according to the scheme **(Figure M-13)** *(Mauri et al. 2004; Prioni et al. 2004).*

[6-^{3}H(IV-Gal)]GM1(Cer-N_3)

Photoactivable GM1, [6-^{3}H(IV-Gal)]GM1(Cer-N_3), bearing the photoactivable group on the fatty acid moiety, was prepared from galactose-tritiated GM1 ([6-^{3}H(IV-Gal)]GM1).

To insert the photoactivable group on fatty acid residue, [6-^{3}H(IV-Gal)]GM1 was firstly submitted to alkaline hydrolysis with KOH 16 M at 90 °C for 18 h, to remove the stearic acid residue followed by acid coupling with 12-aminododecanoic acid.

The reaction occurred adding 350 µmol of 12-aminododecanoic acid, dissolved in 2,5 ml of dry tetrahydrofuran (12.5%, v/v) to 1,5 ml of dimethylformamide (7.5%) containing 80 µmoles of deacyl-GM1, 1 ml of Triton X-100 (5%, v/v), and 15 ml of dry triethylamine (75%, v/v). The reaction mixture was maintained under continuous stirring at 23 °C for 24 h. The mixture was evaporated under vacuum to 1, and 25 ml of ethyl acetate was added *(Sonnino et al. 1989).*

Finally, the aminoderivatives were treated to insert the photoactivable group. The azide-labeling procedure started with the dissolution of the crude aminoderivatives obtained by previous reaction in 0,5 ml of dry dimethylformamide. Then, 1 mg of 4-fluoro-3-nitrophenylazide and 1 µl of tributylamine in 25 µl of dry dimethyl sulfoxide were added under dark conditions. The reaction mixture was stirred at 80 °C for 18 h in dark conditions. After solvent evaporation, the photoactivable compounds were purified by flash chromatography using chloroform/methanol/water, 60:35:8 (v/v/v) *(Sonnino et al. 1989)*. All the derivates were solubilized in methanol and stored at 4 °C. HPTLC analyses were performed using the solvent system chloroform/methanol/0,2% aqueous $CaCl_2$, 60:35:8 (v/v/v). Bound sialic acid was determined by the resorcinol-HCl method *(Svennerholm 1957; Takki-Luukkainen and Miettinen 1959),* pure Neu5Ac being used as the reference standard.

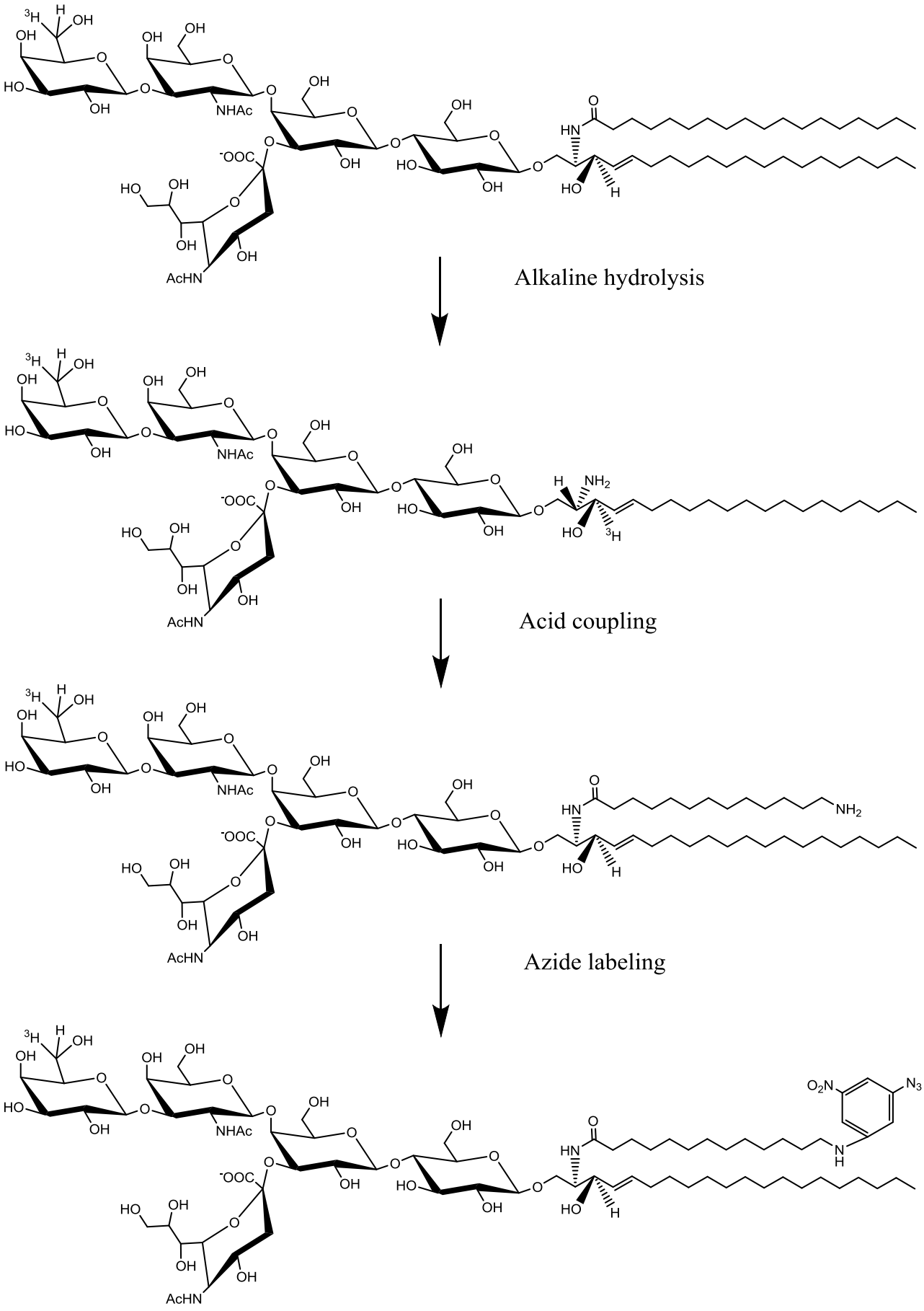

Figure M-13. Scheme for the preparation of [6-^{3}H(IV-Gal)]GM1(Cer-N_3).

6-N_3(IV-Gal)GM1-[Sph-3-^{3}H]

Photoactivable 6-N_3(IV-Gal)GM1-[Sph-3-^{3}H] **(Figure M-14)**, bearing the photoactivable group linked at position 6 of external galactose, was prepared from [Sph-3-^{3}H]GM1.

[Sph-3-^{3}H]GM1 was firstly subjected to enzymatic oxidation at position 6 of the external galactose.

[Sph-3-^{3}H]GM1 (0,41 mCi) was dissolved in 50 µl Triton X-100/1-propanol (18 mg/ml) and the mixture was slowly dried under nitrogen flux. The residue was dissolved in 500 µl of 25 mM phosphate buffer, pH 7,0, 5 mM EDTA, and 450 mU of galactose oxidase were added. The mixture was stirred at 37 °C for 21 h. 450 mU of galactose oxidase were further added and reaction allowed to proceed overnight in the same condition. The reactions products were characterized by HPTLC with the solvent system chloroform/methanol/water, 55/45/10 (v/v/v).

The reaction mixture was dried under vacuum and dissolved in 1 ml of 2,5 mM sodium cyanoborohydride ($NaCNBH_3$) and ammonium acetate (CH_3COONH_4) 1 M in methanol. The reaction was allowed to proceed at 23 °C for 18h. The reaction mixture was dried under vacuum and was purified on a silica gel 100 column chromatography (60 cm × 1.2 cm), eluted first with chloroform/methanol/water 60/35/5 (v/v/v) and then with chloroform/methanol/water 50/40/10 (v/v/v). The reactions products were characterized by HPTLC with the solvent system chloroform/methanol/0,2% aqueous $CaCl_2$ 50:42:11 (v/v/v). Fraction with homogeneous galactosamine containing a radioactive GM1 were dried and the residue solubilised in 100 µl anhydrous DMF.

At this solution were added 1µl triethylamine and 1,5 µmole of 4-fluoro-3-nitrophenylazide, dissolved in 27 µl ethanol. The mixture was stirred at 80 °C for 18 h. The reaction mixture was dried, and [Sph-3-^{3}H]GM1(Gal-N_3) was purified from 4-F-3-NO_2-phenylazide in excess on a reverse phase RP18 column (20 cm × 1 cm) eluited with methanol/water 15:4 (v/v). Fractions containing partially purified [Sph-3-^{3}H]GM1(Gal-N_3) were died and applied on a silica gel 100 column (80 cm × 1.2 cm) equilibrated and eluted with chloroform/methanol/water 76:26:4 (v/v/v). Fractions containing homogeneus 6-N_3(IV-Gal)GM1-[Sph-3-^{3}H] were dried and the residue immediately solubilised in methanol (1,45 µCi/ml) and stored at 4 °C *(Prioni et al. 2004).*

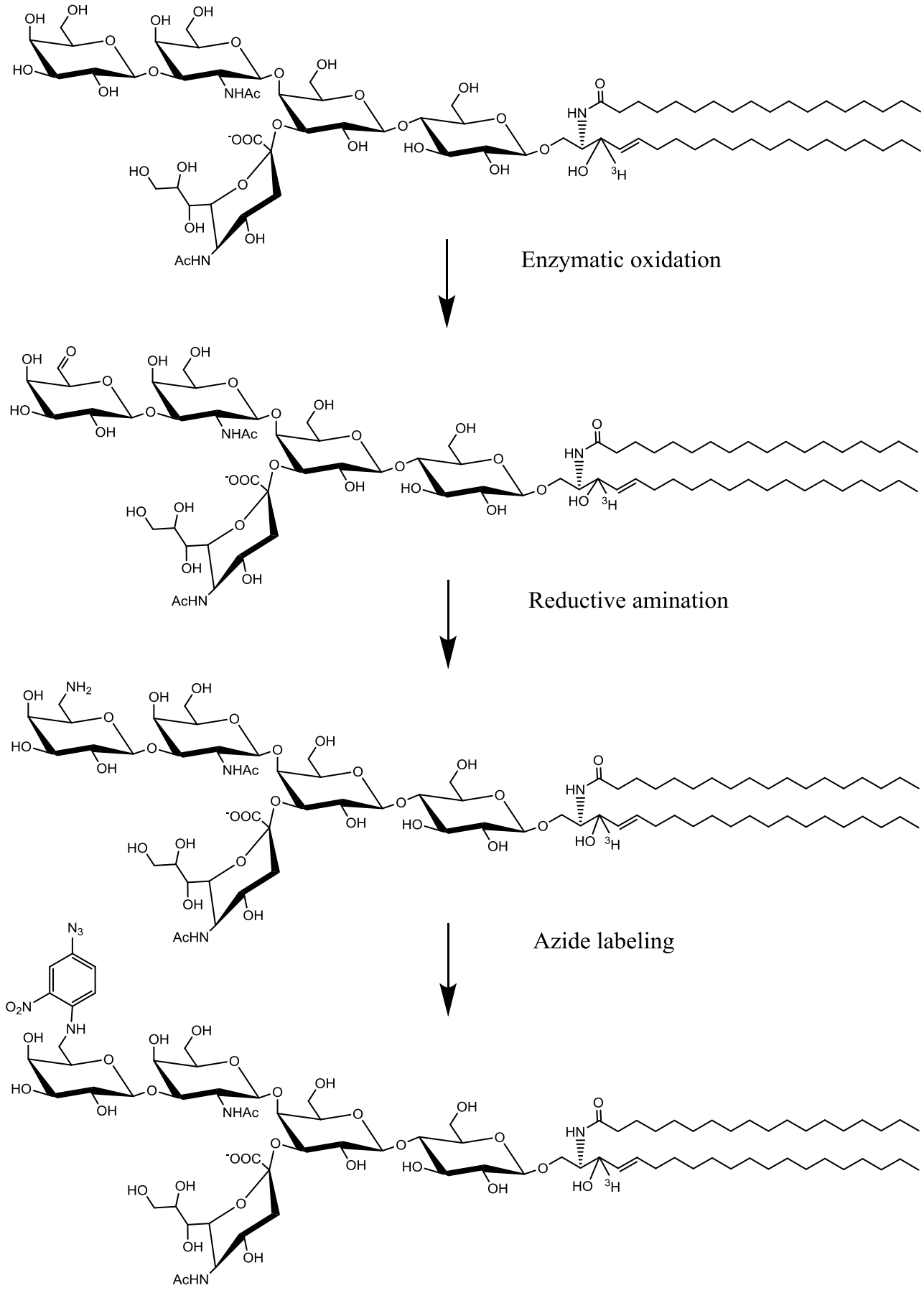

Figure M-14. Scheme for the preparation of [Sph-3-^{3}H]GM1(Gal-N_3).

2.1.10 GM1 oligosaccharide tritium-labeled and photoactivable

Tritium-labeled and photoactivable GM1 oligosaccharide, [6-^{3}H(IV-Gal)OligoGM1(Glc-N_3), was prepared from [6-^{3}H(IV-Gal)]GM1, according to the scheme reported in **Figure M-15**.

[6-^{3}H(IV-Gal)]GM1 was dissolved in the minimum required methanol and maintained under ozone (O_3) at 23 °C for 30 min under continuous stirring. The solvent was then evaporated under vacuum and the residue brought to pH 10.5–11.0 by addition of triethylamine at 23 °C for 18 h. After solvent evaporation [6-^{3}H(IV-Gal)]GM1 oligosaccharide was purified by flash chromatography using chloroform/methanol/2-propanol/water 60:35:5:5 (v/v/v/v) as eluent. HPTLC followed by radio-imaging showed a purity over 98% for the [6-^{3}H(IV-Gal)OligoGM1.

Then an amount of 52 µmoles of [6-^{3}H(IV-Gal)OligoGM1 (0,5 Ci/mmol) were dissolved in 33% ammonia and treated with 1 mg of ammonium hydrogen carbonate at 40 °C for 48 h. The solution was then immediately freezedried *(Lubineau et al. 1995)*.

The crude amino [6-^{3}H(IV-Gal)OligoGM1 was dissolved in 0,5 mL of dry dimethylformamide, then were added under dark conditions 1 mg of 4-fluoro-3-nitrophenylazide and 1 µl of tributylamine in 25 µL of dry dimethylsulfoxide. Maintaining dark conditions for all the process, the reaction mixture was stirred at 80 °C for 18 h.

After solvent evaporation, the [6-^{3}H(IV-Gal)OligoGM1(Glc-N_3) was purified by flash chromatography using as eluent chloroform/methanol/2- propanol/water 60:35:5:5 (v/v/v/v) *(Mauri et al. 2004)*. [6-^{3}H(IVGal)OligoGM1(Glc-N_3) solubilized in methanol was stored at 4 °C. HPTLC analyses were performed using the solvent system chloroform/methanol/0,2% aqueous $CaCl_2$, 60:35:8 (v/v/v). Bound sialic acid was determined by the resorcinol-HCl method *(Svennerholm 1957; Takki-Luukkainen and Miettinen 1959)*.

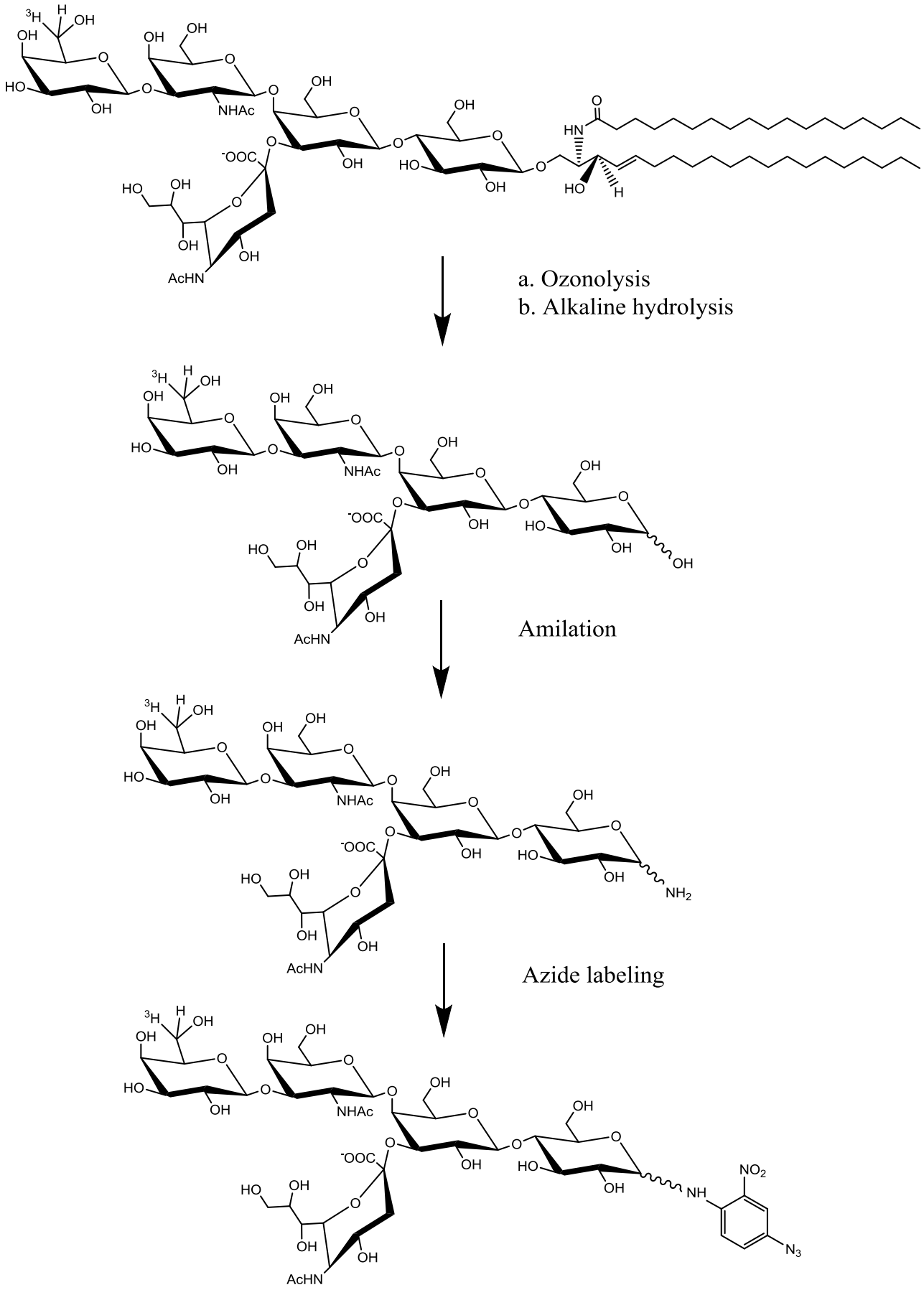

Figure M-15. Scheme for the preparation of [6-^{3}H(IV-Gal)]OligoGM1(Glc-N_3).

2.1.11 *Pseudo GM1*

The PseudoGM1, pseudo tetrasaccharide mimic of ganglioside GM1, was synthesized according to the scheme reported in **Figure M-16** *(Bernardi et al. 1999)* by the group of Dr. Bernardi and it was given to us to test it on N2a cells..

The pseudo GM1 (pseudo tetrasaccharide) was designed to mimic ganglioside GM1. PseudoGM1 preserve the galactose (Gal) and N-Acetylneuraminic acid (Neu5Ac) of the GM1 with the addition of a cyclohexanediol (DCCHD). DCCHD has the same relative and absolute configuration of natural galactose. EESI-MS of PseudoGM1 which was used, is reported in **Figure M-17**.

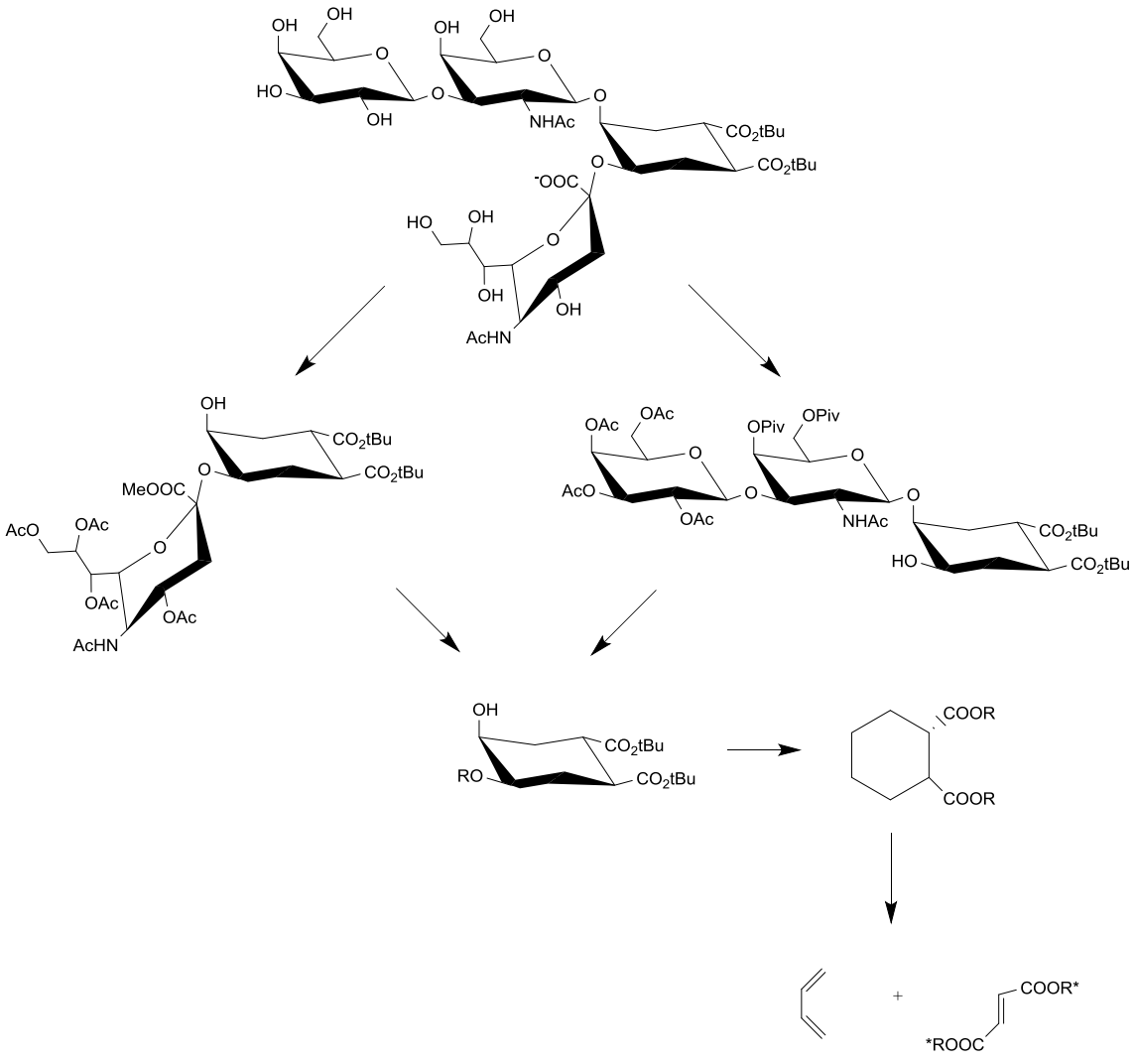

Figure M-16. Retrosynthesis of PseudoGM1 *(Bernardi et al. 1999).*

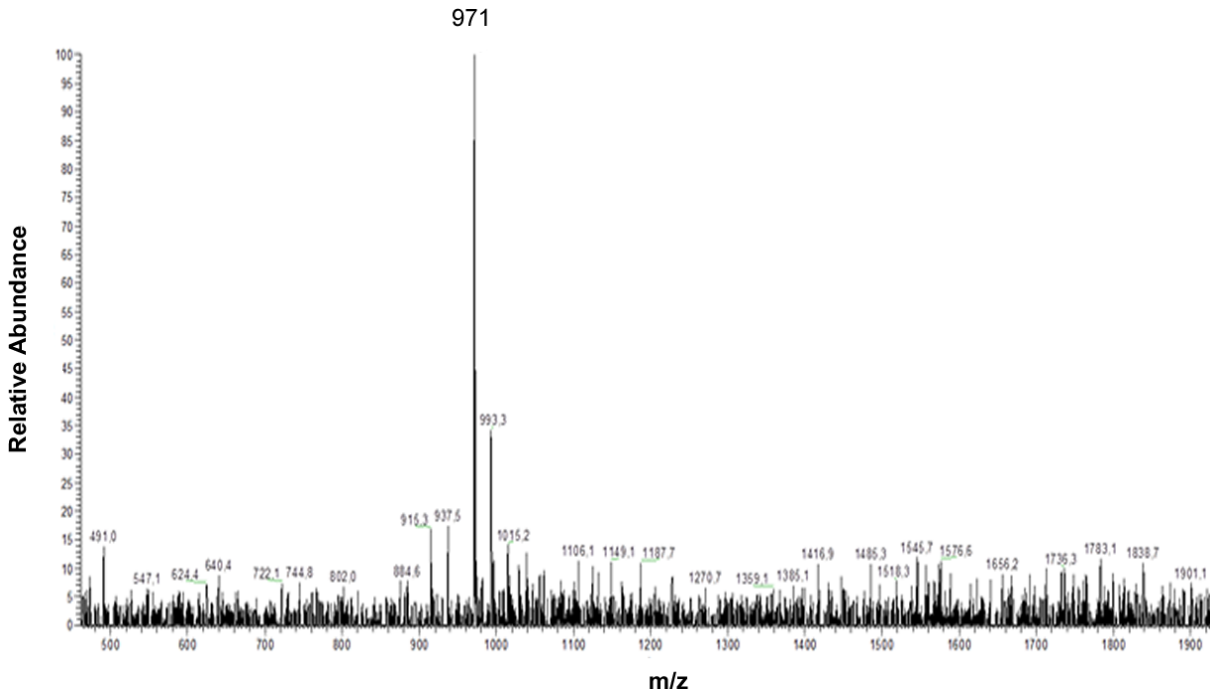

Figure M-17-. PseudoGM1 MS profile ESI-MS (negative-ion mode): m/z= 971 $[M - H]^-$.

2.2. Neuroblastoma cells (N2a)

2.2.1 N2a cell cultures

Neuro2a (N2a) cells were cultured and propagated as monolayer on 75 cm^2 flasks in Dulbecco's modified Eagle's medium-High Glucose medium (DMEM) with the add of 10% fetal bovine serum inactivated (FBS), 1% L-glutamine and 1% penicillin/streptomycin. Cells were incubated at 37 °C in humidified atmosphere of 95% air / 5% CO_2. Every 3-4 days, when growth reached the 80–90% confluence, cells were subcultured to a fresh culture. N2a cells were used in the experiments between the 10th and the 15th passages. Sterilized condition were maintained working under a laminar flow cabinet and by using sterile solutions and materials.

2.2.2 N2a cells treatments: gangliosides, galactose, sialic acid and retinoic acid

N2a cells were plated at $5\times10^3/cm^2$ and incubated for 24 h in complete medium to allow cells attachment. Cells were counted. Growth medium was removed to induce differentiation. Cells were pre-incubated in pre-warmed Transfectagro medium with 2% FBS, 1% L-glutamine, 1% penicillin/streptomycin, for 30 min at 37 °C. Cell treatments were performed in serum reduced culture medium to reduce possible interactions between serum components and exogenous gangliosides or oligosaccharides. In the end, cells were incubated at 37 °C up to 48 h in the presence of 50 μM gangliosides, oligosaccharides, galactose, sialic acid or 20 μM retinoic acid (RA) *(Riboni et al. 1995).* Gangliosides and oligosaccharides were solubilized in methanol. Control N2a cells were incubated in the same conditions without any addition.

2.2.3 TrkA chemical inhibition in N2a cell

To block TrkA activity in N2a cells, the TrkA inhibitor (120 nM), an oxindole compound that acts as a cell-permeable, reversible, potent and highly selective inhibitor of TrkA (IC50 = 0,006 μM) by targeting the kinase's ATP binding pocket, was added to the incubation medium 1 h before the addition of GM1 or OligoGM1 *(Wood et al. 2004).*

2.2.4 Small interfering RNA (siRNA) mediated TrkA knockdown in N2a cells

TrkA knockdown was obtained by RNA interference applying three distinct siRNAs.

1. Mm_Ntrk1_1 (sense 5'-CCAUCAUAAUAGCAAUUAUTT-3', antisense 5'-AUAAUUGCUAUUAUGGAT-3');
2. Mm_Ntrk1_5 (sense 5'-GGUGGCUGCUGGUAUGGUATT-3', antisense 5'-UACCAUACCAGCAGCCACCTG-3');
3. Mm_Ntrk1_6 (sense 5'-CCUUCUUGUGCUCAACAAATT-30', antisense 5'-UUUGUUGAGCACAAGAAGGAG-3').

Non-silencing siRNA with no homology to any known mammalian gene was used (sense 5'-UUCUUCGAACGUGUCACGUdTdT-3', antisense 5'-ACGUGACACGUUCGGAGAAdTdT-3'). Transfection was performed after 24 h from cell plating in antibiotic and serum free culture media with solution containing 25% OptiMEM, 0.25% Lipofectamine 2000 and 50 nM siRNA (16.7 nM of each siRNA). After 6 h, the transfection medium was changed to culture medium containing antibiotic and serum. After 24 h from the silencing, cells were treated with GM1 or OligoGM1 (2.2.2 N2a cells treatments).

2.2.5 Photolabeling experiments on N2a cells

To study the interaction between GM1 and TrkA, cells were incubated with 50 μM [6-^{3}H(IV-Gal)]GM1(Cer-N_3), [Sph-3-^{3}H]GM1(Gal-N_3), and [6-^{3}H(IV-Gal)]OligoGM1(Glc-N_3), for 3 h at 37°C in humidify atmosphere of 95% air / 5 % CO_2 in dark condition. After incubation, medium was removed and cells were illuminated for 40 min under UV light (λ = 360 nm) on ice to induce photo-activation. All the procedures before exposure to UV light were performed in dark room under red safelight. The cells were lyzed by sample buffer containing 0,15 M DTT, 94 mM Tris-HCl, 15% glycerol (v/v), 3% SDS (w/v), 0,015% blue bromophenol (v/v), sonicated by probe (50 W, 30 kHz) and boiled for 5 minutes at 99 °C and subjected to 4–20% sodium dodecyl sulfate–polyacrylamide gel electrophoresis (SDS–PAGE) and blotted on PVDF membrane. Digital autoradiography of the PVDF membrane was performed with Beta-Imager 2000 (Biospace). PVDF membrane was then incubated with anti-TrkA antibody and protein were analyzed *(Sonnino et al. 1989; Sonnino et al. 1992; Chigorno et al. 1990; Loberto et al. 2003; Chiricozzi et al. 2015).*

2.2.6 Determination of cell viability of N2a cells

Cell viability was determined by Trypan blue exclusion *(Mehlen et al. 1988; Aureli et al. 2011)* and by MTT assays *(Mosmann 1983)* after 12, 24 and 48 h treatment with 50 μM GM1, OligoGM1 or RA. After the incubation, 2,4 mM MTT (4 mg/mL in PBS) were added to each well and plates were re-incubated for 4 h at 37°C. Medium was removed and replaced with 2- propanol/formic acid, 95:5 by vol. Plates were agitated for some minutes before to read the absorbance at 570 nm with a microplate spectrophotometer (Wallac 1420 VICTOR2TM; Perkin Elmer).

2.2.7 Morphological analysis and neurite outgrowth evaluation of N2a cells

Cultured cells treated with 50 μM GM1, oligosaccharides or sugars up to 48 hours, were observed by phase contrast microscopy (Olympus BX50 microscope). The neurite-like length was measured on bidimensional images and expressed as the ratio between neurite length and cell body diameter *(Schengrund and Prouty 1988).* Were examined five random fields from each well, giving a total cell count of 200 cells per well.

2.2.8 Immunofluorescence analysis of N2a cells

Treated (24 h treatment with 50 μM GM1 or OligoGM1) or not treated (control) cells were fixed in 4% paraformaldehyde for 20 min at 23 °C. Cells were permeabilized with 0,1% Triton X-100 for 30 min and then treated with a blocking solution (5% donkey serum and 0,2% Triton X-100 in PBS, by vol) for 1 h at 23 °C. Cells were incubated with rabbit polyclonal antibody anti-Neurofilament (NF) for 2 h at 23 °C. After washing with PBS, cells were incubated 1 h with secondary anti-rabbit antibody FITC-conjugated. Fluorescence signal was detected by fluorescence microscope (Olympus U-RFL-T EPI Fluorescence Microscope) and the images were processed by ImageJ software.

2.2.9 Study of interaction between OligoGM1 and N2a cells

Fate of OligoGM1 administered to cells was determined with tritium-labeled OligoGM1([6-^{3}H(IV-Gal)]OligoGM1). After the administration to cell of [6-^{3}H(IV-Gal)]OligoGM1 (50 μM) for different times (0.5, 1, 6, and 24 hours), the medium was removed and the following treatments were performed sequentiall:

1. cells were washed five times with 10% FBS-medium to remove the amount of [6-^{3}H(IV-Gal)]OligoGM1 weakly associated to the cells (serum removable fraction);
2. cells were treated with 0.1% Trypsin-EDTA solution to evaluate the [6-^{3}H(IV-Gal)]OligoGM1 strongly linked to extracellular domain of PM proteins (trypsin removable fraction);
3. cells were lyzed by trypsin-EDTA solution (0.05%-0.02%, w/v in PBS) to evaluate the quantity of [6-^{3}H(IV-Gal)]OligoGM1 internalized by the cells (trypsin stable fraction) *(Chigorno et al. 1985).*

The same procedure was used to determinate the fate of GM1 oligosaccharide photoactivable derivative to N2a cells using tritium-labeled [6-^{3}H(IV-Gal)]OligoGM1(Glc-N_3). The radioactivity was determined by liquid scintillation counting using a beta-counter system. For [6-^{3}H(IV-Gal)]OligoGM1(Glc-N_3) the entire procedure was performed in dark condition under red safelight omitting cell UV illumination to induce photoactivation.

2.2.10 Isolation of detergent-resistant membrane (DRM) fractions in N2a cells

To verify the presence of TrkA in the plasma membrane microdomain, N2a cells were incubated in the absence or in the presence of GM1 or OligoGM1 (50 μM) for 3 h at 37 °C. Detergent-resistant membrane (DRM) were prepared by ultracentrifugation on discontinuous sucrose gradient of cells subjected to homogenization with 1% Triton X-100 *(Chiricozzi et al. 2015; Schiumarini et al. 2017).* Cells were mechanically harvested in PBS 1X and centrifuged at 270 × g for 10 min at 4 °C. Cell pellet was lysed in 1,2 mL of 1% Triton X-100 in TNEV buffer (10 mM TrisHCl 10, 150 mM NaCl, 5 mM EDTA pH 7,5) in the presence of 1 mM Na_3VO_4, 1 mM phenylmethylsulfonyl fluoride, and 75 mU/mL aprotinin and homogenized for 11-folds with tight Dounce. Cell lysate (2 mg of cell protein/mL) was centrifuged for 5 min at 1300 g at 4 °C to remove nuclei and cellular debris and obtain a postnuclear supernatant (PNS). A volume of 1 mL of PNS was mixed with an equal volume of 85% sucrose (w/v) in TNEV buffer containing 1 mM

Na_3VO_4, placed at the bottom of a discontinuous sucrose gradient (30–5%), and centrifuged for 17 h at 200 000 g at 4 °C. After ultracentrifugation, 12 fractions were collected starting from the top of the tube. The light scattering band, corresponding to the DRM fraction, was located at the interface between 5 and 30% sucrose corresponding to fraction 5 or 6. The entire procedure was performed at 0–4 ° C on ice immersion. Equal amounts from each fraction were used for protein and lipid analysis.

2.2.11 Protein analysis and determination in N2a cells

Equal amounts of proteins derived from photolabeled cells from gradient fractions or from GM1/OligoGM1-treated/untreated cells were denatured, separated on 4–20% polyacrylamide gels, and transferred to PVDF membranes using the Trans-Blot® Turbo™ Transfer System. The presence of TrkA was determined by specific primary antibody, followed by reaction with secondary HRP-conjugated antibody. For the time course analysis of TrkA–ERK1/2 activation, proteins derived from GM1/OligoGM1-treated and -untreated cells were denatured, separated on 7.5% polyacrylamide gels, and transferred to PVDF membranes. The presence of TrkA, p-TrkA, extracellular signal-regulated protein kinases 1 and 2 (ERK1/2), NF and p-ERK1/2 was determined by specific primary antibodies, followed by reaction with secondary horseradish peroxidase-conjugated antibodies (HRP-conjugated). The data acquisition and analysis were performed using Alliance Uvitec.

For protein determination, protein concentration (between 0.2 and 1.5 mg/ml) of samples was estimated using a DC™ protein assay kit. The DC (detergent compatible) protein assay is a colorimetric assay for protein concentration following detergent solubilization. The DC protein assay is measured at 650–750 nm. Bovine serum albumin was used as standard.

*2.2.12 Lipid extraction and GM1 detection in N2a cell*s

Total lipids were extracted with chloroform/methanol/water, 2:1:0,1 by vol, followed by a second extraction with chloroform/methanol, 2:1 by vol *(Prinetti et al. 2011).* Lipids were separated by Thin Layer Chromatography (TLC). GM1 ganglioside was specifically detected with HPR-conjugated cholera toxin B (CT-B) staining directly on TLC *(Valperta et al. 2007).* Sample was spotted on a silica gel 60 HPTLC plate and developed in chloroform/methanol/0,2% aqueous $CaCl_2$, 50:42:11 by vol. Following solvent evaporation, the plate was treated for 30 s with a solution of 0,2% (v/v) polyisobutylmethacrilate in hexane for three times and air-dried for 1 h. After 1 h of preincubation at 23°C in PBS containing 3% BSA (w/v), the plate was overlaid with CT-B subunit-HPR conjugated (40 ng) in 1% BSA (w/v) at 23°C for 1 h. After washing three times with PBS, plates were developed with o-phenylenediamine (one tablet in 1,8 ml of citratephosphate buffer 0,05 M (pH 5) and 17 µl of H_2O_2). The amount of GM1 was calculated by comparing the intensity of the spot of the samples with the standard.

2.2.13 Molecular modeling

Crystallographic structure of the extracellular segment of human TrkA in complex with nerve growth factor (NGF) (RCSB PDB ID: 2IFG) was used for molecular docking calculations. Protein complex was submitted to the Molecular Operating Environment 2016.0802 (MOE) Structure Preparation application, in order to fix all issues and to prepare structures for subsequent computational analyses. The OligoGM1 structure was built with the MOE Carbohydrate Builder and a geometry optimization was carried out with MOPAC7 and the PM6 basis set. Molecular docking was carried out through the MOE Dock program, setting as receptor the complex between TrkA and NGF, as ligand the optimized OligoGM1 structure. The binding site was identified at the interface between the two proteins. Before placement procedure, 20 000 rotamers of the ligand was generated, exploring all the molecule rotatable bonds. Alpha PMI placement algorithm, specifically developed for tight binding pocket, was selected. The London dG empirical scoring function was used for sorting the poses. The 30 top-scoring poses was refined through molecular mechanics, considering the receptor as a rigid body, and the refined complexes were scored through the GBVI/WSA dG empirical scoring function, keeping the five top-scoring poses. The top-scoring pose from the docking procedure was refined by using the MOE QuickPrep procedure aimed at relaxing and refining the complex before calculating the approx. binding free energy via the GBVI/WSA dG empirical scoring function *(Naim et al. 2007)*.

2.2.14 Statistical analysis in N2a cells

Data are expressed as mean ± SEM. When the normality of data was not assessed because the number of the samples was too small, data were analyzed for significance by Mann–Whitney test. Otherwise two-way ANOVA test has been applied. The analysis was performed with Prism software (GraphPad Software, version 8.0, Inc. La Jolla, CA, USA).

2.2.15 Other analytical methods in N2a cells

NMR spectra were recorded with a Bruker AVANCE-500 spectrometer at a sample temperature of 298 K. NMR spectra were recorded in CDCl3 or CD3OD and calibrate using the TMS signal as internal reference. Mass spectrometric analysis were performed in positive or negative ESI-MS. MS spectra were recorded on a Thermo Quest Finningan LCQTM DECA ion trap mass spectrometer, equipped with a Finnigan ESI interface; data were processed by Finnigan Xcalibur software system (Thermo Fischer Scientific). All reactions were monitored by HPTLC on silica gel 60 plates. Radioactivity associated with cells and trypsin and serum labile cell fractions was determined by liquid scintillation counting. Digital autoradiography of the PVDF membranes was performed with a Beta-Imager 2000.

Results

1. N2a cell viability

N2a cell was treated with 50 μM of GM1 and OligoGM1 up to 48 h. Trypan blue assay *(Mehlen et al. 1988; Strober, 2001; Aureli et al. 2011)* showed a viability overlapping to that of control cells and over 94% **(Figure R-1).** Cell proliferation was evaluated by 3-(4,5,-dimethylthiazol-2yl)-2,5-diphenyltetrazolium bromide (MTT) reduction assay on N2a cells grown in the absence or presence of GM1 or OligoGM1. After 12 h of treatment, we observed a reduction in cell proliferation **(Figure R-2).**

	Cell viability (%)		
	h 0	h 24	h48
Untreated cells	96.2 ± 2	94.1 ± 1	94.1 ± 2
+ GM1	94.1 ± 2	94.5 ± 2	94.2 ± 1
+ OligoGM1	96.3 ± 1	94.3 ± 2	94.4 ± 2

Figure R-1. Cell viability. The number of living or death cells was determined by Trypan blue assay. Values represent the percentage mean of living cells ± SEM for three different culture preparations (n = 3).

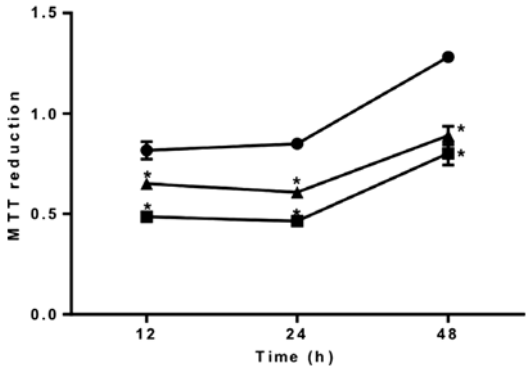

Figure R-2. Cell proliferation. N2a cells grown in the absence (●) or presence of GM1 (□) and OligoGM1 (▲). Results are expressed as mean of absorbance values at 570 nm ± SEM for three different culture preparations (*$p < 0.05$ vs. CTRL, two-way ANOVA, n = 3).

2. Neurite sprouting by administration to N2a cells of OligoGM1, PseudoGM1 and NO_2-OligoGM1

After 24 h incubation of N2a cells with OligoGM1 or GM1, we observed a neuron-like morphology **(Figure R-3)**. After 24h was possible to see the sprouting and elongation of neurites (not present in round-shaped control cells). N2a cells were also treated with Asialo-OligoGM1, OligoGM2, sialyllactose, galactose, or sialic acid. After the treatment with these compounds we didn't observed morphological variation. Only cells treated with fucosylated OligoGM1, showed neurite sprouting and reduction of cell proliferation comparable to OligoGM1. All these results suggests that the neurite sprouting process requires specifically the β-Gal-(1-3)-β-GalNAc-(1-4)-[α-Neu5Ac-(2-3)]-β-Gal-(1-4)-Glc structure. It's possible to conclude that the presence of an α-fucose at position 2 of the external galactose is insignificant for the processes. Also after 24 h

incubation of N2a cells with PseudoGM1 and NO_2-OligoGM1 we didn't observed morphological variation **(Figure R-5)**.

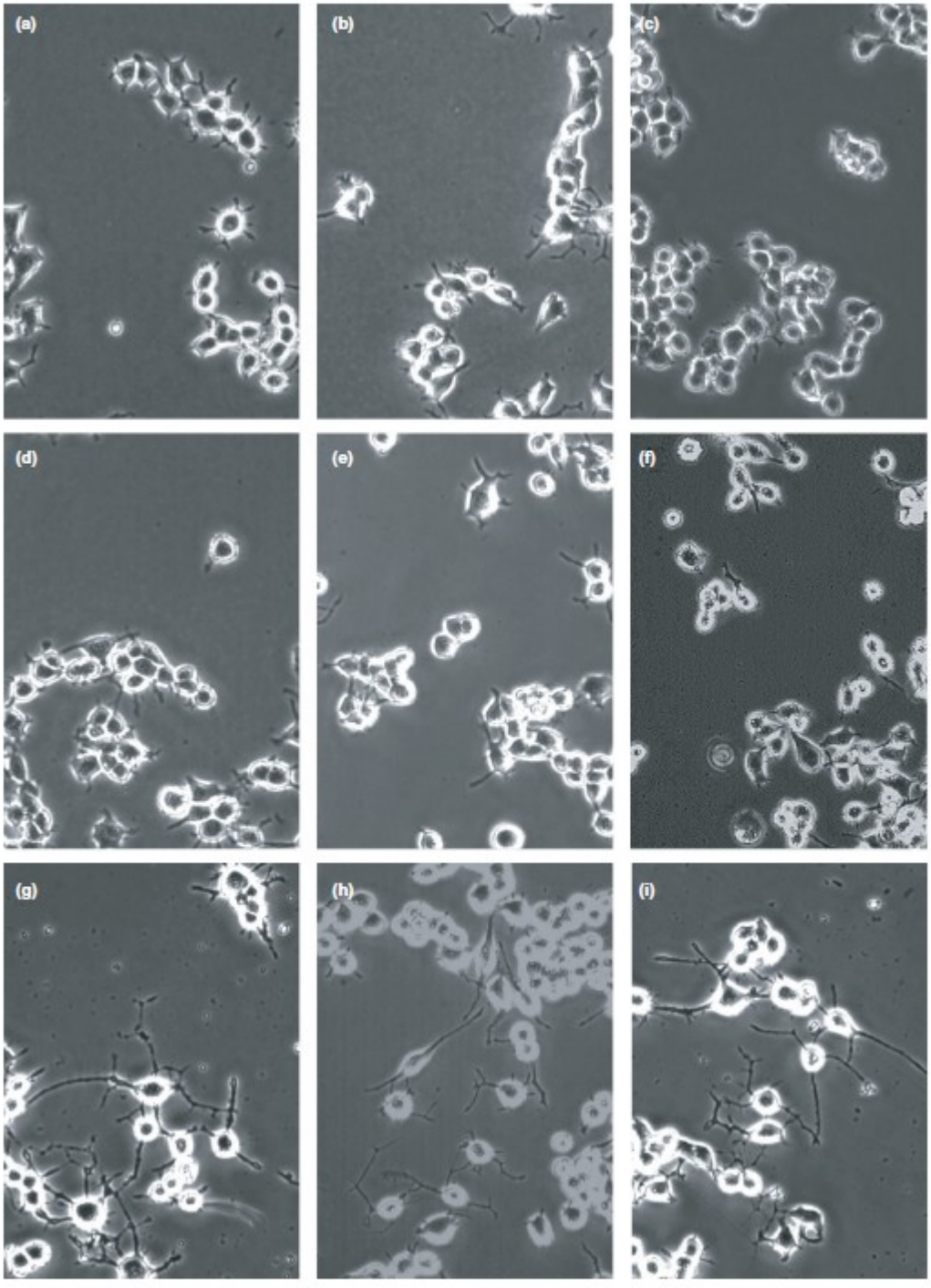

Figure R-3. Effect on the morphology of Neuro2a (N2a) cells after 24 h incubation. N2a cells in the absence **(a)** or presence of 50 µM galactose **(b)**, sialic acid **(c)**, sialyllactose **(d)**, OligoGM2 **(e)**, Asialo-OligoGM1 **(f)**, OligoGM1 **(g)**, Fucosyl-OligoGM1 **(h)** and GM1 **(i)**. Cells were analyzed with phase contrast microscopy with 200× magnification. Images are representative of ten independent experiments (n = 10).

Neurite extensions were measured as the ratio between the length of processes and the diameter of cell body **(Figure R-4)**, after 24 h treatment with OligoGM1. The values observed for the treated cells resulted significantly higher than control after 24 hours. Values obtained with OligoGM1 and GM1 were comparable.

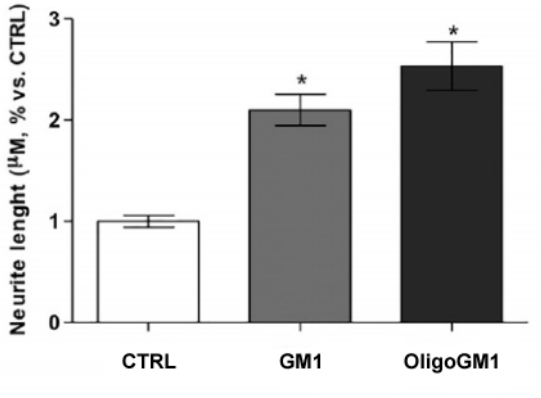

Figure R-4. Characterization of the neurite sprouting in N2a cells after administration of GM1 and OligoGM1. Values are expressed as fold increase over CTRL of mean ± SEM from five different experiments (*$p < 0.01$, Student's t-test, $n = 5$).

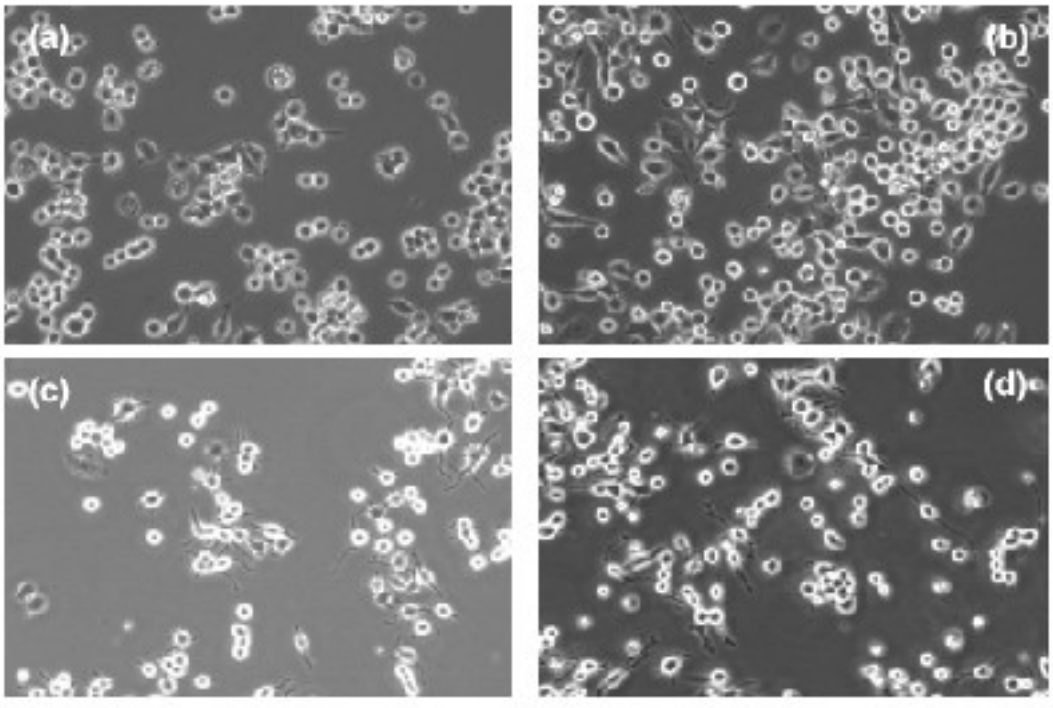

Figure R-5. Effect on the morphology of Neuro2a (N2a) cells after 24 -72 h incubation. N2a cells in the presence of 50 μM of PseudoGM1 after 24 h **(a)** and after 72 h **(b)**. N2a cells in the presence of 50 μM of NO_2-OligoGM1 after 24 h **(c)** and after 72 h **(d)**.

We used immunoblotting to evaluated the expression of heavy, medium, and light intracellular NF subunits (NF-H, NF-M and NF-L), considered markers of neurodifferentiation *(Fukuda et al. 2014).* NF expression

increased after 24 h of treatment with GM1 or OligoGM1 **(Figure R-6)**. α-tubulin (α-tub) was used as internal normalizer. The same results was obtained by immunofluorescence **(Figure R-7)**.

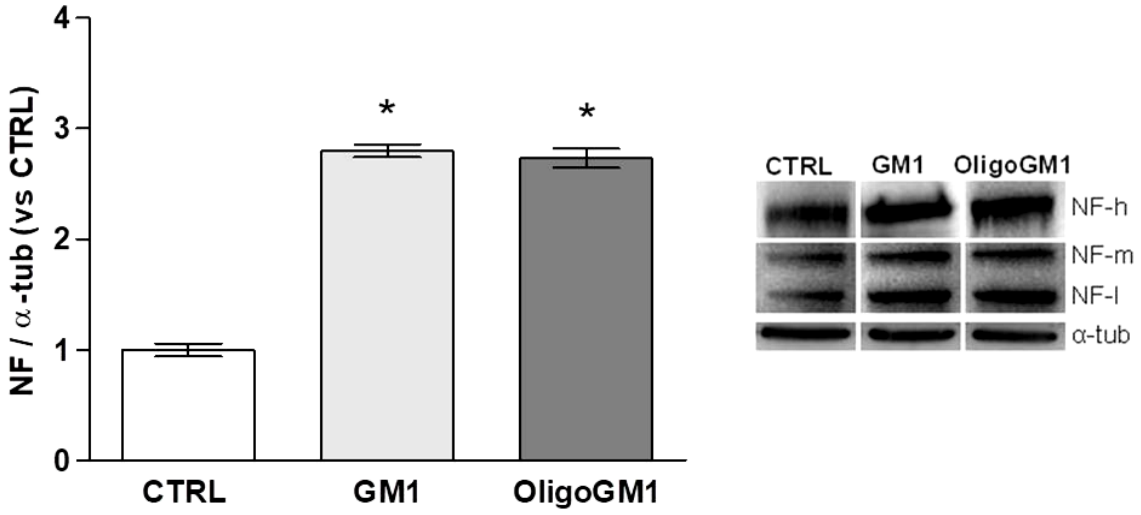

Figure R-6. NF proteins amount. Right: Immunoblotting images (three independent experiments). Left: semiquantitative analysis of NF proteins amount Data are expressed as fold increase over CTRL of mean ± SEM from three different experiments (*p < 0.01, Student's t-test, n = 3).

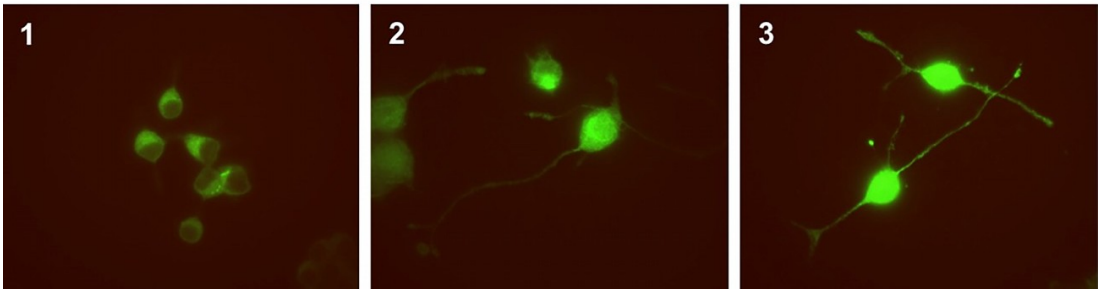

Figure R-7. Immunofluorescence staining of NF proteins. **(1)** CTRL; **(2)** GM1; **(3)** OligoGM1. Images are representative of three independent experiments (n = 3).

3. Fate of the OligoGM1 added to N2a cells

Tritium-labeled OligoGM1 was administered to the N2a cells. At the end of the incubation (0.5, 1, 6, and 24 h treatment), cells were washed with culture medium containing 10% serum to evaluate the quantity of OligoGM1 weakly associated to the cells surface (serum labile) *(Chigorno et al. 1985).* In a second moment cells were treated with trypsin to evaluate a possible portion strongly bond to the extracellular domain of PM proteins (trypsin labile). At the end, cells were lyzed to evaluate the quantity of internalized OligoGM1 (trypsin stabile). In all situation, about 99% of OligoGM1 was found in the serum labile form **(Figure R-8)**. This suggests the association of OligoGM1 with PM proteins. OligoGM1 is not absorb by the cells. The radioactivity associated with each fraction was determined by liquid scintillation counting.

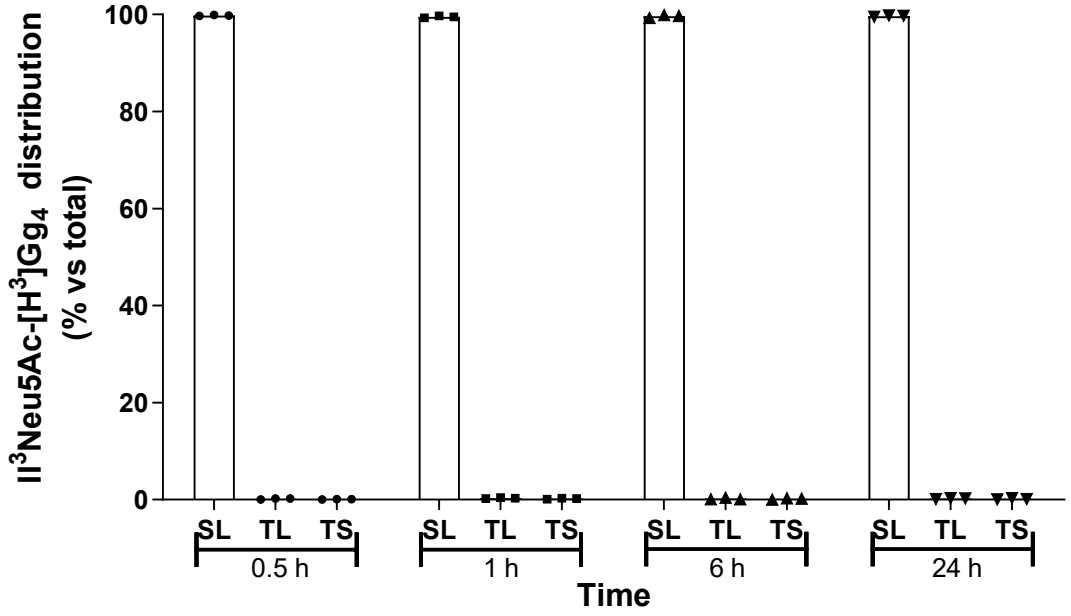

Figure R-8. Association of Tritium-labeled OligoGM1 to N2a cells. Data are expressed as percentage mean of total radioactivity ± SEM of three different experiments (n = 3).

4. TrkA-dependent neuritogenesis induced by OligoGM1

GM1 promotes neurite elongation by amplifying the effect exerted by NGF on TrkA *(Farooqui et al. 1997; Singleton et al. 2000; Duchemin et al. 2002; Da Silva et al. 2005; Mocchetti 2005; Zakharova et al. 2014).*
Starting from this point we wanted to verify the role of OligoGM1 in TrkA activation in N2a cells. Our attention was focused on Tyr490, whose phosphorylation is responsible to the activation of the neuronal differentiation *(Singleton et al. 2000; Duchemin et al. 2002; Huang and Reichardt 2003; Zakharova et al. 2014).* Both in N2a cells treated with GM1 and in those treated with OligoGM1 we observed an increase in the phosphorylation of Tyr490. These results were obtained using immunoblotting analysis **(Figure R-9)**.
In the cells treated with GM1 or OligoGM1, we also checked the activation of MAP kinases. In this case we have verify an increase of ERK1/2 phosphorylation. Blocking TrkA receptor by chemical inhibition we proved that GM1 or OligoGM1 effect was directly mediated by TrkA-ERK pathway *(Wood et al. 2004).*
The addition of TrkA inhibitor, in treated cells, prevented the phosphorylation processes and the neurite elongation **(Figure R-10)**.

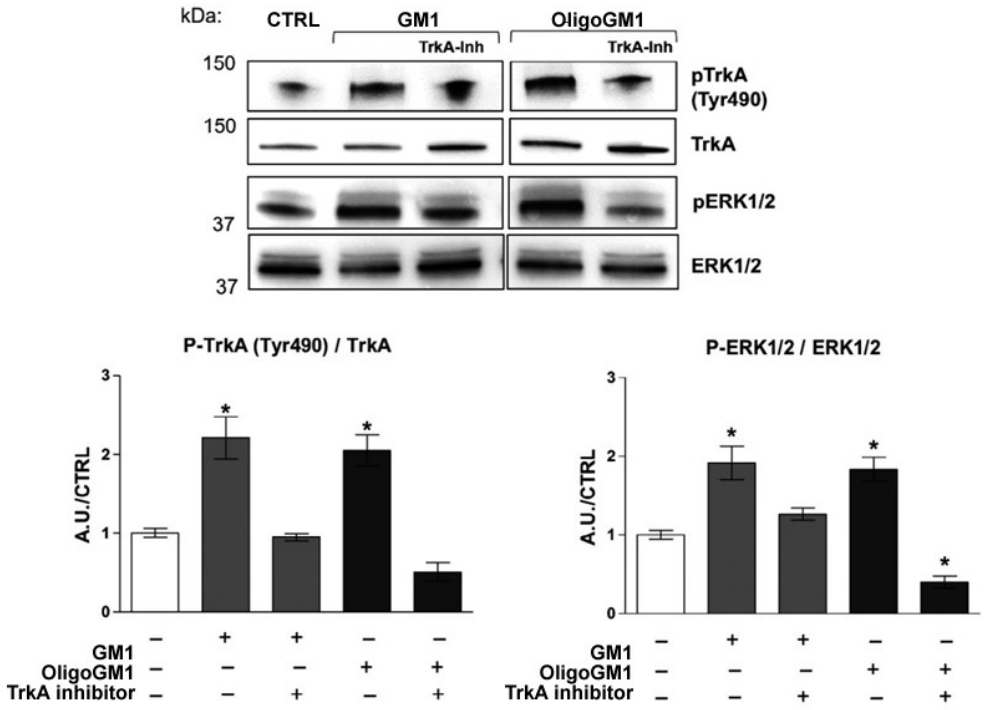

Figure R-9. GM1and OligoGM1 effect on TrkA pathway. Expression of TrkA, phosphorylated TrkA (tyrosine 490, Tyr490), total extracellular signal-regulated protein kinases 1 and 2 (ERK1/2) and phosphorylated ERK1/2 in cell lysate by means of specific antibodies and revealed by enhanced chemiluminescence. Top: immunoblotting images are shown. Bottom: Semiquantitative analysis of phosphorylated TrkA and ERK1/2 related to total level of TrkA and ERK 1/2, respectively. Data are expressed as fold increase over control of the mean ± SEM from five different experiments (*$p < 0.05$, Student's t-test, n = 5).

Furthermore, to prove the necessary requirement of TrkA in OligoGM1-mediated neuritogenesis, TrkA was knocked down using the siRNA approach. Control cells were transfected with scramble-siRNA. Silenced cells, resulting in a 70% reduction of TrkA expression, were incubated with GM1 or OligoGM1 for 24 h and no differentiation, nor the phosphorylation of Erk1/2 **(Figure R-11)** could be observed.

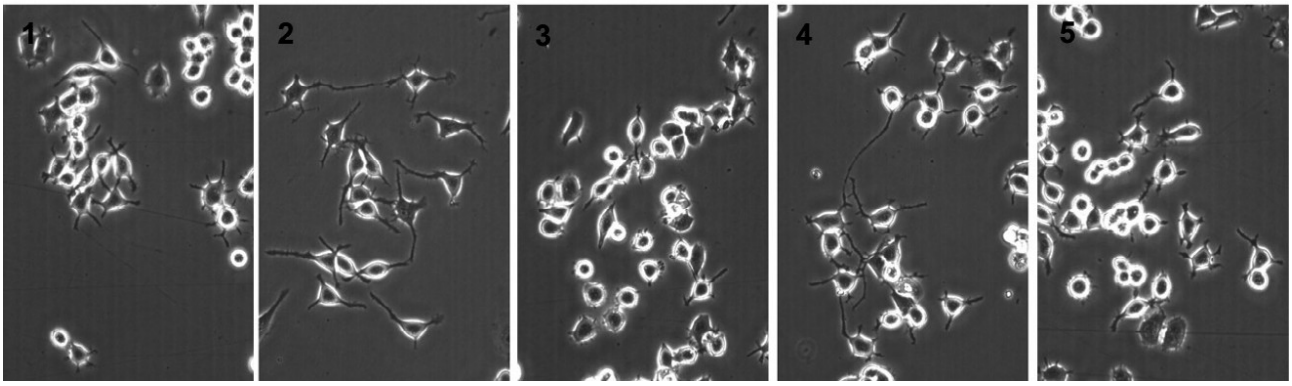

Figure R-10. Morphological analysis of N2a cells. **(1)** control; **(2)** GM1; **(3)** TrkA-Inh + GM1; **(4)** OligoGM1; **(5)** TrkA-Inh + OligoGM1. Cells were evaluated with phase contrast microscopy with 200× magnification. Images are representative of ten independent experiments (n = 10).

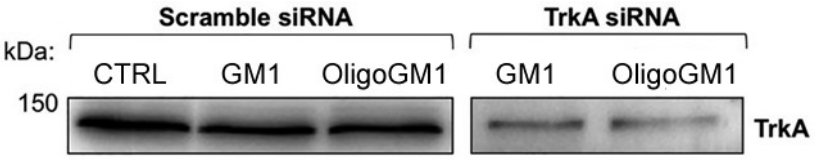

Figure R-11. Effect of GM1 and OligoGM1 on Neuro2a (N2a) cells following silencing of TrkA. Western blotting representative image for TrkA expression in siRNA treated cells.

5. Photolabeling experiments. GM1 and OligoGM1–TrkA interaction in N2a cells

To understand which part of GM1 is involved into the interaction with TrkA receptor we used photoactivable and tritium-labeled GM1 and OligoGM1. We observed that OligoGM1, unlike the GM1, interacts in a non-covalent manner with the cell surface **(Figure R-12)**.

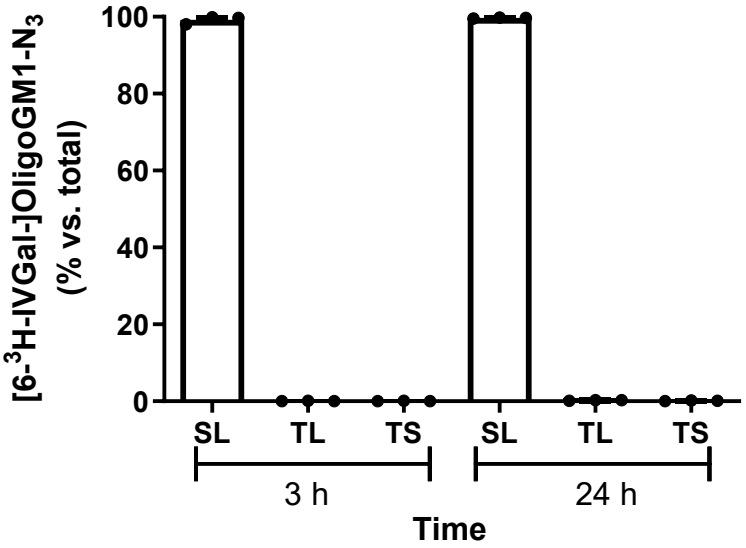

Figure R-12. Association of [Gal-6-^{3}H]OligoGM1(Glc-N_3) to N2a cells. N2a cells were incubate with 50 µM [Gal-6-^{3}H]OligoGM1(Glc-N_3) for 3 and 24 h. The radioactivity associated to each fraction was determined by liquid scintillation counting. Data are expressed as percentage mean of total radioactivity ± SEM of three independent cell culture preparations (n = 3).

Under UV irradiation, the azide of the nitrophenylazide group becomes a nitrene, that immediately generates covalent bonds with adjacent molecules. In this way, proteins interacting with the azide-bearing radioactive molecules become radiolabeled as well *(Sonnino et al. 1989).* Cell proteins were separated by SDS-PAGE, transferred on a PVDF membrane, and visualized by digital autoradiography as well as by colorimetric assay. Among the entire N2a protein pattern **(Figure R-13)**, only few radioactive bands were detected on PVDF.

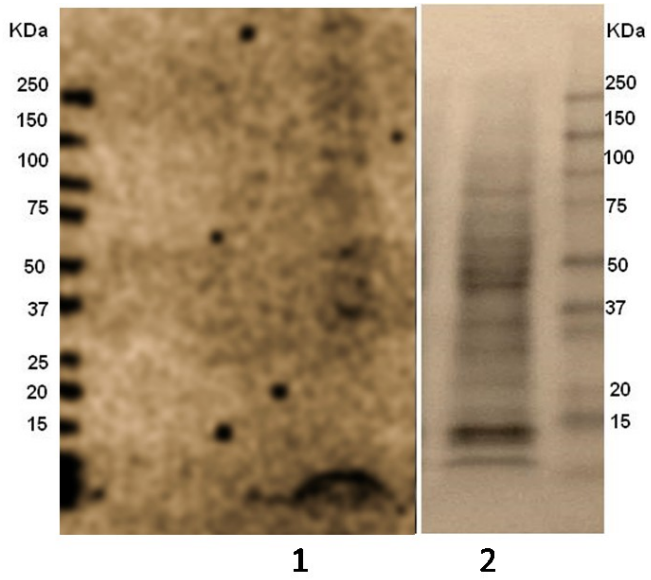

Figure R-13. N2a protein patterns. **1** radioactive tracks on PDVF membrane of N2a tritium labelled proteins interacting with OligoGM1 obtained using [Gal-6-^{3}H]OligoGM1(Glc-N_3) and acquired by digital autoradiography. **2**: entire N2a protein pattern revealed by Ponceau PVDF staining.

The radioactive tracks identify proteins cross-linked with the photoactivated compound. Using GM1 and OligoGM1 derivatives was identified a radioactive protein pattern. The results obtained suggest specific protein–ganglioside and protein– oligosaccharide interactions **(Figure R-14)**. After the autoradiography, the PVDF membranes were immunostained with anti-TrkA antibody. The band corresponding to TrkA signal was found to overlap a radiolabeled band at 140 kDa in cells treated with GM1 derivative, carrying the photoactivable group on the external galactose and with the OligoGM1 derivative, carrying the photoactivable group on the glucose **(Figures R-14 B and R-14 C).** In cells treated with the GM1 derivative with the photoactivable group at the ceramide **(Figure R-14 A)** was not found correspondence of TrkA signal with radioactive track. From what has been observed it is possible to conclude that TrkA–GM1 complex formed through the interaction between the TrkA and the oligosaccharide head of the GM1 does not involve ceramide.

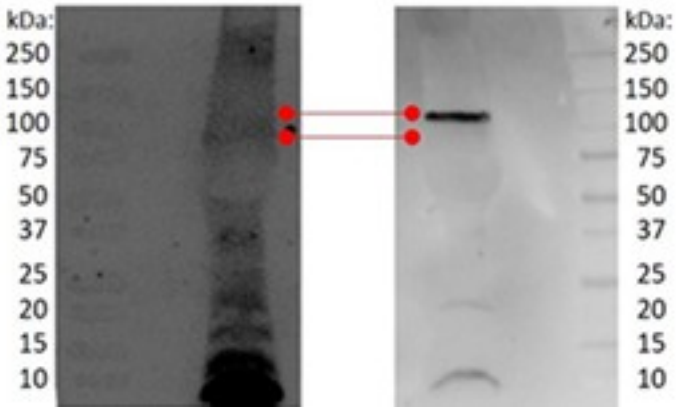

(A)

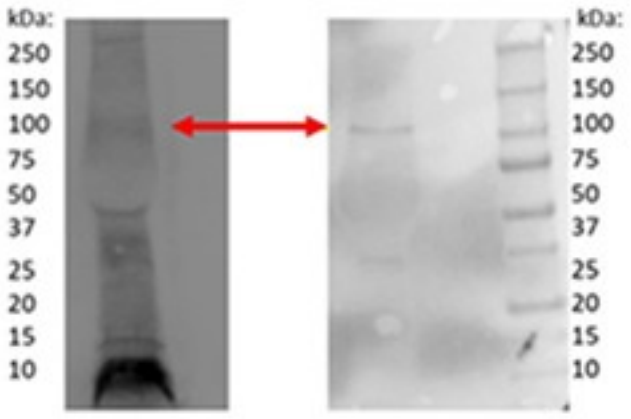

(B)

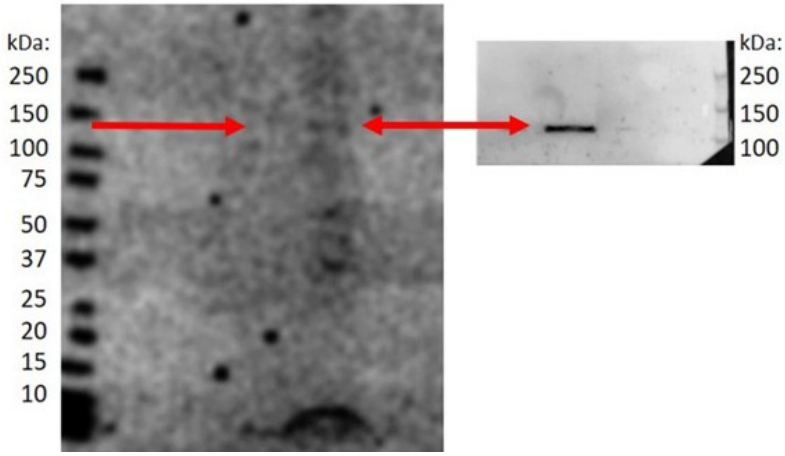

(C)

Figure R-14. Interaction between TrkA and GM1 derivatives in N2a cells. **(A)** Interaction between TrkA and [Gal-6-^{3}H]GM1(Cer-N_3)GM1; **(B)** Interaction between TrkA and [Sph-3-^{3}H]GM1(Gal-N_3)]; **(C)** Interaction between TrkA and [Gal-6-^{3}H]OligoGM1(Glc-N_3). Left: autoradiography. Right: western blotting.

6. Time course of the TrkA–ERK1/2 signaling pathway

GM1 and OligoGM1 activate the TrkA–MAPK pathway after 24-48 h from their exogenous administration. In order to examine the time course of TrkA–ERK1/2 pathway activation induced by GM1 and OligoGM1 the phosphorylation levels of TrkA on Tyr490 and of Erk1/2 on Thr202/Tyr204 were followed by immunoblotting analysis. GM1 and OligoGM1 caused a rapid elevation of TrkA phosphorylation **(Figure R-15)**, detectable after 30 min, and significantly maintained for over the 12h time course. The enhancement in ERK1/2 phosphorylation becoming significant after 6 h from GM1 and OligoGM1 administration **(Figure R-15).** The results revealed that, following GM1 and OligoGM1 treatment, TrkA Tyr490 phosphorylation increased twofold in 3 h and Erk1/2 phosphorylation doubles in 6 h, respect to control untreated cells. Both proteins remained hyperphosphorylated for the following 24-48 h.

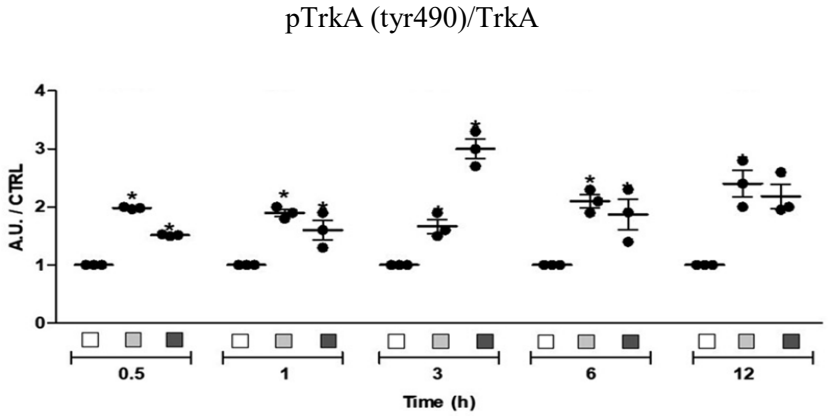

(A)

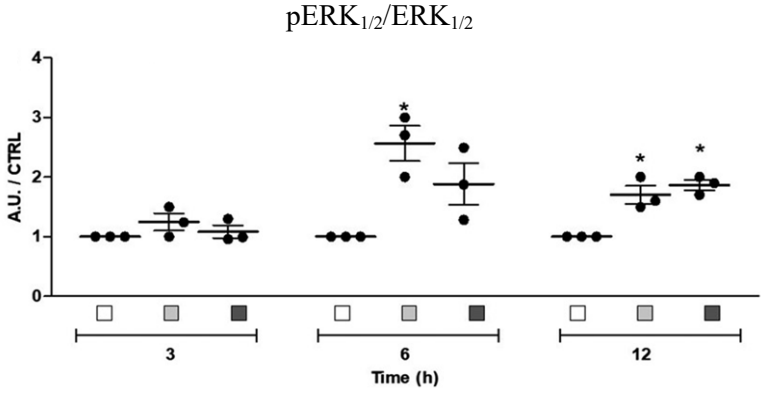

(B)

Figure R-15. Time course of TrkA and ERK1/2 pathway activation followed by N2a differentiation. Expression of TrkA, phosphorylated TrkA (Tyr490), ERK1/2, and phosphorylated ERK1/2 in cell lysate by means of specific antibodies and reveled by enhanced chemiluminescence. Semiquantitative analysis of phosphorylated TrkA **(A)** and ERK1/2 **(B)** related to total level of TrkA andERK1/2 respectively. Data are expressed as fold increase over control of the mean ± SEM from three independent cell culture preparations (*$p < 0.05$, Mann–Whitney test, n = 3). [□ white square: control, ■ light gray square: GM1; ■ dark gray square: OligoGM1].

Morphological analysis revealed the acquisition of neuron-like morphology of N2a cells (sprouting and elongation of neuritis), confirming that the differentiation processes occurred **(Figure R-16).**

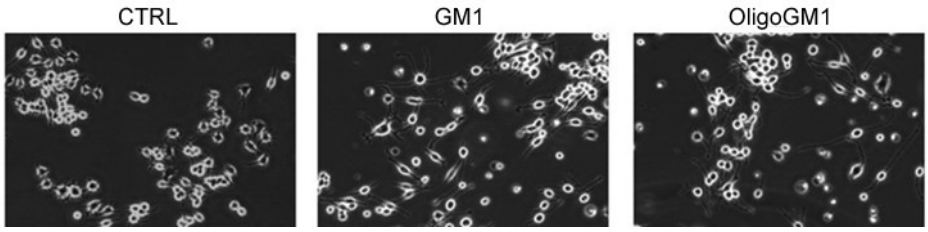

Figure R-16. Morphological analysis of N2a cells. Images are representative of ten independent cell culture preparations (n = 10)

7. Membrane lipid domains characterization

Lipid rafts were isolated as the DRM to better understand if TrkA and GM1 inserted into the external lipid layer of the plasma membrane are near enough to interact or if ganglioside GM1 localizes in lipid membrane domains, the lipid rafts, and that the TrkA receptor places in the fluid membrane environment separated from the lipid rafts *(Limpert et al. 2007; Ichikawa et al. 2009; Pryor et al. 2012).* Lipids were extracted from each fraction, separated by HPTLC and ganglioside GM1 content was revealed by TLC staining with cholera toxin B subunit (CT-B). In all experimental conditions, GM1 was found in the rigid membrane fractions non-solubilized by the detergent **(Figure R-17)**. Differently, in any experimental condition, western blotting analysis revealed that TrkA was present in the fluid membrane fraction, solubilized by the detergent **(Figure R-17)**. This result supports the photoactivable data and show up that TrkA and GM1 interact through the oligosaccharide chain in the extracellular environment since GM1 and TrkA belong to separate membrane portions.

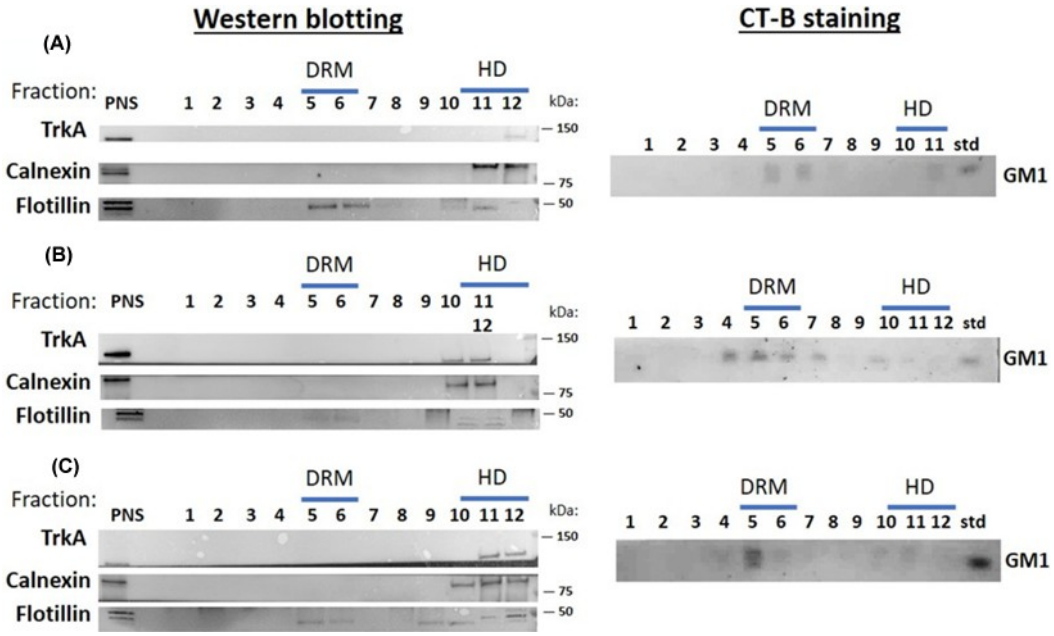

Figure R-17. Sucrose gradient fractions characterization. N2a cells were incubated in the absence **(A)** or in the presence of GM1 **(B)** or OligoGM1 **(C)** for 3 h at 37°C. Cells were subsequently subjected to sucrose gradient ultracentrifugation to prepare plasma membrane microdomains. Left: Immunoblotting against the TrkA, calnexin (HD marker), and flotillin (DRM marker) performed on postnuclear supernatant (PNS) and on the 12 fractions. Images are representative of three independent cell culture preparations. Right: GM1 detection among total lipids extracted from each sucrose fraction, revealed by cholera toxin subunit B (CT-B) TLCstaining (std: GM1 standard).

8. Dynamic calculations for the TrkA-OligoGM1 complex

The availability of the crystallographic structure of the extracellular segment of human TrkA in complex with NGF allowed us to support biochemical data with bioinformatics. The molecular docking of OligoGM1, specifically carried out exploring the interaction interface between TrkA and NGF, showed that OligoGM1 is able to tightly bind both TrkA and NGF contemporarily, producing only one very stable pose, with an approximative binding free energy of - 11.3 kcal/mol **(Figure R-18).**

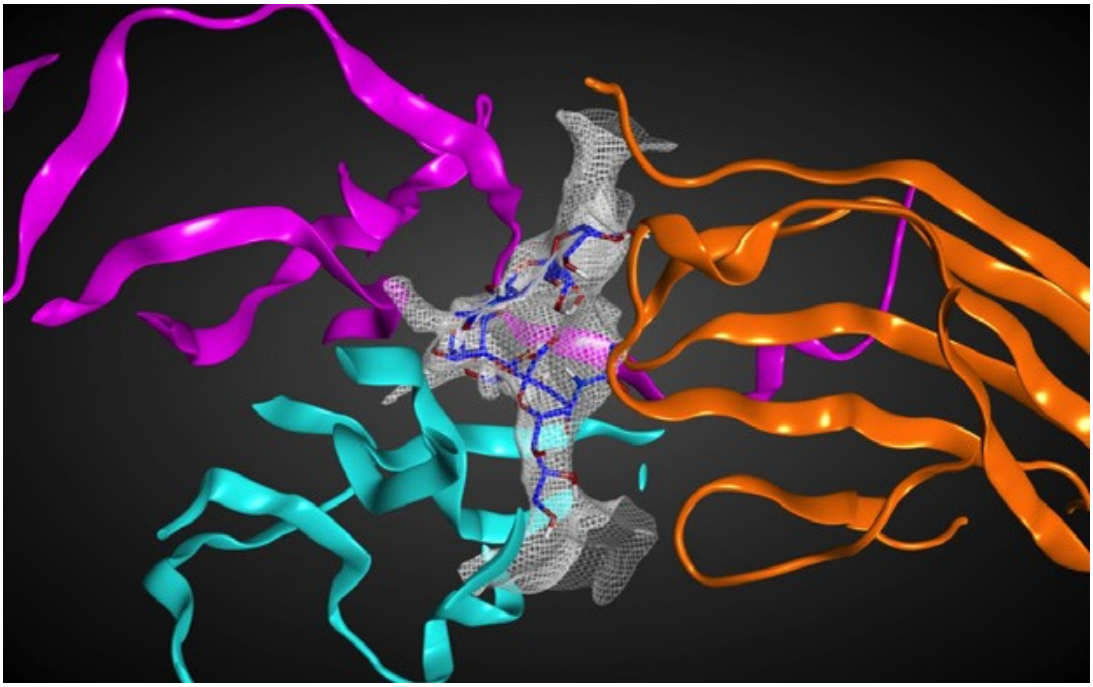

Figure R-18. Molecular dynamic calculations for the complex TrkA-NGF-OligoGM1. Top-scoring docking pose of OligoGM1 in the TrkA-NGF crystallographic complex. TrkA in orange ribbons; two NGF molecules: one in cyan ribbons and one in magenta ribbons. OligoGM1 is represented in sticks, with blue color for carbon atoms and red color for oxygen atoms. Van der Waals interaction surface between OligoGM1 and proteins is represented as a white mesh map.

Discussion

Gangliosides are glycosphingolipids (GSLs) containing one or more sialic acid residues in the sugar moiety., with a strong amphiphilic character due to the presence of a hydrophobic group (lipid moiety) linked to a hydrophilic head group (oligosaccharide chain). Gangliosides for their chemical structure are important mediators of information across the plasma membrane. They are insert into membranes by their lipid moiety with most of the glycan extending outside, in cell surrounding environment. They are present in different tissues but in mammalian they are abundant in nervous cells. Gangliosides are involved in different processes like ion transport, receptor modulation, stem cell biology and they are involved in neurodegenerative disorders. The gangliosides content change during neuron differentiation, aging and neurodegenerative diseases. Gangliosides play also important function in animal cells as antigens, and receptors for microbial toxins as well as mediators of cell adhesion and modulators of signal transduction. Oligosaccharide chain represent the interactive point of gangliosides with other molecules in extracellular environment. It is extremely variable in sugar structure, number, and is characterized by the presence of one or more negative charges in the sialic acid residues.

GM1 is the most studied gangliosides, not only in its complete structure but also for the features of the oligosaccharide chain. GM1 is one of the principal modulator in the nervous system where is involve in maturations of neurons, differentiation, increases responses to neurotrophic factors, protects against neuronal death and reduces brain damage acting on neurotrophic factors. The effects of GM1 are know *in vitro* and *in vivo*, but the molecular mechanism of action underlying the GM1 properties like neurodifferentiation, neuroprotection and its involvement in neurodegeneration, remained difficult to find. We know that, in neuroblastoma cells, the increase of GM1 in the plasma membrane promotes neurite production and cell differentiation, and this increase is necessary for TrkA-mediated neurodifferentiative processes *(Facci et al. 1984).*

The present work aimed to analyze the mechanism of action of GM1, and in particular to demonstrate that the effects of this ganglioside are attributable to the action of its oligosaccharide portion. To reach our purpose we used mouse neuroblastoma cell line Neuro2a (N2a).

For our experiments, we prepared GM1, OligoGM1, their tritiated-and-photoactivable form and No_2-OligoGM1. GM1 was purified from the total ganglioside mixture extract from the brain, while OligoGM1 was prepared by chemical ozonolysis of pure GM1 followed by alkaline fragmentation.

Incubation of N2a cells with OligoGM1 (50 μM) induced in 12 h a reduction of cell proliferation, in 24 h a neuron-like morphology and after 48 h elongation of neurites.

After establishing cell vitality and cell proliferation, we demonstrated that the effect of OligoGM1 was structure-specific. OligoGM1, like GM1, promote neurodifferentiation by increasing both neurite elongation and the expression of neurofilament proteins in N2a cell. A similar effect was obtained with the use of fucosyl-OligoGM1, suggesting that the terminal α-Fuc-(1-2)-β-Gal linkage does not change the molecular conformation required for the activation of the sprouting process. No difference was observed with the administration of asialo-OligoGM1, OligoGM2, OligoGM3, sialic acid or galactose (single components of

Oligo GM1). Considering the results obtained with these tests, we decided to try NO_2-OligoGM1, that was prepared from ozonolysis of deAcGM1, and Pseudo GM1, a mimic of ganglioside GM1. No morphological difference was observed with the use of this GM1 derivative.

With the use of tritium-labeled OligoGM1 we demonstrated that OligoGM1 is not absorb by the cells.

GM1 promotes neurite elongation by amplifying the effect exerted by NGF on TrkA, while the absence of ganglioside GM1 is negatively correlated with TrkA function. OligoGM1, in N2a cells, activates ERK1/2 pathway binding to the NGF specific receptor TrkA present on the cell surface. Both in N2a cells treated with GM1 and in those treated with OligoGM1 we observed an increase in the phosphorylation of Tyr490. The activator for GM1 mediated functions (differentiation and protection) is the interaction between OligoGM1 and TrkA. The addition of TrkA inhibitor, in treated cells, prevented the phosphorylation processes and the neurite elongation.

Photolabeling experiments with photoactivable and tritium-labeled GM1 and OligoGM1 were carried out to verify the interaction between glycosphingolipids and proteins. Cells were incubated with the tritium-labeled photoactivable OligoGM1 and GM1. The subsequent UV-light exposition transforms the photoactivable group into a nitrene, which rapidly covalently links to neighbouring compounds. We observed that OligoGM1, unlike the GM1, interacts in a non-covalent manner with the cell surface.

By SDS–PAGE separation, followed by radioimaging of the blotted material, we identified one band with a molecular mass of 140 KDa. This band corresponding to TrkA signal and overlapped a radiolabeled band in cells treated with GM1 derivative, carrying the photoactivable group on the external galactose and with the OligoGM1, carrying the photoactivable group on the glucose. This suggesting a direct interaction between OligoGM1 and TrkA.

Our results point out that the GM1 oligosaccharide is the structure portion responsible for the neurodifferentiative properties exerted by GM1. OligoGM1–TrkA interaction is due to a membrane reorganization.

Lipid rafts were isolated as the DRM to better understand if TrkA and GM1 inserted into the external lipid layer of the plasma membrane are near enough to interact. Lipids were extracted from each fraction, separated by HPTLC and ganglioside GM1 content was revealed by TLC staining with cholera toxin B subunit (CT-B). In all experimental conditions, GM1 was found in the rigid membrane fractions while TrkA was found in the fluid fraction solubilized by the detergent. To understand how the TrkA–GM1 interaction occurs, we used tritium-labeled and photoactivable GM1 and OligoGM1. The result show up that TrkA and GM1 interact through the oligosaccharide chain in the extracellular environment since GM1 and TrkA belong to separate membrane portions. When TrkA, for its dynamics in the fluid membrane, is near the lipid rafts, the extracellular environment of the soluble portion of TrkA, with an extension of the order of several tens of Å, may reach the GM1 oligosaccharide with no necessity for TrkA to belong to the same lipid membrane domain of GM1. With a bioinformatics study was established that OligoGM1 inserts in a pocket of the TrkA-NGF complex. An increase in energy associated to the complex TrkA-NGF-OligoGM1 indicates greater stability of intermolecular interactions.

All the results lead to the conclusion that the bioactive portion of GM1, in neuronal differentiation and protection, is represented by its oligo chain. These conclusions open up new perspectives on the therapeutic use of gangliosides.

References

- Abad-Rodrıguez J, Dìez-Revuelta N. Axon glycoprotein routing in nerve polarity, function, and repair. Trends Biochem Sci. 2015;40(7):385-96.
- Acquotti D, Cantù L, Ragg E, Sonnino S. Geometrical and conformational properties of ganglioside GalNAc-GD1a, IV4GalNAcIV3Neu5AcII3Neu5AcGgOse4Cer. Eur J Biochem. 1994;225(1):271-88.
- Angata T, Varki A. Chemical diversity in the sialic acids and related alpha-keto acids: an evolutionary perspective. Chem Rev. 2002;102(2):439-69.
- Aureli M, Loberto N, Lanteri P, Chigorno V, Prinetti A, Sonnino S. Cell surface sphingolipid glycohydrolase in neuronal differentiation and aging in culture. J Neurochem. 2011;116(5):891-9.
- Bernardi A, Boschin G, Checchia A, Lattanzio M, Manzoni L, Potenza D, Scolastico C. Synthesis of Pseudo Tetrasaccharide Mimic of Ganglioside GM1. Eur. J. Org. Chem. 1999;1311-17.
- Blennow K, Davidsson P, Wallin A, Fredman P, Gottfries CG, Mansson JE, Svennerholm L. Differences in cerebrospinal fluid gangliosides between “probable Alzheimer’s disease” and normal aging. Aging. 1992;4(4):301-6.
- Braun PE, Snell EE. The biosynthesis of dihydrosphingosine in cell-free preparations of Hansenula ciferri. Proc Natl Acad Sci U S A. 1967;58(1):298-303.
- Breiden B, Sandhoff K. Ganglioside metabolism and its inherited diseases. Methods Mol Biol. 2018;1804:97-141.
- Brodeur GM, Minturn JN, Ho R, Simpson AM, Iyer R, Varela CR, Light JE, Kolla V, Evans AE. Trk receptor expression and inhibition in neuroblastomas. Clin Cancer Res. 2009;15(10):3244-50.
- Chierzi S, Ratto GM, Verma P, Fawcett JW. The ability of axons to regenerate their growth cones depends on axonal type and age, and is regulated by calcium, cAMP and ERK. Eur. J. Neurosci. 2005;21(8):2051-62.
- Chigorno V, Pitto M, Cardace G, Acquotti D, Kirschner G, Sonnino S, Ghidoni R, Tettamanti G. Association of gangliosides to fibroblasts in culture: a study performed with I14Cl-labelled at the sialic acid acetyl group. Glyconj J. 1985;2:279-91.
- Chigorno V, Valsecchi M, Acquotti D, Sonnino S, Tettamanti G. Formation of a cytosolic ganglioside-protein complex fol-lowing administration of photoreactive ganglioside GM1 to humanfibroblasts in culture. FEBS Lett. 1990;263(2):329-31.
- Chiricozzi E, Ciampa MG, Brasile G, Compostella F, Prinetti A, Nakayama H, Ekyalongo RC, Iwabuchi K, Sonnino S, Mauri L. Direct interaction, instrumental for signaling processes, between LacCer and Lyn in the lipid rafts of neutrophil-like cells. J Lipid Res. 2015;56(1):129-41.
- Chiricozzi E, Mauri L, Ciampa MG, Prinetti A, Sonnino S. On the use of cholera toxin. Glycoconj. J. 2018;35(2):161-3.
- Chiricozzi E, Lunghi G, Di Biase E, Fazzari M, Sonnino S, Mauri L. GM1 ganglioside is a key factor in maintaining the mammalian neuronal functions avoiding neurodegeneration. Int J Mol Sci. 2020;21(3):868.

- Corti M, Degiorgio V, Ghidoni R, Sonnino S, Tettamanti G. Laser-light scattering investigation of the micellar properties of gangliosides. Chem Phys Lipids. 1980;26(3):225-38.
- D'Angelo G, Rega LR, De Matteis MA. Connecting vesicular transport with lipid synthesis: FAPP2. Biochim Biophys Acta. 2012;1821(8):1089-95.
- Da Silva JS, Hasegawa T, Miyagi T, Dotti CG. Abad-Rodriguez. Asymmetric membrane ganglioside sialidase activity specifies axonal fate. Nat. Neurosci. 2005;8(5):606-15.
- Dodge JC, Treleaven CM, Pacheco J, Cooper S, Bao C, Abraham M, Cromwell M, Sardi SP, Chuang WL, Sidman RL, Cheng SH, Shihabuddin LS. Glycosphingolipids are modulators of disease pathogenesis in amyotrophic lateral sclerosis. Proc Natl Acad Sci USA. 2015;112(26):8100-5.
- Du J, Meledeo MA, Wang Z, Khanna HS, Paruchuri VD, Yarema KJ. Metabolic glycoengineering: sialic acid and beyond. Glycobiology. 2009;19(12):1382-401.
- Duchemin AM, Ren Q, Mo L, Neff NH, Hadjiconstantinou M. GM1 ganglioside induces phosphorylation and activation of Trk and Erk in brain. J. Neurochem. 2002;81(4):696-707.
- Facci L, Leon A, Toffano G, Sonnino S, Ghidoni R, Tettamanti G. Promotion of neuritogenesis in mouse neuroblastoma cells by exogenous gangliosides: relationship between the effect and the cell association of ganglioside GM1. J. Neurochem. 1984;42(2):299-305.
- Farooqui T, Franklin T, Pearl DK, Yates AJ. Ganglioside GM1 enhances induction by nerve growth factor of a putative dimer of TrkA. J. Neurochem. 1997;68(6):2348-55.
- Fukuda Y, Fukui T, Hikichi C. Ishikawa T, Murate K, Adachi T, Imai H, Fukuhara K, Ueda A, Kaplan AP, Mutoh T. Neurotrophin promotes NGF signaling through interaction of GM1 ganglioside with Trk neurotrophin receptor in PC12 cells. Brain Res. 2014;1596:13-21.
- Ghidoni R, Sonnino S, Tettamanti G, Wiegandt H, Zambotti V. On the structure of two new gangliosides from beef brain. J Neurochem. 1976;27(2):511-5.
- Glanz VY, Myasoedova VA, Grechko AV, Orekhov AN. Sialidase activity in human pathologies. Eur J Pharmacol. 2019;842:345-50.
- Hadaczek P, Wu G, Sharma N, Ciesielska A, Bankiewicz K, Davidow AL, Lu ZH, Forsayeth J, Ledeen RW. GDNF signaling implemented by GM1 ganglioside; failure in Parkinson's disease and GM1-deficient murine model. Exp. Neurol. 2015;263:177-89.
- Hanada K, Kumagai K, Yasuda S, Miura Y, Kawano M, Fukasawa M, Nishijima M. Molecular machinery for non-vesicular trafficking of ceramide. Nature. 2003;426(6968):803-9.
- Hanover JA. Glycan-dependent signaling: O-linked N-acetyl-glucosamine. FASEB J. 2001; 15(11):1865-76.
- Hirabayashi Y, Furuya S. Roles of L-serine and sphingolipid synthesis in brain development and neuronal survival. Prog Lipid Res. 2008;47(3):188-203.
- Holmgren J, Lonnoroth I, Svennerholm L. Tissue receptor for cholera exotoxin: postulated structure from studies with GM1 ganglioside and related glycolipds. Infect Immun. 1973;8(2):208-14.

- Huang EJ, Reichardt LF. Trk receptors: roles in neuronal signal transduction. Ann. Rev. Biochem. 2003;72:609-42.
- Ichikawa N, Iwabuchi K, Kurihara H, Ishii K, Kobayashi T, Sasaki T, Hattori N, Mizuno Y, Hozumi K, Yamada Y, Arikawa-Hirasawa E. Binding of laminin-1 to monosialoganglioside GM1 in lipid rafts is crucial for neurite outgrowth. J. Cell Sci. 2009;122(Pt 2):289-99.
- Irie A, Koyama S, Kozutsumi Y, Kawasaki T, Suzuki A. The molecular basis for the absence of N-glycolylneuraminic acid in humans. J Biol Chem. 1998;273(25):15866-71.
- Ito M., Yamagata T. A novel glycosphingolipid-degrading enzyme cleaves of the linkage between the oligosaccharide and ceramide of neutral and acidic glycosphingolipids. J Biol Chem. 1986;261(30):14278-82.
- Ito M., Yamagata T. Purification and characterization of glycosphingolipid-specific endoglycosidases (endoglycoceramidases) from a mutant strain of Rhodococcus sp. Evidence for three molecular species of endoglycoceramidases with different specificities. J Biol Chem. 1989;264(16):9510-9.
- Itokazu Y, Wang J, Yu RK. Gangliosides in nerve cell specification. Prog Mol Biol Transl Sci. 2018;156:241-63.
- IUPAC-IUB joint commission on biochemical nomenclature (JCBN). nomenclature of glycolipids. Eur J Biochem. 1998;257(2):293-8.
- Kappagantula S, Andrews MR, Cheah M, Abad-Rodriguez J, Dotti CG, Fawcett JW. Neu3 sialidase-mediated ganglioside conversion is necessary for axon regeneration and is blocked in CNS axons. J. Neurosci. 2014;34(7):2477-92.
- Klenk E. Über die natur der phophatide und anderer lipoide des gehirns und der leber bei der niemann-pickschen krankheit. Z Phys Chem. 1935;235:24-36.
- Klenk E. On the discovery and chemistry of neuraminic acid and gangliosides. Chem Phys Lipids. 1970;5(1):193-7.
- Kolesnick RN, Goñi FM, Alonso A. Compartmentalization of ceramide signaling: physical foundations and biological effects. J Cell Physiol. 2000;184(3):285-300.
- Kolter T, Proia RL, Sandhoff K. Combinatorial ganglioside biosynthesis. J Biol Chem. 2002;277(29):25859-62.
- Kolter T, Sandhoff K. Principles of lysosomal membrane digestion: stimulation of sphingolipid degradation by sphingolipid activator proteins and anionic lysosomal lipids. Annu Rev Cell Dev Biol. 2005;21:81-103.
- Kolter T, Sandhoff K. Sphingolipid metabolism diseases. Biocim Biophys Acta. 2006;1758(12):2057-79.
- Kolter T. Ganglioside biochemistry. ISRN Biochemistry. 2012;2012:506160.
- Kooner AS, Yu H, Chen X. Synthesis of *N*-glycolylneuraminic acid (Neu5Gc) and its glycosides. Front Immunol. 2019;10:2004.

- Kracun I, Rosner H, Drnovsek V, Vukelic Z, Cosovic C, Trbojevic-Cepe M, Kubat M. Gangliosides in the human brain development and aging. Neurochem Int. 1992;20(3):421-31.
- Kuhn R, Wiegandt H. Die konstitution der ganglio-N-tetraose und desgangliosids GI. Chem Ber. 1963;96:866-80.
- Ledeen RW. Biology of gangliosides: neuritogenic and neuronotrophic properties. J. Neurosci. Res. 1984;12(2-3):147-59.
- Ledeen RW, Wu G. The multi-tasked life of GM1 ganglioside, a true factotum of nature. Trends Biochem Sci. 2015;40(7):407-18.
- Ledeen RW, Wu G. Gangliosides, α-synuclein, and Parkinson's disease. Prog Mol Biol Transl Sci. 2018;156:435-54.
- Li F, Ding J. Sialylation is involved in cell fate decision during development, reprogramming and cancer progression. Protein Cell. 2019;10(8):550-65.
- Limpert AS, Karlo JC, Landreth GE. Nerve growth factor stimulates the concentration of TrkA within lipid rafts and extracellular signal-regulated kinase activation through c-Cbl-associated protein. Mol. Cell. Biol. 2007;27(16):5686-98.
- Lindner R, Naim HY. Domains in biological membranes. Exp Cell Res. 2009;315(17):2871-8.
- Loberto N, Prioni S, Prinetti A, Ottico E, Chigorno V, Karagogeos D, Sonnino S. The adhesion protein TAG-1 has a ganglioside environment in the sphingolipid-enriched membrane domains of neuronal cells in culture. J Neurochem. 2003;85(1):224-33.
- Lubineau A, Auge J, Drouillat B. Improved synthesis of glycosylamines and a straightforward preparation of Nacylglycosylamines as carbohydrate-based detergents. Carbohydr. Res. 1995;266(2):211-9.
- Maglione V, Marchi P, Di Pardo A, Lingrell S, Horkey M, Tidmarsh E, Sipione S. Impaired ganglioside metabolism in Huntington's disease and neuroprotective role of GM1. J Neurosci. 2010;30(11):4072-80.
- Manev H, Favaron M, Vicini S, Guidotti A, Costa E. Glutamate-induced neuronal death in primary cultures of cerebellar granule cells: protection by synthetic derivatives of endogenous sphingolipids. J Pharmacol Exp Ther. 1990;252(1):419-27.
- Mauri L, Prioni S, Loberto N, Chigorno V, Prinetti A, Sonnino S. Synthesis of radioactive and photoactivable ganglioside derivates for the study of ganglioside-protein interaction. Glycoconj. J. 2004;20(1):11–23.
- Mauri L, Sonnino S, Prinetti A. Chemical and physicochemical properties of gangliosides. Methods Mol Biol. 2018;1804:1-17.
- McGonigal R, Cunningham ME, Yao D, Barrie JA, Sankaranarayanan S, Frewou SN, Furukawa K, Yednock TA, Willison HJ. C1q-targeted inhibition of the classical complement pathway prevents injury in a novel mouse model of acute motor axonal neuropathy. Acta Neuropathol Commun. 2016;4:23.

- Mehlen P, Mehlen A, Godet J, Arrigo AP. hsp27 as a switch between differentiation and apoptosis in murine embryonic stem cell. J Biol Chem. 1988;272(50):31657-65.
- Merrill AH. De novo sphingolipid biosynthesis: a necessary, but dangerous pathway. J Biol Chem. 2002;277(29):25843-6.
- Mocchetti I. Exogenous gangliosides, neuronal plasticity and repair and the nurotrophins. Cell. Mol. Life Sci. 2005;62(19-20):2283-94.
- Mosmann T. Rapid colorimetric assay for cellular growth and survival: application to proliferation and cytotoxicity assays. J Immunol Methods. 1983;65(1-2):55-63.
- Mountney A, Zahner MR, Lorenzini I, Oudega M, Schramm LP, Schnaar RL. Sialidase enhances recovery from spinal cord contusion injury. Proc. Natl. Acad. Sci. U.S.A. 2010;107(25):11561-6.
- Naim M, Bhat S, Rankin KN, Dennis S, Chowdhury SF, Siddiqi I, Drabik P, Sulea T, Bayly CI, Jakalian A, Purisima EO. Solvated interaction energy (SIE) for scoring protein-ligan binding affinities. 1. Exlporing the parameter space. J. Chem. Inf. Model. 2007;47(1):122-33.
- Nikolova-Karakashian MN, Reid MB. Sphingolipid metabolism, oxidant signaling,and contractile function of skeletal muscle. Antioxid Redox Signal. 2011;15(9):2501-17..
- Pitto M, Mutoh T, Kuriyama M, Ferraretto A, Palestini P, Masserini M. Influence of endogenous GM1 ganglioside on TrkB activity in cultured neurons. FEBS Lett. 1998;439(1-2):93-6.
- Pohlentz, G, Klein D, Schwarzmann G. Schmitz D, Sandhoff K. Both GA2, GM2, and GD2 synthases and GM1b, GD1a, and GT1b synthases are single enzymes in Golgi vesicles from rat liver. Proc Natl Acad Sci. U S A. 1988;85(19):7044-8.
- Prinetti A, Prioni S, Chiricozzi E, Schuchman EH, Chigorno V, Sonnino S. Secondary alterations of sphingolipid metabolism in lysosomal storage diseases. Neurochem. Res. 2011:36(9);1654-68.
- Prioni S, Mauri L, Loberto N, Casellato R, Chigorno V, Karagogeos D, Prinetti A, Sonnino S. Interactions between gangliosides and proteins in the exoplasmic leaflet of neuronal plasma membranes: a study performed with a tritium-labeled GM1 derivative containing a photoactivable group linked to the oligosaccharide chain. Glycoconj. J. 2004;21(8-9):461-70.
- Pryor S, McCaffrey G, Young LR, Grimes ML. NGF causes TrkA to specifically attract microtubules to lipid rafts. PLoS One. 2012;7(4):e35163.
- Riboni L, Prinetti A, Bassi R, Caminiti A, Tettamanti G. A mediator role of ceramide in the regulation of neuroblastoma Neuro2a cell differentiation. J Biol Chem. 1995;270(45):26868-75.
- Roisen, F.J., Bartfeld, H., Nagele, R., Yorke, G. Ganglioside stimulation of axonal sprouting in vitro. Science. 1981;214(4520):577-8.
- Rubovitch V, Zilberstein Y, Chapman J, Schreiber S, Pick CG. Restoring GM1 ganglioside expression ameliorates axonal outgrowth inhibition and cognitive impairments induced by blast traumatic brain injury. Sci Rep. 2017;7:41269.
- Saqr HE, Pearl DK, Yates AJ. A review and predictive models of ganglioside uptake by biological membranes. J Neurochem. 1993;61(2):395-411.

- Schengerund CL, Garrigan OW. A comparative study of gangliosides from brains of various species. Lipids. 1969;4(6):488-95.
- Schengrund CL and Prouty C. Oligosaccharide portion of GM1 enhances process formation by S20Y neuroblastoma cells. J. Neurochem. 1988;51(1):277-82.
- Schiumarini D, Loberto N, Mancini G, Bassi R, Giussani P, Chiricozzi E, Samarani M, Munari S, Tamanini A, Cabrini G, Lippi G, Dechecchi MC, Sonnino S, Aureli M. Evidence for the Involvement of Lipid Rafts and Plasma Membrane Sphingolipid Hydrolases in Pseudomonas aeruginosa Infection of Cystic Fibrosis Bronchial Epithelial Cells. Mediators Inflamm. 2017;1730245.
- Schnaar RL, Gerardy-Schahn R, Hildebrandt H. Sialic acids in the brain: gangliosides and polysialic acid in nervous system development, stability, disease, and regeneration. Physiol Rev. 2014;94(2):461-518.
- Schwarzmann G. Labeled gangliosides: their synthesis and use in biological studies. FEBS Lett. 2018;592(23):3992-4006.
- Segler-Stahl K, Webster JC, Brunngraber EG. Changes in the concentration and composition of human brain gangliosides with aging. Gerontology. 1983;29(3):161-8.
- Singer SJ, Nicolson GL. The fluid mosaic model of the structure of cell membranes. Science. 1972;175(4023):720-31.
- Singleton DW, Lu CL, Collela R, Roisen FJ. Promotion of neurite outgrowh by protein kinase inhibitors and ganglioside GM1 in neuroblastoma cells involved MAP kinase ERK1/2. Int. J. Dev. Neurosci. 2000;18(8):797-805.
- Skaper SD, Katoh-Semba R, Varon S. GM1 ganglioside accelerates neurite outgrowth from primary and central neurons under selected culture conditions. Brain Res. 1985;355(1):19-26.
- Solovyeva VV, Shaimardanova AA, Chulpanova DS, Kitaeva KV, Chakrabarti L, Rizvanov AA. New Approaches to Tay-Sachs Disease Therapy. Front Physiol. 2018;9:1963.
- Sonnino S, Chigorno V, Acquotti D, Pitto M, Kirschner G, Tettamanti G. A photoreactive derivative of radiolabeled GM1 ganglioside: preparation and use to establish the involvement of specific proteins in GM1 uptake by human fibroblasts in culture. Biochemistry. 1989;28(1):77-84.
- Sonnino S, Chigorno V, Valsecchi M, Pitto M, Tettamanti G. Specific ganglioside–cell protein interactions: a study performedwith GM1 ganglioside derivative containing photoactivable azide and rat cerebellar granule cells in culture. Neurochem Int. 1992;20(3):315-21.
- Sonnino S, Cantù L, Corti M. Acquotti D, Venerando B. Aggregative properties of gangliosides in solution. Chem Phys Lipids. 1994;71(1):21-45.
- Sonnino S, Nicolini M, Chigorno V. Preparation of radiolabeled gangliosides. Glycobiology. 1996;6(5):479–87.
- Sonnino S, Mauri L, Chigorno V, Prinetti A. Gangliosides as components of lipid membrane domains. Glycobiology. 2007;17(1):1R-13R.

- Sonnino S, Prinetti A. Sphingolipids and membrane environments for caveolin. FEBS Lett. 2009;583(4):597-606.
- Sonnino S, Aureli M, Loberto N, Chigorno V, Prinetti A. Fine tuning of cell functions through remodeling of glycosphingolipids by plasma membrane-associated glycohydrolases. FEBS Lett. 2010;584(9):1914-22.
- Sonnino S, Prinetti A. Membrane domains and the "lipid raft" concept. Curr Med Chem. 2013;20(1):4-21.
- Sonnino S, Aureli M, Mauri L, Ciampa MG, Prinetti A. Membrane lipid domains in the nervous system. Front Biosci. 2015;20:280-302.
- Sonnino S, Chiricozzi E, Grassi S, Mauri L, Prioni S, Prinetti A. Gangliosides in membrane organization. Prog Mol Biol Transl Sci. 2018;156:83-120.
- Stoffel W, LeKim D, Sticht G. Biosynthesis of dihydrosphingosine in vitro. Hoppe Seylers Z Physiol Chem. 1968;349(5):664-70.
- Stoffyn A, Stopffyn P, Yip MC. Chemical structure of monosialoganglioside GM1b biosynthesized in vitro. Biochim. Biophys Acta. 1975;409(1):97-103.
- Svennerholm L. Quantitative estimation of sialic acids II A colorimetric resorcinol hydrochloric acid method. Biochim Biophys Acta. 1957;24(3):604-11.
- Svennerholm L. Chromatographic separation of human brain gangliosides. J Neurochem. 1963;10:613-23.
- Svennerholm L. The gangliosides. J Lipid Res. 1964;5:145-55.
- Svennerholm L. Ganglioside designation. Adv Exp Med Bio. 1980;125:11.
- Svennerholm L, Bostro¨m K, Helander CG, Jungbjer B. Membrane lipids in the aging human brain. J Neurochem. 1991;56(6):2051-9.
- Svennerholm L. Gangliosides -- A new therapeutic agent against stroke and Alzheimer's disease. Life Sci. 1994;55(25-26):2125-34.
- Svennerholm L, Bostrom K, Jungbjer B., Olsson, L. Membrane lipids of adult human brain: lipid composition of frontal and temporal lobe in subjects of age 20 to 100 years. J. Neurochem. 1994;63(5):1802-11.
- Takki-Luukkainen IT,,Miettinen T. Presence of sialic acid and hexosamine in proteins of the aqueous humour. Acta Ophthalmol. 1959;37(2):138-42.
- Tettamanti G, Bonali F, Marchesini S, Zambotti V. A new procedure for the extraction, purification and fractionation of brain gangliosides. Biochim Biophys Acta. 1973;296(1):160-70.
- Todeschini AR, Hakomori S. Functional role of glycosphingolipids and gangliosides in control of cell adhesion, motility, and growth, through glycosynaptic microdomains. Biochim Biophys Acta. 2008;1780(3):421-33.

- Valperta R, Valsecchi M, Rocchetta F, Aureli M, Prioni S, Prinetti A, Chigorno V, Sonnino S. Induction of axonal differentiation by silencing plasma membrane-associated sialidase Neu3 in neuroblastoma cells. J. Neurochem. 2007;100(3):708-19.
- Varki A. Glycan-based interactions involving vertebrate sialic-acid-recognizing proteins. Nature. 2007; 446(7139):1023-9.
- Varki A. Evolutionary forces shaping the Golgi glycosylation machinery: why cell surface glycans are universal to living cells. Cold Spring Harb Perspect in Biol. 2011;3(6):a005462.
- Wiegandt H, Bücking HW. Carbohydrate components of extraneuronal gangliosides from bovine and human spleen, and bovine kidney. Eur J Biochem. 1970;15(2):287-92.
- Wood ER, Kuyper L, Petrov KG, Hunter RN, Harris PA, Lackey K. Discovery and in vitro evaluation of potent TrkA kinase inhibitors: oxindole and aza-oxindoles. Bioorg Med Chem Lett. 2004;14(4):953-7.
- Wu G, Ledeen RW. Stimulation of neurite outgrowth in neuroblastoma cells by neuraminidase: putative role of GM1 ganglioside in differentiation. J. Neurochem. 1991;56(1):95-104.
- Wu G, Ledeen RW. Gangliosides as modulators of neuronal calcium. Prog. Brain Res. 1994;101:101-112.
- Wu G, Lu Z., Kulkarni N, Ledeen RW. Deficiency of ganglioside GM1 correlates with Parkinson's disease in mice and humans. J. Neurosci. Res. 2012;90(10):1997-2008.
- Waetzig V, Herdegen T. MEKK1 controls neurite outgrowth after experimental injury by balancing ERK1/2 and JNK2 signaling. Mol. Cell. Neurosci. 2005;30(1):67-78.
- Yang LJ, Lorenzini I, Vajn K, Mountney A, Schramm LP, Schnaar RL. Sialidase enhances spinal axon outgrowth in vivo. Proc. Natl. Acad. Sci. U.S.A. 2006;103(29):11057-62.
- Yu RK, Bieberich E, Xia T, Zeng G. Regulation of ganglioside biosynthesis in the nervous system. J Lipid Res. 2004;45(5):783-93.
- Yu RK, Nakatani Y, Yanagisawa M. The role of glycosphingolipid metabolism in the developing brain. J Lipid Res. 2009;50Suppl(Suppl):S440-5.
- Yu RK, Tsai YT, Ariga T, Yanagisawa M. Structures, biosynthesis, and functions of gangliosides—An overview. J Oleo Sci. 2011;60(10):537-44.
- Zakharova IO, Sokolova TV, Vlasova YA, Furaev VV, Rychkova MP, Avrova NF. GM1 ganglioside activates ERK1/2 and Akt downstream of Trk tyrosine kinase and protects PC12 cell against hydrogen peroxide toxicity. Neuro chem. Res. 2014;39(11):2262-75.
- Zaprianova E, Deleva D, Ilinov P, Sultanov E, Filchev A, Christova L, Sultanov B. Serum ganglioside patterns in multiple sclerosis. Neurochem Res. 2001;26(2):95-100.